Smart Charging of Plug-in Electric Vehicles in Distribution Systems Considering Uncertainties

by

Nafeesa Mehboob

A thesis
presented to the University of Waterloo
in fulfillment of the
thesis requirement for the degree of
Doctor of Philosophy
in
Electrical and Computer Engineering

Waterloo, Ontario, Canada, 2016

I hereby declare that I am the sole author of this thesis. This is a true copy of the thesis, including any required final revisions, as accepted by my examiners.

I understand that my thesis may be made electronically available to the public.

Abstract

Distribution feeders and equipment are designed to serve peak loads, and in the absence of Plug-in Electric Vehicle (PEV) loads, day-ahead dispatch of feeders is typically performed by optimizing feeder controls for forecasted load profiles. However, due to climate change concerns, the market share of PEVs is expected to increase, and consequently, utilities expect an increase in demand due to these loads charging from the grid. Uncontrolled charging of PEVs may lead to new peaks in distribution feeders, which would require expensive infrastructure and equipment upgrades. Furthermore, PEV loads will represent new sources of uncertainty, temporal and spatial, which will pose a challenge for the centralized control and optimal operation of the grid. In practice, these uncertainties arise as a result of variability in factors such as the number of PEVs connected to the grid for charging, the arrival and departure times of PEVs, and the initial battery State-of-Charge (SoC). Hence, the integration of PEVs into the existing distribution system, without significant infrastructure upgrades, will be possible only through smart charging of these loads, while properly accounting for these uncertainties. The elasticity of PEVs provides a level of flexibility that can be used by utilities or Local Distribution Companies (LDC) to ensure efficient feeder operation, while providing fair and efficient charging to PEV customers.

This thesis presents a novel two-step approach for the fair charging of PEVs in a primary distribution feeder, accounting for the uncertainty associated with PEVs, considering the perspectives of both the LDC and the PEV customer. In the first step of the proposed approach, the mean daily feeder peak demand and corresponding hourly feeder control schedules, such as taps and switched capacitor setpoints, are determined hourly, while minimizing the daily peak demand, taking the existence of PEVs into account. As an alternative to the conventional Monte Carlo Simulations (MCS), a nonparametric Bootstrap technique is used in conjunction with a Genetic Algorithm (GA)-based optimization model, to account for variations in the arrival and departure times, and the initial battery SoC of PEVs, at each node. In the second step, the maximum possible power that can be given to the charging PEVs at each node, while maintaining the peak demand value and

corresponding feeder dispatch schedules defined in the first step, is computed every few minutes and shared fairly among the PEVs.

The proposed technique is validated using the IEEE 13-bus test feeder as well as the distribution feeder model of an actual primary feeder in Ontario, considering significant PEV penetration levels. The potential gain in PEV charging efficiency is quantified for the proposed Bootstrap feeder control schedule with respect to the base schedule (without PEVs). The presented optimization approach is also compared with the current industry practice in Ontario, and a sensitivity-based heuristic technique, demonstrating the advantages and feasibility of the presented technique. The results show that the proposed approach could be implemented in practice due to its reasonable computational burden, and its ability to charge PEV loads better than the current industry practice, or a popular heuristic method, while satisfying feeder and peak demand constraints.

Acknowledgements

First and foremost, I would like to express my sincere gratitude to my advisors Professor Claudio Cañizares and Professor Catherine Rosenberg for their invaluable support, guidance and patience during the course of my PhD studies. It has truly been an honour and privilege to have completed my studies under their supervisions. Their professionalism, thoughtful guidance, and positive feedback have helped me throughout my studies.

I owe my deepest gratitude to my PhD committee for their valuable comments and inputs: Professor João Peças Lopes from the Faculty of Engineering, Porto University, Portugal; Professor Kankar Bhattacharya and Professor Mehrdad Kazerani from the Department of Electrical and Computer Engineering, University of Waterloo; and Professor Srinivasan Keshav from the Cheriton School of Computer Science, University of Waterloo.

My heartfelt thanks and endless appreciation to my family and in-laws for their unconditional support, encouragement, love, and care. To my beloved abbuji (dad), you are my inspiration to excel in everything that I do, and I know I get my passion for knowledge and learning from you. To my beautiful and amazing ammiji (mom), your endless sacrifices, love, and nurturing is the reason that I have been able to reach this point in my life. Whatever I am today, and where I stand today is because of both of you, and I always strive to make you proud. To both my brothers, Abdul Aziz and Khalid, I am blessed to have you looking out for me always. Thank you for being there for me throughout my ups and downs. To my loving husband, Jafar, no amount of thanks will be enough for the way you have supported and encouraged me in my passion to learn. To my wonderful in-laws, I am truly blessed to have you in my life. There was no end to the encouragement I always received from all of you, and it always raised my spirits.

Through the course of my studies, I had the opportunity of working with many brilliant minds and forging great friendships: Mohammad, Sadek, Ahsan, Wajid, Ehsan, Isha, Victor, Behnam, Indrajit, Juan Carlos, Daniel, Mauricio, Fabricio, Adarsh, Felipe, Miguel, Brian, Mehrdad, Behnam, Amr, Amir, Shubha, Bharat, Mostafa, Abdullah, Badr, Mariano, Rajib, Jose, Idrees and many others. I would like to thank all my past and present

colleagues in the EMSOL lab for making it such a friendly and pleasant place to work. I would also like to especially thank Mauricio, Sumit, Isha, Juan Carlos, Daniel, and Amir for their support and inputs during my PhD Research.

I gratefully acknowledge the funding and support provided by the University of Waterloo, Ontario Graduate Scholarship (OGS), and the partners of the Smart Grid Project: Natural Sciences and Engineering Research (NSERC), Hydro One Networks Inc., IBM Corporation, and ABB Corporate Research USA.

Dedication

I dedicate this thesis to my parents, Mr. Mehboob Saghir and Mrs. Shehnaz Bano, and my husband, Jafar Hussain.

Table of Contents

List of Tables

List of Figures

List of Abbreviations

AER	All Electric Range
BEV	Battery Electric Vehicles
CD	Charge Depleting
CI	Confidence Interval
CS	Charge Sustaining
DG	Distributed Generation
DMS	Distribution Management System
DOD	Depth-of-Discharge
DOPF	Distribution Optimal Power Flow
E-REV	Extended Range Electric Vehicle
EV	Electric Vehicle
G2V	Grid-to-Vehicle
GA	Genetic Algorithms
GHG	Green House Gas
HEV	Hybrid Electric Vehicle
ILP	Integer Linear Programming
LDC	Local Distribution Company
LP	Linear Programming
LTC	Load Tap Changing
MCS	Monte Carlo Simulations
MINLP	Mixed Integer Non Linear Programming

MIP	Mixed Integer Programming
NHTS	National Household Travel Surveys
NLP	Non Linear Programming
OpenDSS	Open Distribution System Simulator
OPF	Optimal Power Flow
p.d.f.	Probability distribution function
PEV	Plug-in Electric Vehicle
PHEV	Plug-in Hybrid Electric Vehicle
PSO	Particle Swarm Optimization
SD	Standard Deviation
SRM	Sum Rate Maximization
SoC	State-of-Charge
V2G	Vehicle-to-Grid

Chapter 1

Introduction

1.1 Research Motivation

Governments' long term commitment to emission reduction targets for Green House Gases (GHGs) and air pollutants aims to reduce GHG emissions in Canada through significant new investments in green infrastructure and clean technologies. Therefore, one of the motivations for the shift towards renewable sources of energy for generation is to reduce the carbon footprint on the environment. As a result, the country's energy mix is expected to move towards less carbon intensive energy sources, with large reductions in coal and refined petroleum products, and an increase in alternative greener sources of energy [1]. Furthermore, and in tandem with GHG reductions in the electrical system, a similar trend is being incentivized in the auto industry, as transportation is a major contributor to Green House Gas (GHG) emissions, as shown in Figure 1.1, where it can be seen that 23% of Canada's GHG emission is from the transportation sector, a significant contributor, based on 2013 data [2]. Under a long-term emission reduction scenario, the share of electricity as an energy source in the transportation sector is expected to increase, which would translate to an increase in market share of Plug-in Electric Vehicles (PEVs).

The fact that PEVs can recharge their batteries from the grid means a significant

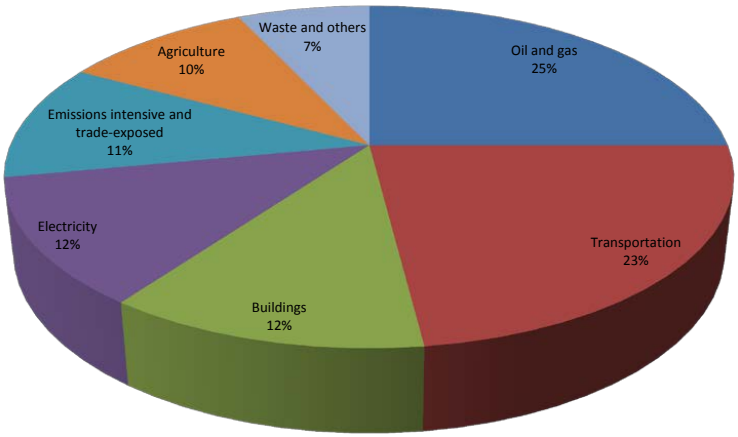

Figure 1.1: Distribution of GHG emissions by economic sector in Canada (2013).

reduction in the carbon footprint of the transport sector. A large increase in the number of PEVs, however, will also result in substantial power being drawn from the grid to recharge these vehicles, depending on the time and location of these loads [3]. Therefore, uncoordinated charging of these PEV loads, which is the current industry practice, can impact grid operation adversely, as the PEV penetration level increases [4]. Hence, in order to maintain the reliability and security of the grid, the utilities have to ensure that the grid is equipped to handle these additional loads, which have a high degree of temporal and spatial uncertainty.

The main issues which can be foreseen with the increase in PEV loads is the burden on the existing grid assets resulting in higher system peak and congestion, especially at the distribution level, if the charging is not done smartly. If a large number of PEVs start charging coincidentally, this can create new system peaks, undervoltage at the nodes or feeder overloading, and various other problems [3]. This would be a concern in residential neighbourhoods if the power delivered to PEV loads is not controlled, as most people would reach home from work in the early evening and start charging their vehicles at

about the same time. Since the peak period for a residential neighbourhood also coincides with this time window, it is important to ensure that the charging of PEV loads does not create a higher or a new peak in the system. If this happens, then infrastructure upgrades and increase in power generation will be necessary; however, this will require significant capital investment. Hence, minimizing the daily peak demand while charging PEVs is one of the objectives of this work, similar to the PeakSaver and PeakSaver Plus programs in Ontario [5]. This is based on the elastic nature of PEV loads, which facilitate control over their charging profiles. Smart-charging approaches would help in better utilizing the existing assets through coordinated charging of PEVs. Investigating mechanisms to incentivize PEV customer participation in smart charging programs is not within the scope of this work; however, the presented work could be used by technical and policy bodies in government and utilities to evaluate the impact and value of the proposed smart charging methodologies.

The distribution feeders in a conventional power system are designed to serve forecasted loads, and not PEV loads, which introduce uncertainties in addition to the increase in demand, and hence pose a challenge for the optimal operation of the grid [4]. These uncertainties are temporal and spatial in nature, arising due to the variability in arrival and departure times, initial battery State-of-Charge (SoC), number of PEVs charging, etc. [6]. At present, electricity grids are highly underutilized during off-peak hours, and are able to accommodate uncontrolled charging of PEVs at low PEV penetration levels. However, for medium-to-high PEV penetration levels, it is important to ensure efficient feeder operation through coordinated charging of the PEV loads and proper dispatch of feeders to properly account for the uncertainties. To accomplish this, on the one hand, the utility's concern of the creation of higher system peaks due to the charging of PEVs, which may result in higher operational costs and require infrastructure upgrades, should be considered. On the other hand, the needs of customers to charge their PEVs in a fast and fair manner should also be taken into account. Hence, both perspectives are considered in this work to find a balance between these two conflicting objectives, by decoupling the smart PEV charging problem into two centralized scheduling problems with different time

scales - day-ahead dispatch of taps and capacitors, and scheduling power to charging PEVs every few minutes.

1.2 Literature Review

This section presents a detailed literature review of relevant research papers in the areas of optimal operation of Smart Grids, smart charging of PEVs, and impact of PEV integration on distribution systems.

1.2.1 Optimal Operation of Smart Grids

At present, electrical grids are underutilized during off-peak hours and are able to accommodate the uncontrolled charging of low penetration of PEVs; however, for significant penetration levels of PEVs, it is crucial for utilities to plan for the optimal operation of the grid [3]. The work presented in [7] proposes a three-phase Distribution Optimal Power Flow (DOPF) modeling framework and a novel method to solve the scheduling problem by transforming the Mixed-Integer Non-Linear Programming (MINLP) problem into a Non-Linear Programming (NLP) problem. The algorithm implements an Optimal Power Flow (OPF) technique to schedule optimal hourly tap and capacitor settings for a 24-h period, while minimizing energy drawn from the substation and satisfying grid constraints. However, it does not consider PEV loads.

A modeling framework proposed in [4] considers PEV loads and aims to determine the optimal PEV charging schedule for a 24-h period, as well as tap and capacitor settings, bus voltages and feeder currents, while satisfying system operating conditions. The objective functions implemented in this work are the minimization of total energy drawn, the cost of charging PEVs, and the system losses. However, the model uses continuous taps and capacitors for quantities that are discrete in practice. It also does not consider the customer perspective in terms of fairness in charging.

The authors in [8] also investigate decentralized and centralized charging of PEVs by comparing their performance in a residential distribution system, considering the physical and operational limits of the system. This work also accounts for the variability in duration of charging, initial SoC, charging start time, residential load and location of PEVs. The centralized charging strategy proved to be more efficient in utilizing the network capacity, while satisfying operational constraints. However, the work does not consider different battery types or higher penetration levels for PEVs. A drawback of this strategy is that it resulted in a higher system peak, which is undesirable from the utility's perspective.

The next step in the realization of Smart Grids would be to move from day-ahead planning to optimizing network operation in real-time. A smart Distribution Management System (DMS) is proposed in [9], which can be used to achieve optimal network operating conditions in real-time. However, this work has not considered PEVs, which would have a significant impact on the system loading.

The authors of [10] propose a fast-response algorithm to mitigate voltage variability due to fast changes in the active power generated or consumed by distributed energy resources (renewable generation sources, PEVs, etc.), by using a loss-minimization objective function. It is assumed that conventional voltage regulation devices operate using a slower timescale (every hour) for some optimization problem, and voltage mitigation, using a distributed algorithm, is performed dynamically. However, the perspective considered in this work is utility-centric, and does not consider the consumer perspective.

Utilities adopt load management strategies to optimize network operations, which may involve conflicting aspects that are economical or technical in nature or relate to quality and reliability of service. A demand response strategy at the household level is presented in [11] to accommodate uncontrolled PEV charging while keeping the peak demand fixed. It allows customers to manage their own loads based on a maximum demand limit set by the utility. However, with increasing PEV penetration, the customer may be impacted negatively and the utility may need to adopt other system-level strategies for peak minimization.

A novel three-stage voltage deviation minimization approach is proposed in [12]. It

considers both PEVs and distributed generation sources. The maximum power deliverable to PEVs is computed in the first stage, followed by the minimization of active power curtailed by distributed generation sources in the second stage, and lastly, the minimization of voltage deviation is performed in the third stage. While this work takes into account customer satisfaction, the implicit objective of this work is to relax tap operation, and does not address peak minimization.

Based on the aforementioned shortcomings in the existing technical literature, the research proposed here aims to implement a centralized strategy for the optimal operation of feeders through day-ahead dispatch of distribution feeders, while minimizing the system peak, considering the uncertainties associated with PEV loads and feeder limits. The grid will be accurately modeled using the DOPF model approach, considering discrete taps and capacitor variables, and the customers' perspective will be taken into account, as described next.

1.2.2 Smart Charging of PEVs

Employing smart charging strategies, utilities will be able to enhance the utilization of the grid and accommodate a higher penetration of PEVs at reduced capital investments, since uncontrolled charging would cause new peaks in the system, increasing operational costs for utilities. Thus, there are several works in the literature that address dynamic or real-time charging of PEV loads in distribution systems using a centralized or decentralized approach.

In [13, 14, 15, 16, 17, 18, 19, 20], the authors take the vehicle perspective only, ignoring the grid; hence, the practical feasibility of the proposed algorithms for centralized and decentralized charging of PEVs from a grid perspective cannot be analysed or verified. The authors in [21] propose to enhance system asset utilization by minimizing variations in the system load profile considering PEV loads at different penetrations, accounting for the variation in initial SoC of the battery and charging start time. However, this optimization model does not include grid or operating constraints, which makes it difficult to evaluate

the feasibility of the results; it also does not consider a mix of different PEV battery sizes. A dynamic tariff scheme is used in [22], which proposes a charging algorithm which aims to minimize charging costs and avoid grid congestion, from the day-ahead planning perspective. This, however, does not take into consideration the spatial uncertainty associated with PEV charging, different penetration levels, or the different types of PEVs, but it does consider the grid constraints.

The decentralized charging strategies proposed in [23] aim to schedule PEV loads in real-time and in a fair manner, while considering the operational constraints of the grid; this charging strategy ensures fairness in the frequency in which PEVs are allowed to charge from the grid, but not in terms of the energy they receive, and has a high communication overhead. The decentralized charging strategy proposed in [24] for real-time PEV charging is fast and robust, but this is possible due to simplified power flow equations ignoring the resistance of the distribution feeders, thus linearizing the constraints.

In [4, 25, 26, 27, 28, 29, 30, 31], centralized strategies to charge PEVs dynamically are proposed. However, [25] uses a computation timeframe of 1 h, which is not fast enough for dynamic charging of PEVs, as this would mean that if a PEV arrives after the load profile for the next hour has been computed, it would have to wait up to an hour before it is able to charge from the grid; in addition, the uncertainty associated with initial battery SoC is not considered in this work. In [26], a cost minimizing strategy benefiting the utility alone is proposed, but does not consider fairness in charging for all PEVs, while in [27], fair PEV charging leads to an increase in system peak, which is not favourable to the utility. A joint Optimal Power Flow (OPF) and PEV charging approach is proposed in [28]; however, the uncertainties associated with PEVs are not considered, which is an important factor in real-time charging of PEVs. In [4] and [29, 30, 31], the authors consider the uncertainty associated with PEVs, but [29] only considers the randomness in the arrival times of PEVs, and proposes a priority-based charging scheme that does not ensure fairness in charging. In [31], the dynamic nature of the PEVs is considered while maximizing the power given to PEVs, but a simplified DC grid model is used to linearize the constraints and reduce computational burden.

A two-stage optimization model is proposed in [32] to schedule charging of PEVs, where the power margins are computed in the first stage, and the charging profiles are then computed in the second stage. The limitation of this work is that it does not consider the uncertainties associated with PEVs, and assumes the arrival times and energy required by the vehicles are known through forecasting techniques. In addition, the optimized feeder load profile has a new system peak, even with unused capacity in the off-peak hours.

In order to encourage change in customer behaviour, charging schemes would be most effective if they were associated with pricing incentives by the utilities. From the customers perspective, they would be interested in minimizing the costs associated with charging their PEVs, while the utilities would want to minimize their operating costs. Both these perspectives are addressed in [33], where generation and PEV charging costs are optimized using an OPF model; however, it only assumes a single PEV at each node and no variation in charging start time or initial SoC. Another limitation of this work is that it is topology dependent and can only be solved if the topology meets a specific condition.

Considering the aforementioned papers, the proposed approach uses a centralized approach to provide fair charging of PEVs, while considering PEV-related uncertainties, namely arrival and departure times, initial battery SoCs, and the number of charging PEVs. In addition, an accurate and realistic model of an unbalanced three-phase feeder is used, and the utility's standpoint is also taken into account.

1.2.3 PEV Impact Studies on Distribution Systems

The impact of PEVs on distribution systems at high penetration levels is a concern for utilities with regard to their effect on network equipment, system upgrades, system stability, voltage profiles, reliability, security and quality of service to the customers. This requires detailed and realistic analyses of feeder operation, considering uncertainties associated with PEVs and base load profiles.

The impact of Plug-in Hybrid Electric Vehicles (PHEVs) on the power grid is studied

in [34], using statistically analysed data based on the National Household Travel Surveys (NHTS) to build aggregate load curves for the PHEVs. However, this paper does not consider the system or its operating limits, and hence provides limited insight into the impact of PHEVs on the power grid. A novel GA-based method is presented in [35], which aims to maximize PEV penetration and allocate Distributed Generation (DG) to mitigate the impacts of high PEV penetration. It uses Monte-Carlo simulation to generate an annual PEV energy consumption model for uncontrolled charging, which accounts for the diversity in usage, battery capacity, driver habits, and effects of ambient temperature. This work, however, in spite of using accurate and detailed modeling of PEV parameters to maximize PEV penetration, only considers an uncontrolled charging scenario.

One possible impact of higher PEV penetrations would be the need for system upgrade as well as the increase in system losses in distribution systems, due to increased loading. An approach to evaluate the impact of PEV penetration from this perspective is presented in [36], which is used to analyze two real systems. However, it uses a deterministic model with PEV parameters defined in the scenarios and driving patterns assumed in this work. Another limitation of this work is that it does not consider the base load growth over the planning period of 2020-2050.

In [37], the authors propose a methodology to determine the loading profile due to charging of EVs from the grid, while considering a mix of different battery types and variation in charging start times and initial SoCs of the PEVs. This loading profile is applied to four charging scenarios to study its impact on the grid. However, the physical and operational constraints of the grid are not considered in the model.

A probabilistic power flow approach is presented in [38] to analyze the impact of PHEVs on the grid by developing a single PHEV charging profile, which can be modified for different types of PHEVs, based on their market share, All-Electric Range (AER), battery capacity, distance travelled, energy consumption per mile, energy requirement, charging current, and charging time. Queuing theory is used to develop an aggregate charging profile for multiple PHEVs using the single profile for charging stations and residential

areas; however, it only considers the case of uncontrolled charging and there is no analysis on the effect of this charging scenario on system peak. Also, using a single profile for multiple PHEVs is not an accurate assumption, as it does not consider the uncertainties of various PHEVs separately.

In [39], the authors compare the long-term impact of controlled versus uncontrolled PEV charging on distribution systems in terms of cost of energy losses and reinforcement of network assets, minimizing energy losses and combined peak load of EV and the household. This work uses transportation data to develop EV profiles based on driving patterns; however, it normalizes the aggregate of these profiles to the level of a single EV, which is then multiplied by the number of EVs to get the aggregate demand profile, which eliminates the variability in energy requirement of different types of EV batteries. It also does not consider the possibility of clustered growth of the EV population.

Based on the aforementioned papers, the proposed work aims to account for uncertainties associated with PEV load profiles, and thus optimally operate distribution feeders, considering the perspectives of utility and the customer, to minimize the impact on the grid from PEV charging.

1.3 Research Questions

Considering the spatial and temporal uncertainties associated with PEV loads and the challenges of operating the distribution feeder in an optimal manner, while charging these highly stochastic loads in a fair and efficient manner, the following research questions were defined:

- Are conventional feeder control methods for voltage regulation adequate to operate the distribution feeders in an optimal manner, with the increase in PEV market share?

- How significant are the benefits, in charging and feeder operation, of using a feeder control schedule, that accounts for PEV uncertainty, compared to a heuristic approach and the standard industry practice?
- Is it possible to implement proportional fairness in charging PEV loads, using a detailed AC model for a three-phase unbalanced distribution feeder, in quasi-real-time? How fast can these computations be performed?

These questions led to the problem formulation, assumptions used, and the development of the proposed smart charging approach in this thesis.

1.4 Research Objectives

From the literature review and discussions presented in the previous sections, the main research objectives of the present research are as follows:

- Develop an optimization framework for the optimal operation of primary distribution feeders and smart charging of PEVs, considering feeder characteristics and limitations, as well as the uncertainties associated with PEVs. This framework will allow for consideration of both the utility (peak minimization) and the PEV customer (fairness in charging), interests that are conflicting in nature.
- Develop an approach to estimate the mean daily feeder peak demand and the most likely hourly feeder control schedules, considering various PEV uncertainties, for significant PEV penetration levels.
- Develop a model to address the perspective of PEV customers, by computing the maximum power that can be given to aggregate PEV loads in a fair manner, without exceeding a peak demand value or feeder operational limits. The proposed approach will be benchmarked against a popular sensitivity-based heuristic approach and current industry practices to compare its performance with respect to PEV charging.

- Validate the proposed technique using the IEEE 13-bus test feeder as well as a real primary distribution feeder.

1.5 Thesis Outline

The remainder of this thesis is structured as follows:

- Chapter 2 briefly discusses the background topics pertaining to the research carried out in this thesis. Thus, a brief description of the DOPF model is presented first, followed by some basic concepts related to PEVs. Thereafter, a brief overview of mathematical programming models and modeling tools is provided, followed by a summary of the main concepts of Genetic Algorithms (GA) used in this work. Finally, a brief outline of the non-parametric Bootstrap technique, utilized here to efficiently deal with uncertainties, is presented.

- Chapter 3 presents the first step of the proposed approach, which determines the most likely day-ahead feeder control settings, while considering PEV uncertainties. First, the problem formulation for the proposed approach is presented; next, the methodology used in the implementation of the Bootstrap estimation, and the GA-based optimization model, that allows accounting for PEV uncertainties, is discussed. Finally, a description of the test systems used in this thesis, as well as the assumptions made, are presented, followed by a presentation and discussion of the results.

- Chapter 4 presents the second step of the proposed approach, which computes fair PEV charging schedules with minimum impact on the distribution feeder. First, the optimization approach is described, followed by a brief description of the current industry practices for feeder voltage regulation and PEV charging, which is used as a benchmark for comparison purposes. Next, a popular heuristic approach is presented, which is used as the other benchmark to evaluate the performance of the proposed technique. Finally, the results for the fair charging of PEVs for the test

feeders used in this thesis are discussed and analyzed, comparing them against current utility practices and the heuristic approach, showing this technique's feasibility and advantages.

- Chapter 5 summarizes the main research contributions, and identifies some directions for future research.

Chapter 2

Background

Nomenclature

Indices

N	Total number of nodes in the system
LN	Number of load nodes in the system
T	Number of time intervals
B	Number of feeders in the system
n, p	Node indices, representing feeder node and phase
q	Iteration index
b	Feeder index
t	Time interval index
i	LTC tap index
j	Switched capacitor index
l	PEV index
k	Number of elements in the original sample and Bootstrap replicates
M	Number of Bootstrap replicates

Functions

f	Objective function
g	Functions representing equality constraints
h	Functions representing inequality constraints
$\hat{F}$	Empirical probability distribution of original sample
F_B	Bootstrap estimate of sampling distribution of the desired statistic

Parameters

$\underline{tap}_i$	Lower limit for LTC tap
$\overline{tap}_i$	Upper limit for LTC tap
$\overline{cap}_j$	Upper limit for switched capacitor [kVAr]
$\overline{\lvert I \rvert}_b$	Current carrying capacity of feeder [A]
$\underline{V}_n$	Minimum voltage limit [p.u.]
$\overline{V}_n$	Maximum voltage limit [p.u.]
P_n^G	Real power generation [kW]
Q_n^G	Reactive power generation [kVAr]
P_n^D	Real power demand [kW]
Q_n^D	Reactive power demand [kVAr]
$\lvert Y \rvert_{np}$	Magnitude of admittance [S]
Y	Phasor admittance
θ_{np}	Angle of admittance [rad]
nev_n	Number of PEVs
Mcp	Maximum limit of single charging point [kW]
$Epev_{l,n}$	Battery capacity of single PEV load [kWh]
$Epev_n$	Battery capacity of aggreate PEV load [kWh]
$SoC_{l,n}^f$	SoC of single PEV load at the end of charging period [%]
$BCap_l$	Battery capacity of single PEV [kWh]
T_n^{Arr}	Arrival time of aggregate PEV load

T_n^{Dep}	Departure time of aggregate PEV load
ω	GA population size
cr	Crossover rate
mr	Mutation rate

Variables

x, y	Decision variables
δ_n	Voltage angle [rad]
$\|I\|_b$	Magnitude of feeder current [A]
$\|V\|_n$	Magnitude of node voltage [p.u.]
V_n	phasor node voltage [p.u.]
I_n^{inj}	phasor current injection [A]
P_n^{pev}	PEV load [kW]
$SoC_{l,n}^i$	SoC of single PEV load at the beginning of charging period [%]
X	Original sample
X^*	Bootstrap replicate
σ_B	Bootstrap standard deviation
${\sigma_B}^2$	Bootstrap variance
$\hat{T}$	Statistic of interest for original sample
T_M^*	Statistic of interest for Bootstrap replicate

2.1 Introduction

This chapter presents a background review of the main concepts and tools pertaining to the research presented in this thesis. First, a brief description of the DOPF model, including objective functions and constraints, is presented in Section 2.2, followed by some basic concepts related to PEVs, such as their types, charging levels, charging schemes,

their basic design concepts, and battery charging principles in Section 2.3. Section 2.4 provides an overview of mathematical programming and modeling tools relevant to the present research, and Section 2.5 briefly summarizes the main concepts of GA used to solve the resulting optimization problems. Finally, Section 2.6 provides an overview of the non-parametric Bootstrap technique, and computation of confidence intervals, variance, and standard deviation, used to efficiently deal with PEV uncertainties.

2.2 DOPF Model

An important modeling framework used by power engineers for optimal operation and planning of power systems is the OPF, which optimizes an objective function to find the optimal settings of a given network while satisfying system operating and security constraints. In general, the OPF problem can be expressed in the following form:

$$\min \quad f(x) \tag{2.1}$$

$$\text{s.t.} \quad g(x) = 0 \tag{2.2}$$

$$h(x) \leq 0 \tag{2.3}$$

$$x \geq 0 \tag{2.4}$$

where x represents a vector of decision variables; $g(x)$ describes the power flow equations of the system and other relevant equality constraints; and $h(x)$ represents a vector of nonlinear functional and control variables, with lower and upper bounds characterizing the operational limits of the system, such as transformer tap, load curtailment, node voltage, and feeder current limits. The objective function $f(x)$ may be consumer-centric, utility-centric, or a combination of both perspectives, such as minimizing system losses, installation cost of new capacitors, number of control actions, etc.

The OPF problem in a distribution system is referred to as a DOPF [7]. In this work, a DOPF is used to optimize feeder controls, i.e., taps and capacitors, for daily peak

minimization to perform day-ahead dispatch of feeders considering PEV charging control and uncertainties. Then, the fair scheduling of PEV charging is performed periodically (every few minutes) at each node, so as to not exceed the optimal daily feeder peak demand obtained for the feeder dispatch, and to not violate the feeder operational limits.

2.2.1 Distribution System and Components

The distribution system is the final tier in the power delivery network and connects the transmission network to the customers' electric utility connection points, as illustrated in Figure 2.1. The distribution substation is the point where the distribution system begins, which may be fed directly through a transmission line, or one or more sub-transmission lines [40]. Distribution systems operate in the voltage level range of 4.16 to 34.5 kV, and usually have a radial configuration.

Distribution systems are usually unbalanced, i.e., the loads on each phase, as well as the number and spacing of phase conductors may vary. Power flow calculations for a distribution system using conventional power flow methods such as Gauss-Siedel and Newton-Raphson have shown poor convergence because of the difference in topology and higher R/X ratio of distribution systems. Hence, techniques such as forward-backward sweep may be applied instead. In this work, the distribution feeder is modeled in OpenDSS [42], which performs power flow computations using a novel iterative power flow algorithm, as explained in [43].

The components of the distribution system include [40]:

- *Distribution substation*: This is the junction where the sub-transmission system connects to the primary distribution network. Here, the voltage is stepped down from the sub-transmission voltage to distribution system voltage level. The substation houses power transformers, voltage regulators, monitoring equipment, and switchgear.
- *Feeders*: Starting from the distribution substation, overhead lines or underground

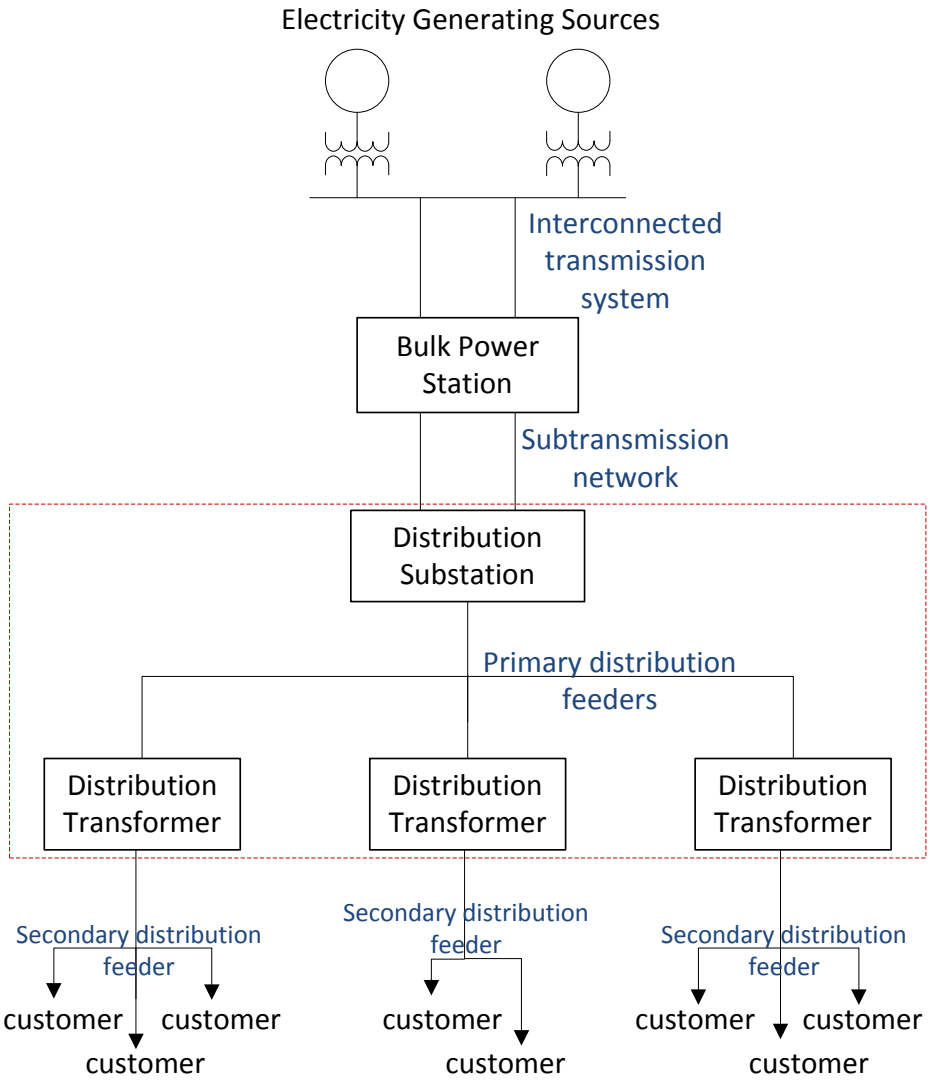

Figure 2.1: Power delivery network from generation to customer [40, 41].

cables transport the electric power, usually radially, to the load centers. These feeders can constitute one or more circuits that are three-phase, two-phase, or single-phase.

- *Distribution transformers*: These transformers step down the voltage level from the primary distribution level to the required voltage level, depending on the type of cus-

tomer; for residential services, the rated voltage is 120/240 V, and for commercial and small industrial customers, the rated voltage may be up to 480 V. As a result, these transformers are sized based on the input voltage and the desired output voltage.

- *Control devices*: Ensuring the reliability and quality of electric power at the customer level is done through voltage regulation at the distribution substation or along the distribution feeder. LTC transformers and switched capacitors help in voltage regulation by keeping the voltage deviation at the buses within 5% [44]. This means that the voltage magnitudes at the load buses should be maintained between 0.95 and 1.05 p.u. The LTC transformer has the capacity to correct the sending end voltage at the substation by 10%, in increments of 5/8 % for a 32-tap transformer.

  Line drop compensation is a technique used to control the changing of taps in a regulator using a compensator circuit, which is a scaled representation of the feeder circuit, and potential and current transformers at the feeder level. The R and X values in the compensator circuit are scaled representations of the feeder impedance, and the voltage at the regulation point is represented by the equivalent voltage drop across the relay in this circuit, which is then used to determine the regulator tap position, thus maintaining the voltage at the regulation point within limits.

  Switched capacitors are also used for reactive power support, in addition to voltage regulation and may be single-phase, two-phase or three-phase capacitor banks connected in wye or delta configurations. Unlike fixed capacitors, these capacitors can help improve the voltage profile by providing reactive support in kVAr blocks. For example, a 5 block capacitor with 50 kVAr blocks has a total kVAr capacity of 250 kVAr and can be dispatched in increments of 50 kVAr.

- *Protection devices*: Devices such as switches, circuit breakers, and fuses are used to enhance system security and reliability. They also protect the equipment from damage due to overcurrent during faults. In addition, tie switches and line sectionalizers are used to reconfigure the network in case of faults.

- *Loads*: Loads differ based on customer type, i.e., residential, commercial, or industrial. Customer loads may be modeled as constant impedance, constant current, constant power, or a combination of them, based on their behaviour with respect to voltage.

2.2.2 Objective Functions

The objective function optimized in the OPF model may be, for example, any one or a combination of the following [6]:

- Cost of operation or increase in cost.
- Deviation from desired settings.
- Real power losses.
- Cost of load curtailment.
- Number of control operations.
- Installation cost of new capacitors or reactors.
- Cost of MVAr supplied.
- Total emissions.

In this work, the feeder controls, i.e., taps and capacitors, are first optimized for daily peak demand minimization to perform day-ahead dispatch of feeders considering PEV charging control and uncertainties. Peak demand minimization is important from the utility perspective due to increase in demand from charging PEVs, and incentive-based programs such as Ontario's PeakSaver and PeakSaver PLUS initiatives [5]. These initiatives are meant to reduce peak demand in power networks to alleviate grid capital investments in generation, transmission, and distribution equipment. The fair scheduling of PEV charging

is then maximized periodically (every few minutes) at each node, so that demand does not exceed the optimal daily feeder peak demand obtained for the feeder dispatch, and does not violate the feeder operational limits.

2.2.3 DOPF Constraints

- *Equality Constraints*: The equality constraints may comprise of the power balance equations for real and reactive power, which govern the flow of power through the network [6]:

$$P_n^G - P_n^D = \sum_{p=1}^{N} |V|_n |V|_p |Y|_{np} \cos\left(\theta_{np} + \delta_p - \delta_n\right) \; \forall \; n = 1, .., N \tag{2.5}$$

$$Q_n^G - Q_n^D = -\sum_{p=1}^{N} |V|_n |V|_p |Y|_{np} \sin\left(\theta_{np} + \delta_p - \delta_n\right) \; \forall n = 1, .., N \tag{2.6}$$

where P_n^G and Q_n^G represent the real and reactive generation at node n, respectively; P_n^D and Q_n^D represent the real and reactive demand at node n, respectively; $|V|_n$, $|V|_p$ represent the voltage magnitudes at node n and p, respectively; $|Y|_{np}$ represents the magnitude of admittance between nodes n and p; θ_{np} represents the angle of admittance between nodes n and p, and δ_n, δ_p represent the voltage angles at node n or p.

In this work, the equality constraints based on the approach used by the power flow program OpenDSS [42], which uses the following phasor current injections I_n^{inj} and voltages V_n at each node:

$$\left[I_n^{inj}(V_n{}^q)\right] = \left[Y\right]_{nxn} \left[V_n{}^{q+1}\right] \quad \forall \; n = 1, .., N \tag{2.7}$$

to compute the feeder currents and node voltages, where q is an iteration index starting at q=0, as explained in [43].

- *Inequality Constraints*: In this work, inequality constraints include the physical limits representing the physical bounds of the system, such as Load Tap Changing (LTC) transformer taps, switched capacitors, and charging point capacity, which cannot be violated, as follows:

$$0 \leq Ppev_n \leq Mcp\ nev_n \quad \forall\ n = 1, 2, .., LN \tag{2.8}$$

$$\underline{tap}_i \leq tap_i \leq \overline{tap}_i \quad \forall\ i \tag{2.9}$$

$$0 \leq cap_j \leq \overline{cap}_j \quad \forall\ j \tag{2.10}$$

The power flow computations performed using OpenDSS also incorporate the transformer taps and switched capacitors in the model using the appropriate admittance matrices. Inequality constraints also include the following node voltage and feeder current limits representing the operating limits of the system:

$$\underline{V}_n \leq |V|_n \leq \overline{V}_n \quad \forall\ n = 1, 2, .., LN \tag{2.11}$$

$$0 \leq |I|_b \leq \overline{|I|}_b \quad \forall\ b = 1, 2, .., B \tag{2.12}$$

2.3 Plug-in Electric Vehicles

PEVs have the potential to reduce the carbon footprint of the transportation sector due to higher energy efficiency and reduced fossil fuel usage compared to conventional vehicles. In addition, PEVs are capable of providing ancillary services to the grid in vehicle-to-grid (V2G) mode; however, the present work only considers the grid-to-vehicle (G2V) mode in which the PEVs charge their batteries from the grid.

2.3.1 Types of PEVs

PEVs comprise of vehicles with electric and hybrid-electric power trains, specifically, Plug-in Hybrid Electric Vehicles (PHEVs), Extended Range Electric Vehicles (E-REVs) and

Battery Electric Vehicles (BEVs) [3]. PHEVs can be considered as the intermediate stage in the transition of Hybrid Electric Vehicles (HEVs) to EVs. HEVs have a battery storage system to complement the conventional powertrain, with this technology being able to channel a significant amount of the vehicle's kinetic energy lost while braking to the energy storage system through regenerative braking, therefore, reducing the overall consumption of fuel. On the other hand, PHEVs include a unidirectional on-board charger in addition to the battery, and thus, can be recharged by plugging into the grid [45].

PHEVs have the advantage of two on-board energy sources, so that the vehicle can utilize the battery for travel, and if the battery gets depleted beyond a certain SoC during a trip, it can switch to the internal combustion engine. The distance that the PHEV covers using the battery alone is known as the AER. Thus, PHEV 20 represents a PHEV with an AER of 20 miles. Similarly, PHEV 40 and PHEV 60km would represent AERs of 40 miles and 60 km, respectively.

The BEV is similar to the PHEV, except that it has only one source of energy, which is the battery, and they are also recharged from the grid. It is solely dependent on battery, and thus the AER of a BEV is restricted by the battery size; as a result, the size of the battery in a BEV is usually larger than that in a PHEV, as it must be sized to meet all of the technical specifications of the vehicle, except range. The BEV has an all-electric powertrain while the PHEV has both electric and conventional powertrains, differing in complexity.

E-REVs are similar to the BEV in that they also have an all-electric powertrain. However, on longer trips when the battery on its own would not be sufficient, gasoline power generators recharge the battery [3].

2.3.2 Charging Levels

It is estimated that most of PEV battery charging will be done at home over several hours through the night using power outlets provided in residential garages. The PEV will most

likely be used during the day to commute in the city for work or other errands, making after-office hours the ideal time for charging. The time it takes to charge the PEV battery completely depends on the charging level employed [3, 45]:

- *Level 1 (slowest)*: This charging level uses the standard 120 V, single-phase ac electrical outlet found in residential garages, with a maximum continuous current in the range of 12-16 A. No new installation is required for this charging level, and hence, the customers do not face any financial obstacles in adopting this charging method. However, depending on the PEV battery size, it may take 8-30 hours to charge the battery completely. This charging rate may affect the battery life and performance negatively for some battery systems. Level 1 charging may be the typical choice for charging at home or the office.

- *Level 2 (faster)*: A 240V, single-phase ac supply, with a maximum continuous current in the range of 32-70 A is used for this charging level. To avail this charging level option in a residential garage, an upgrade is most likely required, which translates into an initial setup investment by the customer. For the safety of users, this level also requires grounding and ground-fault protection. In addition, a no-load make/break interlock is required so that the vehicle cannot start while the battery is charging, as well as a safety breakaway for the cable and connector. Using this charging level, a PEV battery may recharge completely in 2-6 h, depending on the battery size and type. This charging level may be adopted for charging at private or public outlets.

- *Level 3 (fastest)*: This charging level is still in the development stage; however, it is expected to have the ability to recharge 50% of an EVs battery capacity within 10 minutes, operating with a 480 V or higher three-phase circuit. There are several concerns with this charging level. Most of the PEVs have a single-phase on-board charger; however, to charge at this level, an off-board 3-phase charger equipped with a regulated ac-to-dc converter will be needed, which would be an added cost. The power drawn by this level is quite high (50 -100 kW), requiring upgrade of most

utility transformers in residential and some commercial areas. The typical use of this charging level would be commercial, most likely in charging stations.

2.3.3 Charging Schemes

- *Uncoordinated Charging*: This scheme does not involve any schedule to charge PEVs; thus, the vehicles start charging immediately after they are plugged in. This, however, is not the best utilization of the grid and could overload the transformers and feeders, since PEVs would most likely be charged after the customer arrives at home in the evening, which coincides with peak demand for residential areas, thus adding to the system peak [4].

- *Coordinated Charging*: To maximize PEV penetration and optimize the utilization of the grid without threatening its security, coordinated charging schemes are required. This is referred to as "smart" charging and could involve charging PEVs during off-peak hours and distributing the charging schedule over a longer period of time, so as to utilize the grid more efficiently. To implement smart charging, a bidirectional communication system is needed to facilitate exchange of information between the PEV and the LDC. Pricing incentives may be effective in encouraging customers to adopt smart charging strategies, which would help in reducing charging costs [4]. This work also uses coordinated charging to achieve a specific objective, and assumes that a bidirectional communication network is already in place.

2.3.4 Basic PHEV Design Concepts

Battery SoC in a PEV is synonymous to the fuel gauge in a conventional vehicle. Battery SoC is expressed in percentage; for example, a fully charged battery would be at 100% SoC, and a completely depleted battery would be at 0% SoC. Battery SoC represents the current state of the battery in terms of the amount of charge remaining for use by the PEV. In

this work and without loss of generality, only one type of PEV has been considered, i.e., a mid-size sedan PHEV 30km, with a battery capacity of 8.14 kWh. The battery capacities for different types of PHEV 30km are listed in Table 2.1 [3].

Table 2.1: Battery capacity of different types of PHEV 30km.

Vehicle Type	**Battery Capacity [kWh]**
Compact sedan	6.86
Mid-size sedan	8.14
Mid-size SUV	10.29
Full-size SUV, van, pickup truck	12.43

There are two operating modes for a PEV, i.e., charge-depleting (CD) and charge-sustaining (CS) modes. In the former, the PEV derives its power from the battery, while in the latter, fuel is the source of energy used by the vehicle after the battery SoC has reached its minimum level. The distance the PEV travels during the day will gradually deplete the battery in CD mode until the minimum battery SoC level, after which the PEV switches to CS mode. This total distance that the PEV covers in CD mode is the AER of the vehicle. Depth-of-Discharge (DOD) refers to the percentage of battery capacity for which the PEV can operate in CD mode; most batteries have a suggested maximum DOD level for their optimal utilization. In this work, a maximum DOD of 70% and a minimum battery SoC of 20%, below which the PEV switches to CS mode, are assumed [46, 47, 48].

At the end of the day, the PEV is connected to the grid for charging, and thus the corresponding SoC is the starting point for the charging cycle. Hence, the energy required by each PEV $Epev_{l,n}$ at node n from the grid can be computed as follows:

$$Epev_{l,n} = \left(SoC^{f}_{l,n} - SoC^{i}_{l,n}\right) Bcap_{l} \quad \forall\, n = 1, .., LN, \ \forall\, l = 1, .., nev_{n} \tag{2.13}$$

In the first step of the proposed approach, the initial battery SoC of the aggregated PEV

load SoC_n^i at node n is assumed to be a random variable following an appropriate p.d.f., while the final battery SoC of the aggregated PEV load SoC_n^f is required to be at least 90% at the end of the charging period.

2.3.5 PEV Battery Charging

The rate of charge depletion of each PEV depends on its AER and the efficiency of the electric drive. In addition, because of the limit on DOD of the battery, the usable energy of the battery is less than the battery capacity. For example, the mid-size sedan PHEV 30km has a battery capacity of 8.14 kWh, but as a result of the 70% DOD limit, the usable battery energy is 5.7 kWh. In this work, aggregated PEV loads are considered at the load nodes,where nev_n represents the number of PEVs considered at load node n, and thus the initial battery SoC SoC_n^i corresponds to aggregated values of the actual PEVs at node n. Therefore, the energy delivered to the aggregate PEV load $Epev_n$ at node n is given by:

$$Epev_n = \sum_{t=1}^{T} P_{n,t}^{pev} \quad \forall\ n = 1, .., LN \tag{2.14}$$

The goal is to deliver the energy defined by (2.14) over the charging period T_n^{Arr} to T_n^{Dep}, which are random variables following appropriate p.d.f.s in the first step of the proposed technique. With this consideration, the power delivered to the charging PEVs at each load node gives the aggregated PEV charging load profile for that node over the charging period. The power delivered to each aggregated PEV load is limited by:

- *System Operating Limits*: The voltage limits at each load node and the feeder current limits.
- *Charging Point Limit*: The maximum power that can be delivered to the aggregated PEVs determined by the charging level available to these loads.

Given the initial battery SoC of a single or aggregated PEV load, and assuming that the battery will be fully charged at the end of the charging period, there are two ways to

determine the charging schedule of this PEV load: power scaling and time scaling. The power scaling (constant time) method determines the power delivered to each aggregated or single PEV load during each hour for the duration of the charging period. The time scaling (constant power) method uses the maximum power delivery capacity of the charging point; thus, it delivers the maximum power allowed by the charging point every hour, until the battery is recharged completely [49].

Table 2.2 provides an example to illustrate the aforementioned charging methods. Thus, for a charging schedule where the initial battery SoC is 0% and the final battery SoC is 100%, the power delivered to the PEV each hour is the maximum allowed by the charging point capacity for both methods. In this example, charging Level 1 is used, which means the power delivered is 1.4 kW. At this rate, the PEV battery is charged at constant power for the first four hours, and the remaining battery 1.26 kW is provided in the fifth hour. On the other hand, if the initial and final SoC difference is 70%, in the time scaling method, the battery is charged at the maximum power allowed by the charging level, i.e., 1.4 kW, for the first three hours; thus, the remainder of the battery is charged at 0.6 kW in the fourth hour. In the power scaling method, the SoC difference scales the power delivered to the battery each hour by multiplying this difference with the maximum power delivered; thus, the battery is charged at 0.98 kW for the first four hours and at 0.88 kW in the fifth hour.

2.3.6 Optimal PEV Dispatch Techniques

Optimal PEV dispatch techniques may be classified based on the type of control used, the scheduling timeline used, as well as the objective to be achieved [50]. Centralized (at the aggregator or utility level) or decentralized (individual electric vehicles) scheduling of PEV loads falls under the former category, where the control schemes differ based on the scheduling entity. Centralized schemes are better for operating feeders under optimal conditions [4]; however, decentralized schemes have the advantage of robustness in some scenarios [51, 52, 53, 54, 24].

Table 2.2: Comparison of time scaling and power scaling for compact sedan PHEV 30km charging at Level 1.

$SoC^f - SoC^i$	**Scaling**	**Power delivered during hour** k **[kW]**					**Total**
		P_1^{pev}	P_2^{pev}	P_3^{pev}	P_4^{pev}	P_5^{pev}	**kWh**
100%	Power & time	1.4	1.4	1.4	1.4	1.26	6.86
70%	Power	1.4*0.7=0.98	0.98	0.98	0.98	0.88	4.8
	Time	1.4	1.4	1.4	0.6	0	4.8

Day-ahead or dynamic (real-time or periodic) scheduling of PEV charging falls under the scheduling timeline dispatch techniques. Day-ahead scheduling of PEV loads are based on probabilistic models deriving information from driving patterns and behaviour. However, this approach is not robust, given the constantly evolving behaviour of consumers and their driving patterns; this is accounted for in dynamic scheduling of PEV charging [55]. Finally, in the context of objectives to be achieved, dispatch of PEVs may be used with the objective to balance the load, reduce congestion, or minimize costs [50].

The work presented here decouples the fair PEV charging problem into two centralized scheduling problems with different time scales, i.e., a day-ahead dispatch of feeder controls that minimizes daily peak demand from a utility perspective, and fair scheduling of PEVs from a customer perspective, using a time scale of a few minutes.

2.4 Mathematical Programming

Optimization models have numerous applications in almost every area, as they aim to solve any given problem in an optimal manner. These models describe the problem in a mathematical form using equations, also known as constraints, to relate outputs and inputs. The objective function describes the function to be optimized, i.e., minimizing or

maximizing certain function. The constraints of the model define the search space of the feasible region.

With larger and more complicated models these days, it is important to determine the appropriate algorithms and methods to solve them [56]. Thus, optimization models are classified into different categories based on the data type of decision variables, the objective function, and the type of constraints, which determine the solution techniques to be used, as discussed next.

2.4.1 Linear Programming [57]

A mathematical model which optimizes a linear objective function subject to linear constraints (equality or inequality), and has continuous variables is called a Linear Programming (LP) problem. The feasible region in an LP model is defined by the area enclosed by the constraints, and the decision variables are continuous, with the optimal solution, if any, being given by one or more extreme points in the feasible region. An LP problem can be stated as (2.1)-(2.4), where $f(x)$ is a linear objective function to be minimized, $g(x)$ represents linear functions describing the equality constraints, and $h(x)$ represents linear functions describing the inequality constraints.

To solve an LP model, the simplex method is one of the most commonly used methods. By expressing the LP problem in a standard format, the simplex method finds the optimal solution starting at any extreme point and moving through the corner points along the boundary of the feasible region in the direction of improvement. However, with large number of variables, the simplex method requires large number of iterations; in this case, interior point methods are preferred, as they are known to converge to the optimal solution in less number of iterations. Unlike the simplex method, interior-point methods generate points that lie inside the feasible region.

2.4.2 Non-Linear Programming [57]

A mathematical model which optimizes an objective function subject to constraints where either the objective function or constraint(s) or both are non-linear, and has continuous variables is a NLP model. Thus, in (2.1)-(2.4), $f(x)$ is a linear or non-linear objective function to be minimized, $g(x)$ represents linear or non-linear functions describing the equality constraints, and $h(x)$ represents linear or non-linear functions describing the inequality constraints. Quadratic programming is a special case of NLP, where the objective function has a quadratic form and the constraints are linear. One of the challenges with solving NLP models is the possibility of converging to a local optimum instead of a global optimum.

First-order methods such as steepest descent method determine the search direction using the first order derivatives of the equations. Even though this method has high accuracy, it may be slow to converge because of the zigzag nature of the search direction; the conjugate gradient method tries to correct for this zigzagging problem. Second-order methods such as Newton's method work with function values, first-order and second-order partial derivatives (Hessian matrix) of the constraints, and converge fast when in the vicinity of a local optimum. The disadvantage of Newton's method is that it is computationally expensive to compute the Hessian matrix and its inverse, and the search would fail in case of a singular Hessian matrix [58].

2.4.3 Mixed Integer Nonlinear Programming [59]

LP problems with only discrete variables, known as Integer Linear Programming (ILP) problems, are generally more difficult to solve than LP problems. This is because the extreme points of the feasible region no longer guarantee optimality, as these points may or may not be integers. They employ different techniques such as branch-and-bound or branch-and-cut methods, which involve solving multiple iterations of LP relaxations of the ILP problem.

NLP problems, where some variables are discrete and others are continuous, are referred

to as MINLP problems, and can be expressed as follows:

$$\min \quad f(x, y) \tag{2.15}$$

$$\text{s.t.} \quad g(x, y) = 0 \tag{2.16}$$

$$h(x, y) \leq 0 \tag{2.17}$$

$$x \geq 0 \tag{2.18}$$

$$y \in \mathbb{Z} \tag{2.19}$$

For example, the variables representing hourly LTC tap and capacitor settings are discrete in practice, while the variables representing the charging rate of aggregated PEV loads at the load nodes are continuous. Hence, in this work, the optimization model used in the first step is an MINLP problem, while the optimization model in the second step simplifies to an NLP problem, as a result of the day-ahead dispatch of the feeder in the first step.

MINLP problems are difficult to solve due to the added complexity resulting from the combinatorial nature of Mixed Integer Programming (MIP) problems, and the difficulty in solving non-convex NLP problems. There are various techniques which are capable of solving the MINLP problem and may be classified into:

- *Conventional optimization methods*: Branch-and-Cut, Outer Approximation, Generalized Bender's Decomposition, and Branch-and-Bound methods are popular conventional optimization techniques that have been explored extensively to solve MINLP problems. These methods generally decompose MINLP problems into related NLP or MIP problems, and solve them successively to obtain solutions. These approaches only guarantee convergence to a global optimum under convexity, converging to local minima most of the time.

- *Meta-heuristic methods*: More recently, population-based meta-heuristic methods such as GA, Particle Swarm Optimization (PSO), and Ant Colony Optimization have been used widely to solve NLP and MINLP problems, as these methods have

high probability of converging to the global optimum [60]. While these methods work by finding a set of solutions that is improved iteratively, the PSO technique is inherently continuous and is poorly suited for discrete variables, and the Ant Colony optimization method is better suited for discrete or combinatorial optimization problems [61]. Furthermore, PSO is more computationally efficient in solving continuous problems compared to GA; however, for MINLP problems, the former does not offer significant computational savings compared to the latter [62].

Other meta-heuristic methods such as Tabu Search and Simulated Annealing have also been proposed in the literature to solve MINLP problems, which are trajectory-based methods. Tabu search has difficulties in traversing through continuous search spaces, and is better suited for discrete optimization problems [63]. Simulated Annealing, on the other hand, is guaranteed to converge in the limit; this may not be practically useful because the computational time increases exponentially with the size of the problem [63]. Furthermore, it is difficult to define a good cooling schedule for this technique.

This work employs GA, an established and widely-used meta-heuristic technique, as the optimization tool to minimize the daily feeder peak demand in the first step, and then provide fair charging of PEVs in the second step. This population-based search technique is chosen because, compared to other MINLP solution techniques, it is more likely to provide high quality solutions with high probability due to its random search strategy, and even though it does not guarantee convergence to a global optima, it is likely to find it. This technique can also handle discrete and continuous variables efficiently, and is more robust with respect to its search parameters. Furthermore, it allows to easily incorporate external solvers that can handle specific constraints, such as power flow solvers, as in the case of this work.

2.4.4 Mathematical Modeling Tools

There are many commercial modeling tools/solvers such as GAMS, CPLEX, and MATLAB, which can be used to simulate and solve mathematical models. This work uses a combination of MATLAB [64] for GA-based optimization, and OpenDSS [42] for feeder modeling and power flow computations.

MATLAB is a powerful tool developed by MathWorks used extensively for numerical computation and data manipulation. This tool works with matrices and built-in functions, which makes it a powerful simulator. MATLAB has a GA optimization toolbox; however, the toolbox does not have the capability to interface with OpenDSS. Hence, the GA solution procedure was coded in MATLAB script.

OpenDSS is the open-source software developed by Electric Power Research Institute (EPRI), also known as Open Distribution System Simulator, used as a comprehensive distribution system simulation tool. This software can be run as a stand-alone program or through a COM server interfaced with other platforms such as MATLAB or Visual Basic. This software is capable of performing many types of analysis and simulation such as distribution planning and analysis, harmonics analysis, analysis of distributed generation interconnections, etc. OpenDSS also has the option of selecting solution modes, namely, snapshot power flow, daily power flow, yearly power flow, harmonics, fault study and others. OpenDSS has its own script to model power grids, and can display and/or export desired quantities.

2.5 Genetic Algorithms (GA)

Solution approaches which use exhaustive search strategies to find the best solution by enumerating all possible solutions, evaluating their fitness and reporting the best one, are not feasible for systems with large number of variables. For example, a system with 20 binary decision variables would require the generation and evaluation of 2^{20} (over a

million) possibilities. In addition, problems that are highly non-linear in nature and have large number of variables would have a search space with numerous peaks and valleys. Techniques working with one search direction at a time would be computationally intensive, and thus population-based search techniques would be a better alternative. Meta-heuristic methods such as tabu search, simulated annealing, GA, etc., are well suited to solve highly non-linear problems or large combinatorial problems. They do not, however, guarantee global optimality of the solution, but have a high probability of finding the global optimum.

GA uses a global search strategy of smart randomization to search irregular search spaces. Inspired by the evolutionary model, GA works with a population of individuals, which are solutions spread across the search space [65], and the goal is to find the minimum or maximum of some objective function f, also known as the fitness function.

A simple GA, described in [66], starts with an initial population of size ω, made up of feasible individuals. An individual in this population is made up of chromosomes, which are the encoded decision variables. The three basic operators of GA are parent selection, crossover, mutation. Thus, first, a pair of individuals are selected randomly for reproduction; second, crossover occurs using these selected individuals, with a crossover probability cr; and third, each bit in the selected individuals are mutated (flipped from zero to 1, and vice versa), with a mutation probability mr. As a result, two new offsprings are generated, which are then evaluated for fitness, i.e., they are checked to see if they satisfy the constraints of the problem.

The population is updated with the best fit individuals, which can be done either by complete or partial replacement of the old population. By completely replacing the old population with the newly generated individuals, there is a probability of losing the best individual; thus, it is better to use the partial replacement method, also known as the elitist approach. In the partial replacement method, a percentage of the population with the worse-fit individuals are replaced by the new offsprings. This process directs the population towards a global optimum until the convergence criteria are satisfied.

It is better to choose a larger population size, as it leads to better convergence because

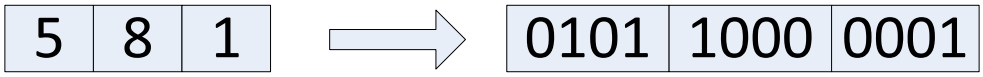

Figure 2.2: Binary encoding of an individual.

of the larger pool of diverse individuals available in a larger population. At the same time, crossover and mutation maintain diversity in the population to ensure that the entire sample space is scoped.

As for encoding the population, there are various encoding schemes that are used for the individuals in a population such as binary, hexadecimal, decimal, etc. The simplest scheme is the binary integer coding, where each gene in an individual is encoded as a binary string, as illustrated in Figure 2.2.

2.5.1 Parent Selection

This operator imitates the process of natural selection, as seen in evolution. The fitter individuals have a greater chance of progressing to the next population and the weaker individuals get weeded out from the population eventually [67]. There are various methods which can be used to select parents for crossover, such as weighted roulette wheel selection, tournament selection, etc.

One of the commonly used methods of parent selection is the weighted roulette wheel selection. In the case illustrated in Figure 2.3, the inner wheel is divided into slots that are sized in proportion to the individual fitness values. The slots on the outer rim of the wheel represent the sum of the fitness values divided into equal parts. A uniform random variable in the interval (0, 1) is chosen and multiplied with the sum of all the fitness values to give a value, say R. The individual selected for the crossover is identified at the point where the partial sum of the fitness values exceeds R [66], thus resulting in individual 1 being selected for crossover out of individuals 1-4.

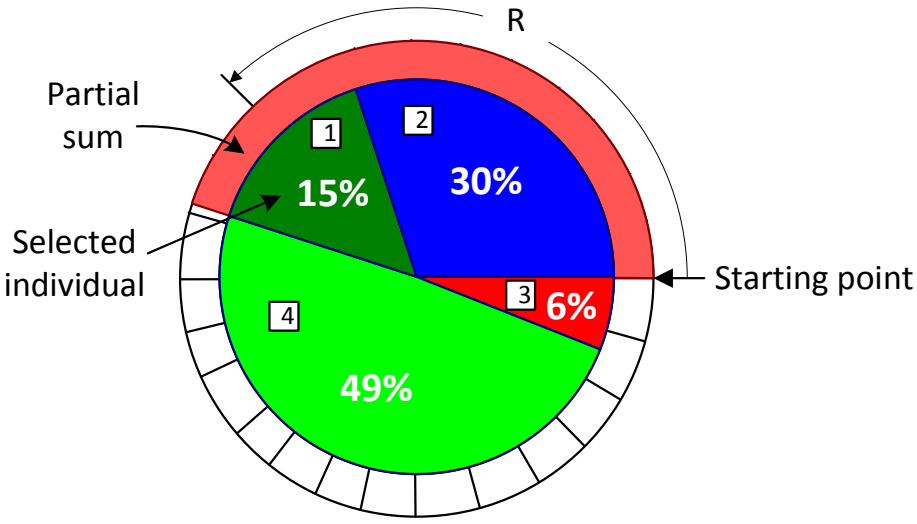

Figure 2.3: Weighted roulette wheel used for parent selection.

2.5.2 Crossover

This operator is instrumental in the exchange of information between the randomly chosen parent individuals to create 2 new offsprings. There are several crossover techniques such as single-point crossover, two-point crossover, uniform crossover, etc. In single-point crossover, the two parent chromosomes are interchanged to the right of a randomly selected point to create new individuals, unlike the two-point crossover where the two parent chromosomes exchange the part of the chromosome between two randomly selected points, as shown in Figure 2.4. In uniform crossover, the parent individual of each bit in the offspring is chosen randomly.

2.5.3 Mutation

This operator is crucial in maintaining the diversity of the population so that the solution does not fall into local minima. It is used to flip a random bit within individual chromosomes. As in evolution, mutation does not occur very frequently, thus this operator has a

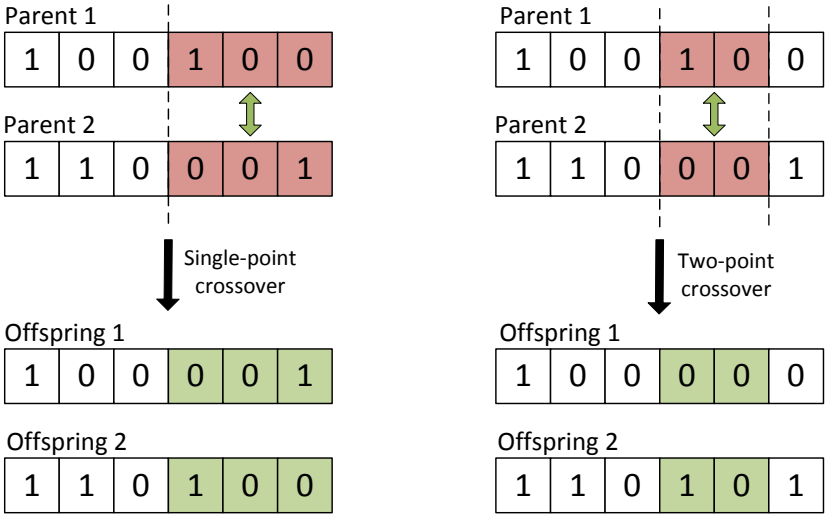

Figure 2.4: Single-point and two-point crossover.

low value to reflect this occurrence. As in the case of crossover, there are single-point and multiple-point mutation, as illustrated in Figure 2.5.

2.5.4 Convergence Criteria [68]

One of the challenges associated with GAs is determining the convergence or stopping criteria. A simplistic approach, that is often used, is to stop when a fixed number of

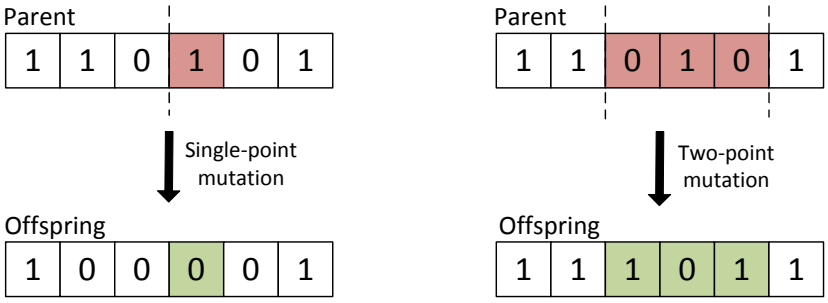

Figure 2.5: Single-point and two-point mutation.

iterations are completed. A more sophisticated alternative is to stop after either the average of the current generation, or preferably, the running average of the best fitness values appears to have reached steady state value. In this work, the GA stops if any of the criteria are satisfied:

- Change in the best fitness value over a specified number of generations does not exceed the specified tolerance value.
- Maximum number of generations are completed.
- The average fitness value of the population converges to the best fitness value.

2.6 Bootstrap Method

The nonparametric Bootstrap method, a well-established statistical method formalized by Efron [69, 70], has been widely employed as an alternative to MCS because of its reduced computational burden [71]. This is a resampling technique used to estimate the statistics of a population with an unknown distribution function F through random sampling with replacement of the original sample of size k, and is particularly effective when the original sample is difficult to obtain or obtained using computationally expensive methods. Sampling with replacement means that each element for the Bootstrap sample is selected separately at random from the original data set and, as a consequence, there is a possibility that one element may occur multiple times in a given Bootstrap sample. The basic idea is that, if the original sample is a good approximation of the population, the technique will provide a good approximation of the sampling distribution of the desired statistic [72].

The Bootstrap method is based on the following:

- The distribution function of the original sample is an estimate of the unknown distribution function of the population.

- Random resampling with replacement from the original sample.

Hence, as the original sample size increases in size, it contains more information about the population, and consequently, approaches the distribution of the population. Furthermore, if the original sample's size k is large enough, then, as the number of Bootstrap replicates M tends to infinity (large number), the Bootstrap estimate of the sampling distribution approaches the sampling distribution of the statistic of interest for the original sample.

2.6.1 Implementation

A graphical illustration of the Bootstrap method, presented in Figure 2.6, follow the steps outlined below [69]:

- Construct an empirical probability distribution $\hat{F}$ of the original sample by assigning equal probabilities to each element of the original sample $X = \{x_1, x_2, x_3, ..., x_k\}$, and calculate the statistic of interest $\hat{T}$ for it.
- Draw a Bootstrap sample $X^* = \{x_1^*, x_2^*, x_3^*, ..., x_k^*\}$ of size k randomly with replacement from the original data set.
- Generate M Bootstrap samples $\{X_1^*,\ X_2^*,\ X_3^*,...,\ X_M^*\}$, and compute their corresponding Bootstrap statistic $\{T_1^*,\ T_2^*,\ T_3^*,\ ...,\ T_M^*\}$, where M is a large number.
- Construct a relative frequency histogram using the M number of Bootstrap statistics $\{T_1^*,\ T_2^*,\ T_3^*,\ ...,\ T_M^*\}$ by assigning equal probabilities to each.
- The resulting distribution F_B gives the Bootstrap estimate of the sampling distribution of the statistic of interest $\hat{T}$.

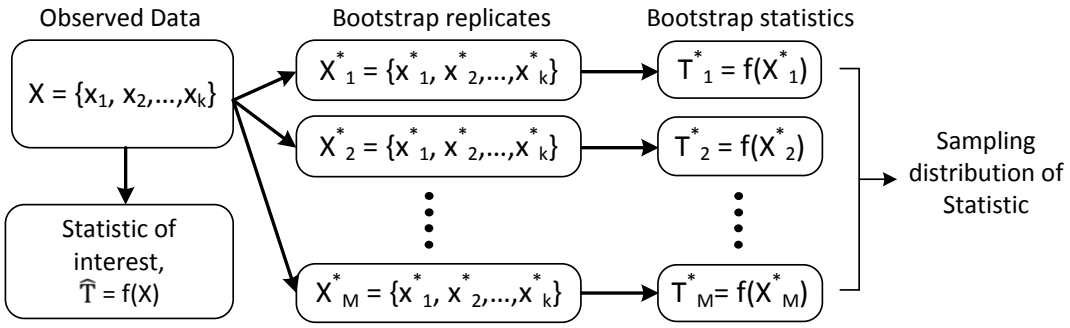

Figure 2.6: Graphical illustration of the Bootstrap method.

2.6.2 Confidence Intervals

The Bootstrap Confidence Interval (CI) is estimated using the Bootstrap percentile method by computing the desired Bootstrap percentiles after ranking the Bootstrap statistics in ascending order, as follows, for a 95% CI [73, 74]:

$$CI_{95\%} = \left[\hat{T} - \left(T^*_{2.5\%} - \hat{T}\right), \hat{T} - \left(T^*_{97.5\%} - \hat{T}\right)\right] \tag{2.20}$$

where $T^*_{2.5\%} = T^*_{\lfloor 0.025M \rfloor}$, and $T^*_{97.5\%} = T^*_{\lceil 0.975M \rceil}$. Confidence intervals suggest that the statistic of interest lies within its bounds with a specified probability. It is important to note, however, that this method requires that the Bootstrap distribution F_B is approximately symmetrical around the sample mean and continuous.

2.6.3 Variance and Standard Deviation

The Bootstrap variance ${\sigma_B}^2$ and Bootstrap standard error σ_B of a statistic are simply the variance and standard deviation (SD) of the Bootstrap distribution of the statistic, i.e., the variance and SD of M values of T^*. Hence, the Bootstrap variance and SD are given by [74, 75]:

$${\sigma_B}^2 = \frac{\sum\limits_M \left(T^* - \frac{\sum_M T^*}{M}\right)^2}{M-1} \tag{2.21}$$

$$\sigma_B = \sqrt{\frac{\sum\limits_{M} \left(T^* - \frac{\sum_{M} T^*}{M} \right)^2}{M-1}} \tag{2.22}$$

2.7 Summary

In this chapter, a brief overview of the DOPF model and its applications, together with pertinent aspects of distribution systems and its components was presented. Relevant background information about PEVs, their types, charging levels, charging schemes, their basic design concepts, battery charging, and optimal dispatch techniques were also explained. The different categories of mathematical programming problems, as well as the mathematical modeling tools used in this work, were described, followed by a detailed discussion on the GA technique used to solve DOPF problems. Finally, an overview of the non-parametric Bootstrap technique, and the computation of confidence intervals, variance, and standard deviation was presented.

Chapter 3

Day-Ahead Dispatch of Distribution Feeders

Nomenclature

Indices

N	Total number of nodes in the system
LN	Number of load nodes in the system
B	Number of feeders in the system
n	Node index
b	Feeder index
t	Time interval index
i	LTC tap index
j	Switched capacitor index
k	Number of elements in the original sample and Bootstrap replicates
M	Number of Bootstrap replicates
m	Bootstrap replicate index

Parameters

τ_1,τ_2	Time steps
pr	PEV penetration level
AHD_h	Average monthly electricity consumption of a household [KWh]
Nev_h	Number of PEVs per household
$\underline{tap}_i$	Lower limit for LTC tap
$\overline{tap}_i$	Upper limit for LTC tap
$\overline{cap}_j$	Upper limit for switched capacitor [kVAr]
$\overline{\|I\|}_b$	Current carrying capacity of feeder [A]
$\underline{V}_n$	Minimum voltage limit [p.u.]
$\overline{V}_n$	Maximum voltage limit [p.u.]
P_n^{spec}	Specified active power for aggregated base load [kW]
SoC_n^f	SoC at the end of charging period [%]
EVr	Electric range of PEV [km]
$BCap_l$	Battery capacity of single PEV [kWh]
$nev_{n,t}$	Number of PEVs
Mcp_l	Maximum limit of single charging point [kW]
Mop	Maximum control operations per hour for taps (Mop_{tap}) and capacitors (Mop_{cap})
$\overline{Epev}_n$	Battery capacity of aggregate PEV load [kWh]
$\overline{Pcp}_{n,t}$	Charging point limit of aggregate PEV load [kW]
Con	Hourly feeder control schedule

Variables

SoC_n^i	SoC at the beginning of charging period [%]
EVd_n	Distance travelled by aggregate PEV load [km]
T_n^{Arr}	Arrival time of aggregate PEV load
T_n^{Dep}	Departure time of aggregate PEV load
$P_{n,t}^{bl}$	Base load active power demand [kW]
$P_{n,t}^{pev}$	PEV load active power demand [kW]

$tap_{i,t}$	Tap setting
$cap_{j,t}$	Capacitor switch setting
P^{max}	Daily feeder peak demand [kW]
$\|I\|_{b,t}$	Magnitude of feeder current [A]
$\|V\|_{n,t}$	Magnitude of node voltage [p.u.]
X^*	Bootstrap replicate
$\hat{P}^{max}$	Mean daily feeder peak demand for original sample [kW]
$\hat{C}on$	Mean hourly feeder control schedule
$\hat{P}^{max*}$	Mean daily feeder peak demand for Bootstrap replicate [kW]
$\hat{C}on^*$	Mean hourly feeder control schedule for Bootstrap replicate
$E[P^{max}]$	Bootstrap estimate of daily feeder minimum peak demand [kW]
$E[Con]$	Bootstrap estimate of hourly feeder control schedule
T	Computation time for one GA run
NC	Number of workstations

3.1 Introduction

This chapter presents the optimization framework to compute a day-ahead feeder control schedule that would allow for optimal operation of the grid within operating limits and the minimization of peak demand when charging PEVs, which is the objective of the first step. The hourly feeder control schedule and the corresponding daily peak demand value are computed using the GA-based optimization model for various realizations of the arrival and departure times, as well as the initial battery SoC [76]. These control schedules and the corresponding peak demand values, in conjunction with a non-parametric Bootstrap approach, are then used to compute the most likely feeder control schedule and peak demand value. There are other ways to select this feeder control schedule, such as the

base schedule (without any PEVs) or automatic voltage regulation. The feeder control schedule chosen is one that both aims to maximize the power delivered to aggregated PEV loads and minimize the risk of operating limit violations, as discussed in more detail in this chapter later.

The remainder of this chapter is organized as follows: Section 3.2 presents the problem formulation for the day-ahead dispatch of distribution feeders (Step I) and the fair charging of PEVs (Step II), followed by the implementation of Bootstrap estimation and GA-based optimization model in Sections 3.3 and 3.4, respectively. Finally, the results for the first step of the proposed approach are discussed in detail, as well as the test systems used, and the assumptions made in this work.

3.2 Problem Formulation

A radial primary distribution feeder, with a specified number of nodes as well as controllable LTC taps and switched capacitors, is considered in this work. It is assumed that aggregated base and PEV loads are present at each load node. Note that the present work deals with aggregated PEV loads at each node, and hence does not deal with individual PEV charging control, which requires the representation of the secondary distribution network. Furthermore, for purposes of simulation, it is assumed that the power delivered to a load node is distributed properly among all PEVs connected for charging. It is also assumed that feeder controllable variables, such as tap and capacitor settings, can be adjusted at hourly discrete time intervals. Furthermore, the hourly base load profiles for each load node is assumed known through proper forecasting methods for a 24 h period (e.g. [77, 78]), and are modeled as constant impedance loads, i.e., the power delivered to these loads depends on the node voltage at their respective nodes. As a result, base loads become decision variables, with small variation from the specified values. On the other hand, PEV loads, which are assumed to be controllable in smaller time steps, are associated with temporal and spatial uncertainties, i.e., the times of arrival and departure, the initial SoC, and the

number of charging PEVs at any given time.

This work addresses the PEV-related uncertainties in two steps, as shown in Figure 3.1. First, the day-ahead dispatch of distribution feeders is performed considering uncertainty in initial battery SoC, and the arrival and departure times as follows:

- *Initial Battery SoC*: The initial battery SoC of aggregate PEV load at node n is calculated using:

$$SoC_n^i = \left(1 - \frac{EVd_n}{EVr}\right) 100 \quad \forall\ n = 1, .., LN \tag{3.1}$$

  based on the aggregated daily distance travelled by the electric vehicles EVd_n, which is a random variable following a given probability distribution function (p.d.f.). All variables, parameters and indices in this and other equations are defined in the Nomenclature. The variation in initial battery SoC affects the total energy drawn from the grid by the charging PEVs.

- *Arrival and departure times*: The aggregated arrival and departure times of PEV loads at each node follow a given p.d.f., accounting for the temporal uncertainty of these loads, thereby dictating the total time available to charge the PEVs to a specific battery SoC.

The base load profile, PEV and feeder parameters, feeder limits, and aggregated charging limits are inputs to the first step. In this step, tap and capacitor schedules, as well as the PEV charging, are computed for τ_1 for various realizations of the above-mentioned uncertainties, while minimizing daily feeder peak demand, and satisfying all feeder and PEV-related constraints based on an optimization approach. These tap and capacitor schedules and daily feeder peak demand values are then used to compute the most likely feeder control schedule and the mean peak demand value, which is the output of this step. These values serve as inputs to the second step, which performs aggregated PEV charging control; aggregated PEV charging limits, and feeder limits and parameters are also inputs

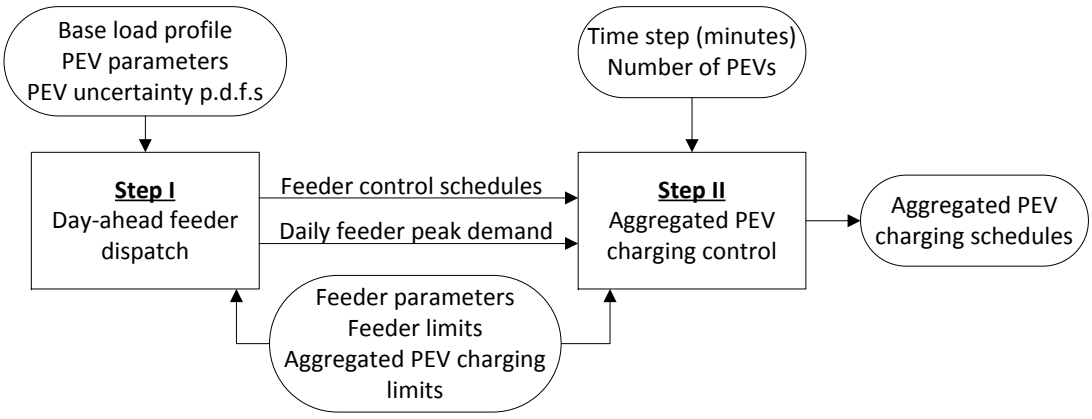

Figure 3.1: Schematic approach of the proposed approach.

for the second step. The output of the second step is the desired aggregated PEV charging rates, which is computed every few minutes.

It is important to note that, in the first step, all the PEVs at a node are assumed to be aggregated into one uncertain and variable load at charging nodes, so that uncertainties on PEV arrival and departure times, as well as initial battery SoCs are all represented through a combined stochastic load. On the other hand, in the second step, the stochasticity associated with each PEV at a node, in terms of the arrival and departure times, and the initial battery SoC is considered using the same p.d.f.s used in the first step. Based on this, the number of PEVs can be computed for each time interval for simulation purposes. In practice, this information will be relayed through the communication network, which is assumed to already exist.

3.3 Bootstrap Estimation

A distinct PEV scenario or a realization is generated based on the random variables, namely the aggregated daily distance travelled EVd_n, and the aggregated arrival and departure times of the total PEV load at each load node, T_n^{Arr} and T_n^{Dep}, where each of them is

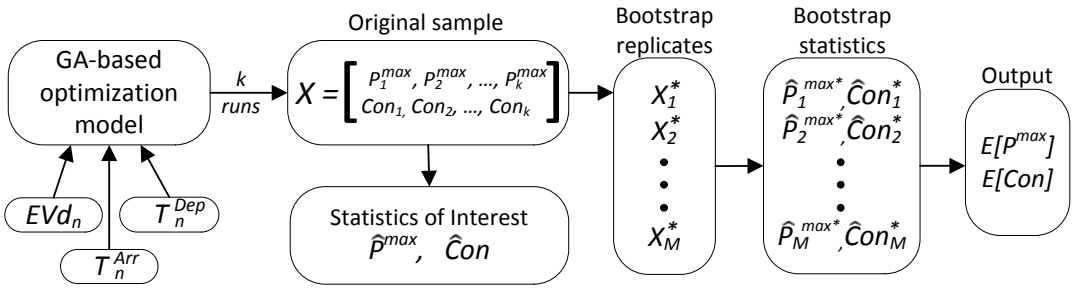

Figure 3.2: Bootstrap estimation of daily feeder minimum peak demand and hourly feeder controls.

modeled using appropriate p.d.f.s. The variation in aggregated daily distance travelled EVd_n affects the aggregated initial battery SoC SoC_n^i, which in turn affects the total energy drawn from the grid by the charging PEVs, while the variation in arrival and departure times dictates the total charging time available to the PEVs to reach $SoC_n^f\%$ of their aggregated battery capacity.

The implementation of the non-parametric Bootstrap technique is illustrated in Figure 3.2. Here, for a finite number of realizations k, the minimum daily feeder peak demand and their corresponding discrete feeder controls, comprising of hourly tap and capacitor settings, are computed using a GA-based optimization model, while satisfying the operational and physical limits of the feeder. Thus, the independent observations obtained populate the original sample of size k, which is then resampled to generate M Bootstrap replicates, each of size k. Consequently, the desired statistics of interest, i.e., mean daily feeder minimum peak demand $\hat{P}^{max}$ and the most likely hourly tap/capacitor settings $\hat{C}on$, are computed for the original sample, as well as for each Bootstrap replicate ($\hat{P}^{max*}$ and $\hat{C}on^*$). These M Bootstrap statistics are, then, used to obtain the sampling distributions of the desired statistics. The Bootstrap estimates of the mean feeder minimum peak demand $E[P^{max}]$ and the most likely feeder control schedule $E[Con]$, which are the outputs of the process, are obtained by computing the mean of their respective sampling distributions, provided they approximate to a normal distribution.

The Bootstrap CI as well as the Bootstrap variance and standard error of the mean daily system peak are calculated using (2.20), (2.21), and (2.21), respectively, as explained in Section 2.6. Note that in the case of the hourly tap/capacitor schedules, each observation in the original sample is a block of data comprised of hourly schedules for each LTC transformer tap and capacitor.

3.4 GA-based Optimization Model

3.4.1 DOPF Model

The minimum daily feeder peak demand and their corresponding discrete feeder controls, comprising of hourly tap and capacitor settings, are computed using a GA-based optimization model, while satisfying the operational and physical limits of the feeder, for the following objective function:

$$\min \ P^{max} = \max_{t=1,..,24} \sum_{n=1}^{N} \left\{ P_{n,t}^{bl} + P_{n,t}^{pev} \right\} \tag{3.2}$$

This objective function minimizes the daily feeder peak demand, which is the maximum value of the demands (sum of the PEV and base loads at all the nodes) during each time interval t experienced at the substation end of the feeder over the 24 h period.

The constraints of the GA-based optimization model are as follows:

- *PEV charging constraints*: The following constraints ensure that the PEV battery capacity is not exceeded, and the minimum battery SoC at the end of the charging period is $SoC_n^f\%$ of the battery capacity, respectively:

$$\sum_{t=1}^{24} P_{n,t}^{pev} \leq \overline{Epev}_n \ \ \forall \ n = 1, .., LN \tag{3.3}$$

$$\sum_{t=1}^{24} P_{n,t}^{pev} \geq \left(SoC_n^f - SoC_n^i \right) \overline{Epev}_n \ \ \forall \ n = 1, .., LN \tag{3.4}$$

where

$$\overline{Epev}_n = \sum_{l=1}^{nev_n} BCap_l \;\; \forall\, n = 1, .., LN \tag{3.5}$$

Note that, for the PEV penetration levels considered in this work, constraint (3.4) is feasible for all generated realizations for a specific SoC_n^f; however, this may not be the case for higher PEV penetration levels. In that case, feasibility may be restored at the cost of a lower final battery SoC, SoC_n^f.

- *System limits*: The physical limits of the system, i.e., power delivered to the PEV at the charging point, transformer taps, and switched capacitors are the following:

$$0 \leq P_{n,t}^{pev} \leq \overline{Pcp}_{n,t} \;\; \forall\, n = 1, ..., LN, \;\forall\, t \tag{3.6}$$

$$\underline{tap}_i \leq tap_{i,t} \leq \overline{tap}_i \;\; \forall\, i, t \tag{3.7}$$

$$0 \leq cap_{j,t} \leq \overline{cap}_j \;\; \forall\, j, t \tag{3.8}$$

where

$$\overline{Pcp}_{n,t} = \sum_{l=1}^{nev_{n,t}} Mcp_l \;\; \forall\, n = 1, .., LN, \;\forall\, t \tag{3.9}$$

The node voltage and feeder current limits are also considered as follows:

$$\underline{V}_n \leq |V|_{n,t} \leq \overline{V}_n \;\; \forall\, n = 1, .., LN, \;\forall\, t \tag{3.10}$$

$$0 \leq |I|_{b,t} \leq \overline{|I|}_b \;\; \forall\, b = 1, .., B, \;\forall\, t \tag{3.11}$$

- *Power flows*: The power flows are determined using OpenDSS [42] at each t.

- *Control operations*: The following constraints limit the number of control operations by taps and capacitors performed every hour:

$$|tap_{i,t} - tap_{i,t-1}| \leq Mop_{tap} \;\; \forall\, i, t \tag{3.12}$$

$$|cap_{j,t} - cap_{j,t-1}| \leq Mop_{cap} \;\; \forall\, j, t \tag{3.13}$$

3.4.2 Implementation

The modeling framework consists of an optimization block implemented using GA in MATLAB [64], and power flow calculations performed using OpenDSS [42]. Each individual in the population contains the hourly charging rate of aggregate PEV loads at each node, and hourly tap and capacitor settings for each LTC transformer, and is represented using a binary encoding scheme.

The flowchart in Figure 3.3 outlines the steps followed to implement this method. First, an initial population of feasible individuals is generated, followed by the application of GA operators (parent selection, crossover, and mutation) to generate new offsprings in each generation, as explained in Section 2.5. Thereafter, each of the newly generated offsprings are evaluated for PEV-related, number of control operations limit, and feeder physical limit violations. The feasible offsprings are forwarded as input data to OpenDSS to perform power flow calculations, which then returns the actual charging rates delivered to PEVs and base load at each node, node voltages, and feeder currents. In the case of infeasible offsprings, they are corrected to restore feasibility, while maintaining randomness, before they are sent to OpenDSS. These node voltages and feeder currents are then checked for operating limit violations, and the non-violating feasible offsprings are then stored. After the generation of the required number of feasible offsprings, the new population is created through partial replacement by replacing the worst fit individuals with the new offsprings. The GA terminates when the change in best fitness value does not exceed the tolerance for a specified number of generations, when the average fitness of the population equals the best fitness value, or when the maximum number of generations is exceeded.

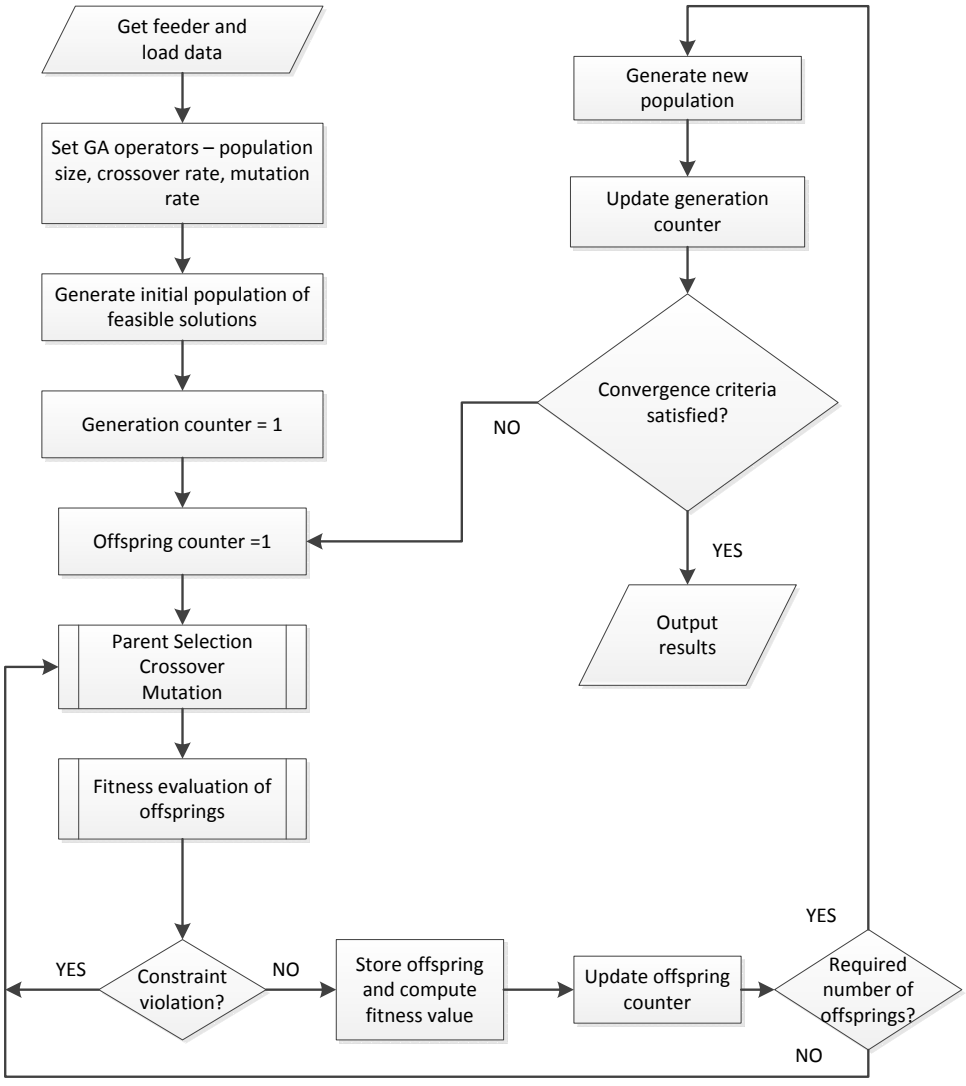

Figure 3.3: Flowchart of the GA-based optimization.

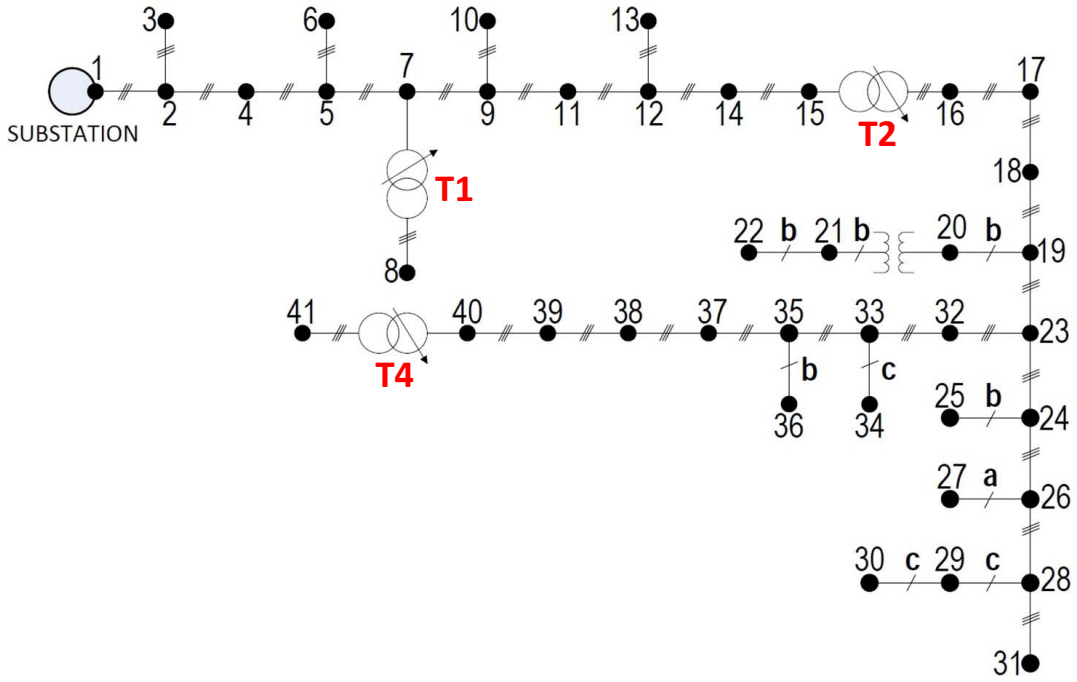

Figure 3.4: Real distribution feeder.

3.5 Results

3.5.1 Test Systems

Real Distribution Feeder

One of the test systems used for this work is the real distribution feeder shown in Figure 3.4, which is an unbalanced three-phase system with three LTC tranformers $T1$, $T2$, and $T4$; there are no switched capacitors in this feeder. The hourly feeder base load profile for the 24 h period is shown in Figure 3.5 [4].

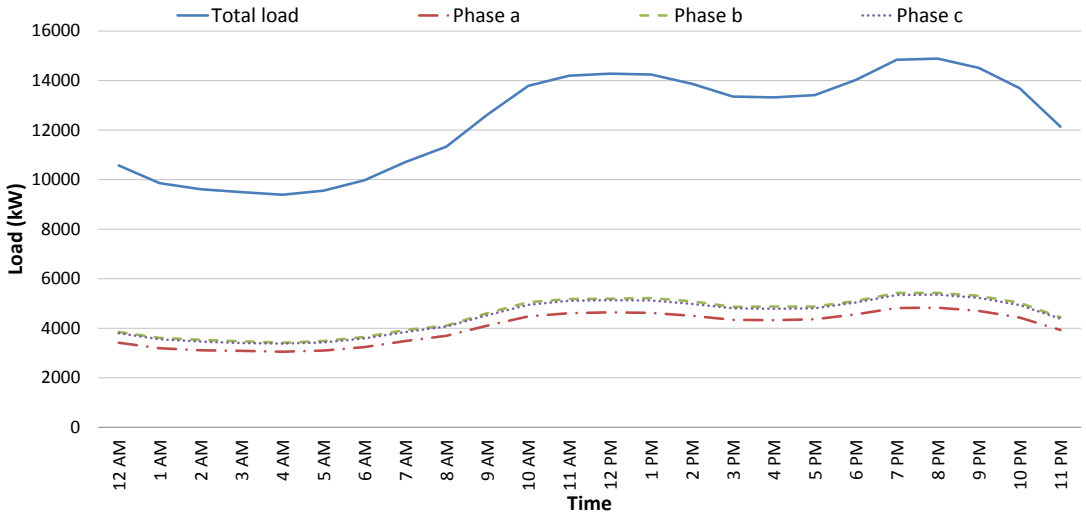

Figure 3.5: Hourly aggregated base load profile for the 24 h period (Real distribution feeder).

IEEE 13-Bus Test Feeder

The other test system used to validate the proposed approach is the IEEE 13-bus test feeder, shown in Figure 3.6, with one LTC transformer and switched capacitors at bus 611 and bus 675. These capacitors are modeled as multiple switching banks, which can be dispatched in discrete blocks, i.e., the capacitor banks in each phase at bus 675 are assumed to have five blocks of 100 kVar, and those at bus 611 with 5 blocks of 50 kVar in phase c. The 24 h aggregated base load profile for this feeder is shown in Figure **??**.

3.5.2 Assumptions

The following assumptions are made in this work:

- A 24 h time horizon is considered, with time steps of τ_1=1 h, since taps and capacitors are typically fixed every hour, and τ_2=5 min for the day-ahead dispatch of distribution

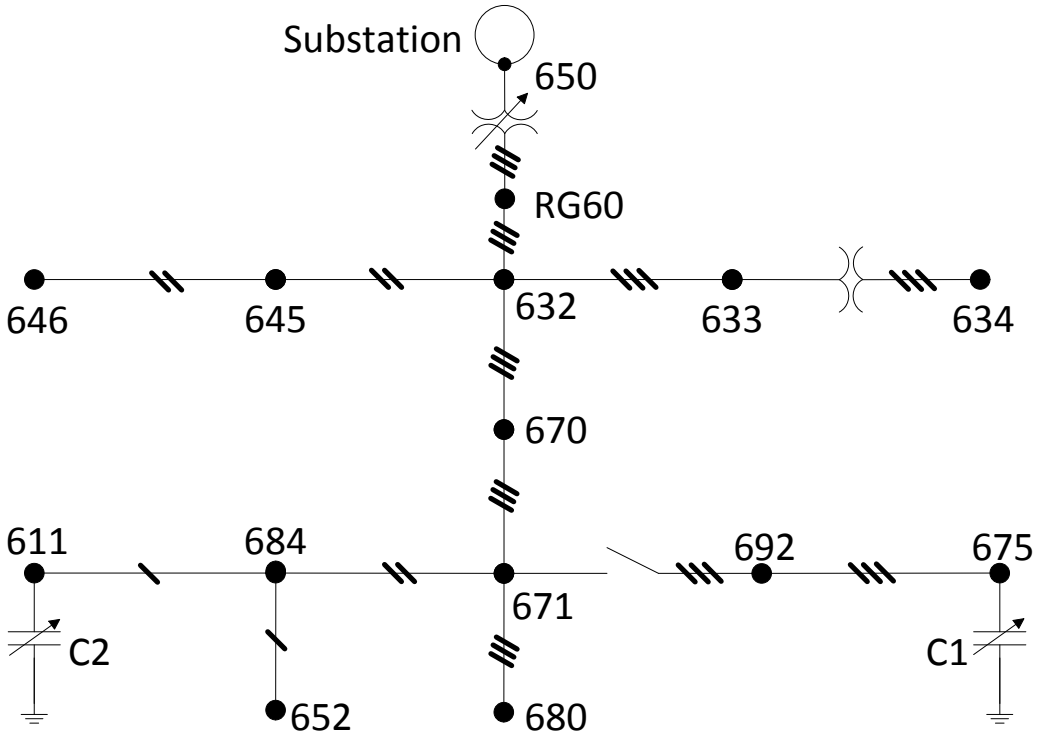

Figure 3.6: IEEE 13-Bus test feeder.

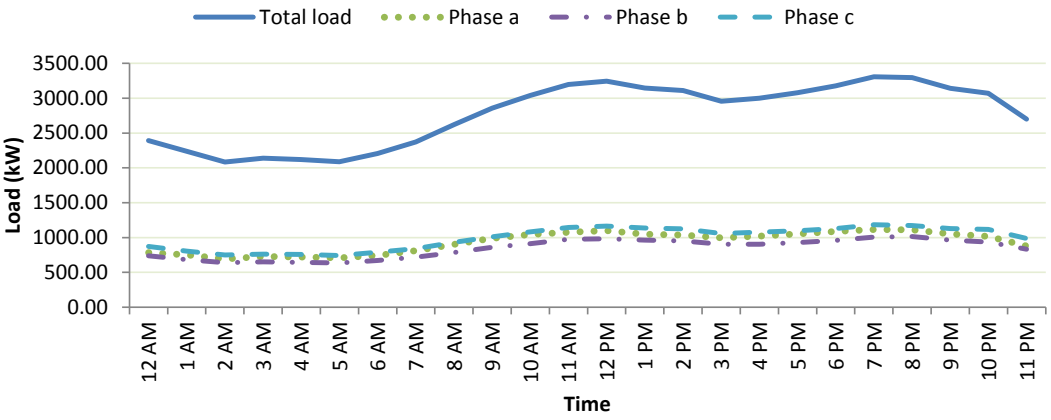

Figure 3.7: Hourly aggregated base load profile for the 24 h period (IEEE 13-bus test feeder).

feeders and fair charging of PEVs, respectively. Note that from the power system perspective, 5 min intervals would be sufficiently fast for PEV charging, since a finer granularity would increase voltage fluctuations, which may have detrimental effects on the lifetime of equipment and appliances serviced by the feeder.

- The hourly base load for the 24 h period (shown in Figures 3.5 and 3.7) is extracted from [4], and is comprised of typical non-flexible residential loads, assuming that these are known through forecasting techniques (e.g. [77, 78]), with a daily system peak occuring at 7 pm. All the base loads at a load node are aggregated, since this work focuses on the primary distribution feeder.

- The only controllable loads considered in this work are PEVs operating in the G2V mode. V2G capability is not considered in this work, in view of the practical implementation objectives of the work presented in this thesis, in the short-to-medium term, since this option will not be available for the foreseeable future, due to concerns with significant battery degradation [79, 80], which would directly affect PEV manufacturer warranties. It is also assumed that the power delivered to a node is distributed equally among the PEVs connected for charging at that node.

- It is assumed that a household can have a maximum of one PEV Nev_h, and the average monthly electricity consumption of a household AHD_h is 1500 kWh. Based on the PEV penetration level pr, which is the percentage of PEVs in the total number of vehicles, the number of PEVs per node is then estimated as follows [81]:

$$nev_n = \left\lfloor pr \cdot \left\lfloor \frac{P_n^{spec} \cdot Nev_h}{AHD_h} \right\rfloor \right\rfloor \tag{3.14}$$

  This means that, for a PEV penetration level of 100%, a total of 7240 PEV loads will charge from the feeder in the case of the real distribution feeder, and a total of 1642 PEV loads in the case of the IEEE 13-bus test feeder. The PEV penetration levels considered in the following are 30%-60% for the former, and 60% for the latter.

- In the day-ahead dispatch step, the number of charging PEVs nev_n, computed based on the PEV penetration level [81], remains constant throughout the specific charging period T_n^{Arr} to T_n^{Dep}. In addition, the arrival and departure times of PEVs are modeled as normal distributions centered around 5 pm and 7 am [82], respectively, as shown in Figure 3.8. In the second scheduling step, the distribution functions from the first step are applied to each PEV at a node n. Hence, the number of PEVs charging from the grid at node n is computed for each time interval, based on the total number of PEVs connected to the grid for charging. In addition, only one charging window is considered during a 24 h period.

- Only a PHEV 30km mid-size sedan with a battery capacity of 8.14 kWh is considered, with Level 2 charging, i.e., up to a maximum of 4.8 kW, without loss of generality.

- In the day-ahead dispatch of feeders, the intial battery SoC is modeled based on the daily distance travelled, which is a random variable following a lognormal distribution [37], as shown in Figure 3.9. In the second step, this distribution function is applied to each PEV at a node to determine the vehicle's SoC. It is also assumed that only the PEVs that need charging are connected to the grid, i.e., if the battery is fully charged, the built-in charger disconnects from the grid. Furthermore, it is also assumed that PEVs will not drop out of the charging process in the middle of the given time interval t.

- In this work, the maximum number of control operations Mop_{tap} or Mop_{cap}, i.e., tap or capacitor operations, is limited to 3 per hour.

- Only the constant current charging mode of the battery is considered.

- The communication network relaying real-time information, such as number of charging PEVs or charging rate at each node, is assumed to already be in place.

- In the case of the real distribution feeder, the upper and lower voltage limits are assumed to be 0.9 and 1.1 p.u., respectively, since the test feeder base data, with

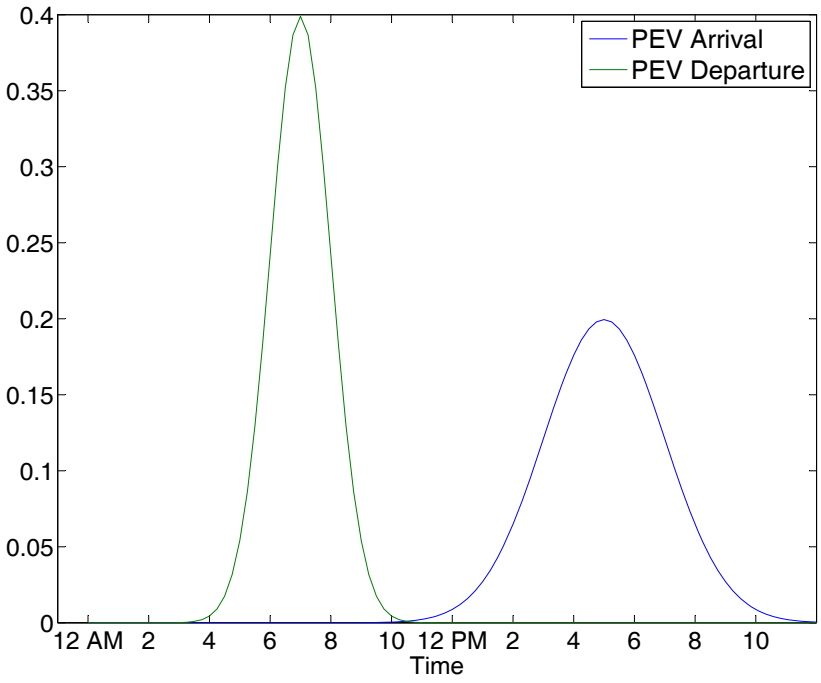

Figure 3.8: Probability density functions of arrival and departure times of aggregate PEV loads per node [82].

no PEVs, already presents voltages outside the standard +/-6% tolerance defined in [83]. However, for the IEEE 13-bus test feeder, the upper and lower voltage limits are assumed to be between 0.95 and 1.05 p.u.

3.5.3 Results For Real Distribution Feeder

Impact of Sample Size on Bootstrap Estimates

For a PEV penetration level of 30%, the GA-based optimization model is used to generate k= 25, k=30, and k=35 independent observations of the daily feeder peak demand and

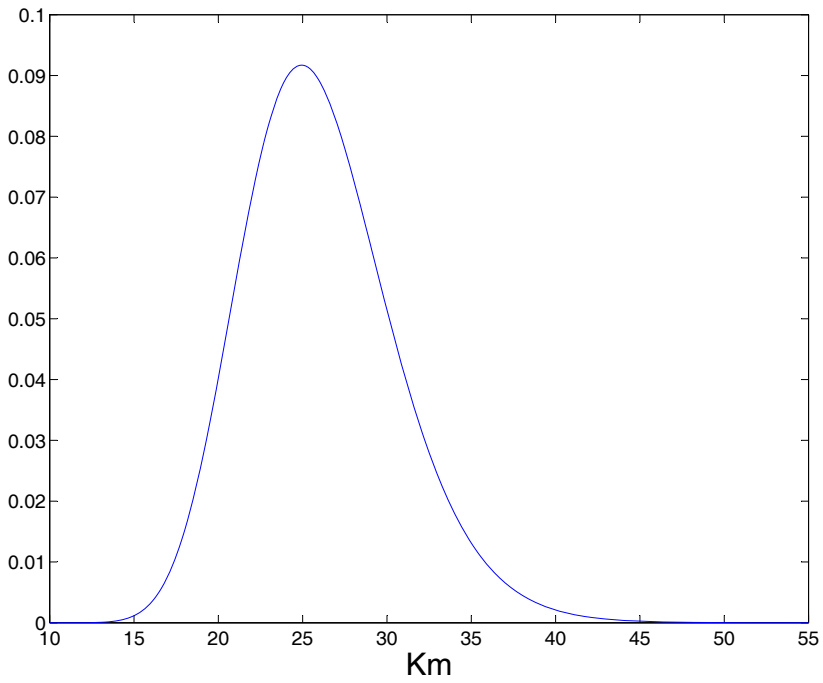

Figure 3.9: Probability density function of daily distance travelled by aggregate PEV loads per node [37].

their corresponding hourly LTC tap schedules to make up the original sample, which is then used to generate M=15,000 Bootstrap replicates. Thus, Bootstrap estimates of daily feeder peak demand $E[P^{max}]$, hourly feeder control $E[Con]$, and PEV charging schedules were computed for the 3 sample sizes. The estimates for the mean daily feeder minimum peak demand, presented in Table 3.1, for varying sample sizes are approximately the same and are not impacted by the increase in sample size, thereby suggesting that the sample sizes used are sufficiently large, as expected from the analysis of the resulting Bootstrap distributions.

The estimates for the mean feeder PEV charging schedules are shown in Figure 3.10. Observe that the varying sample sizes do not affect the mean feeder PEV charging sched-

Table 3.1: Bootstrap estimates of mean daily feeder peak demand for the real distribution feeder for PEV penetration level = 30%.

Statistic [kW]	k=**25**	k=**30**	k=**35**
Sample Mean	13,190.02	13,191.2	13,192.80
Bootstrap Mean	13,190.02	13,191.25	13,192.77
Bootstrap σ	11.02	11.04	10.34
95% CI	[13,167.98, 13,211.92]	[13,169.62, 13,212.91]	[13,172.53, 13,213.07]

ules; however, the Bootstrap tap schedules for transformers $T1$, $T2$, and $T4$ in phase b do show slight differences, as seen in Figures 3.11, 3.12, and 3.13, respectively. Furthermore, it can be seen that, at the farthest node, i.e., bus 41 phase b right after transformer $T4$, the mean PEV charging schedules are practically the same, as seen in Figure 3.14, while the hourly tap settings for transformer $T4$ at bus 40 phase b (see Figure 3.13) vary slightly with sample sizes. This suggests that basically the same PEV charging schedules can be handled by more than one possible tap setting.

Estimation of Mean Daily Feeder Peak Demand and Feeder Control Schedules

Based on the discussion in the previous sections, the empirical distribution function of the original sample of size k=25 and the sampling distribution of the mean daily feeder peak demand obtained for the real distribution feeder using the Bootstrap technique are presented for PEV penetration levels of 30%, 40%, 50%, and 60% in Figure 3.15. Observe that while the distribution of the original sample is asymmetrical, the Bootstrap distribution is nearly normal and approximately symmetrical about the mean as desired, since, according to the central limit theorem, the sampling distribution of the sample mean should approximate a normal distribution, if the size of the sample is large and the observations are

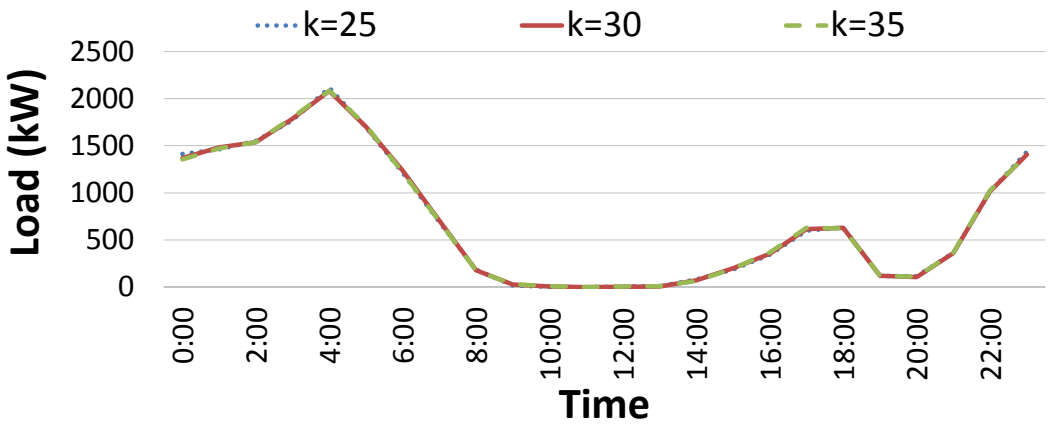

Figure 3.10: Bootstrap estimates of the mean total PEV load for the real distribution feeder for different sample sizes.

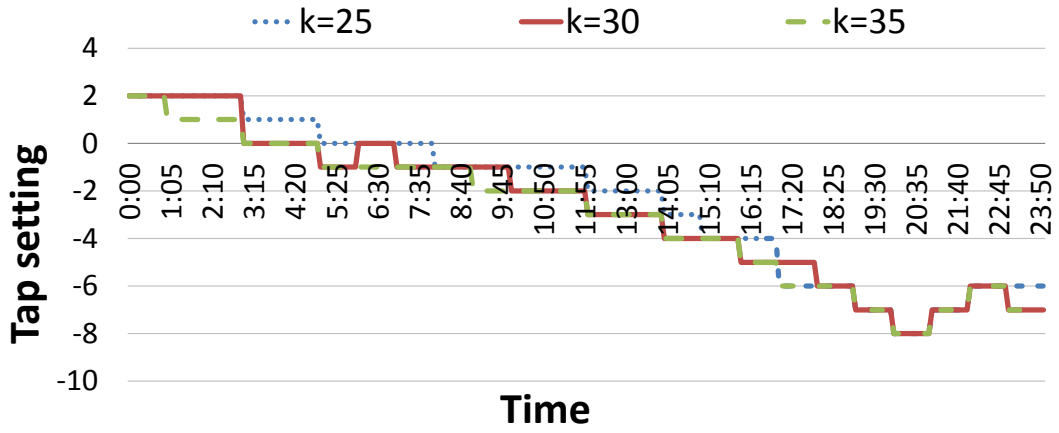

Figure 3.11: Bootstrap results of the hourly tap settings for transformer $T1$ at bus 7 phase b in the real distribution feeder for different sample sizes.

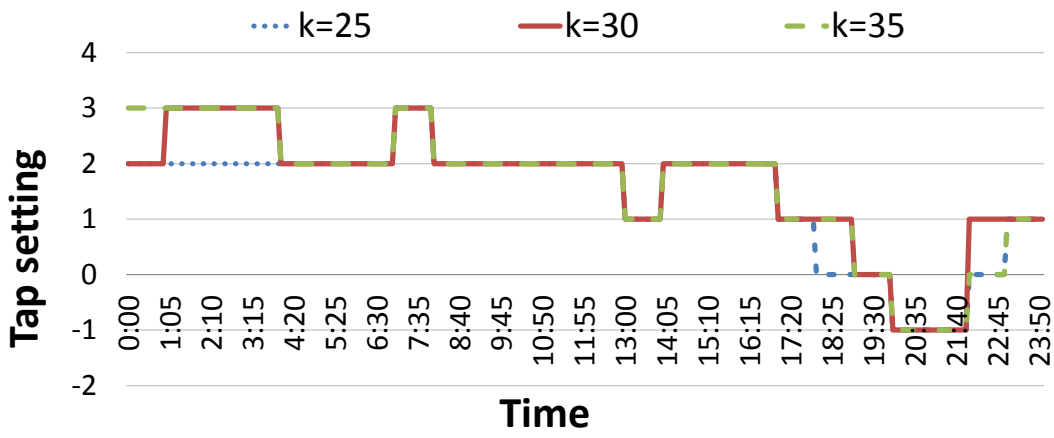

Figure 3.12: Bootstrap results of the hourly tap settings for transformer $T2$ at bus 15 phase b in the real distribution feeder for different sample sizes.

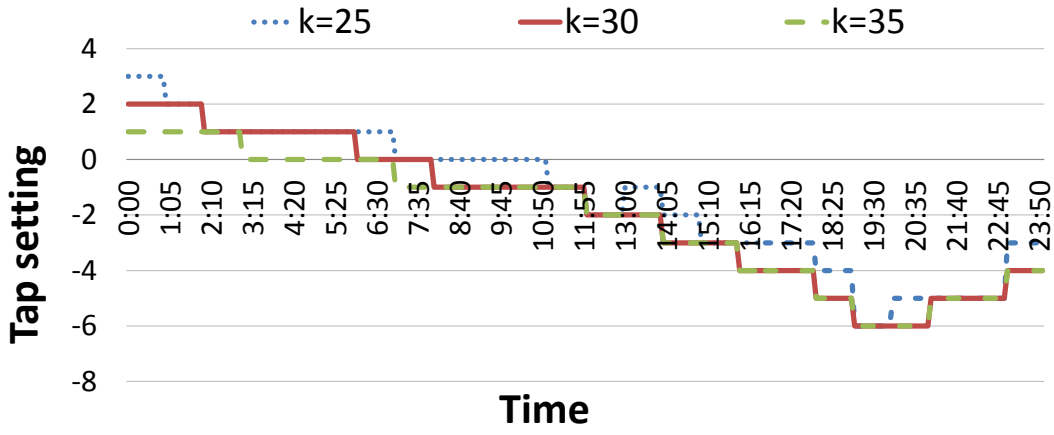

Figure 3.13: Bootstrap results of the hourly tap settings for transformer $T4$ at bus 40 phase b in the real distribution feeder for different sample sizes.

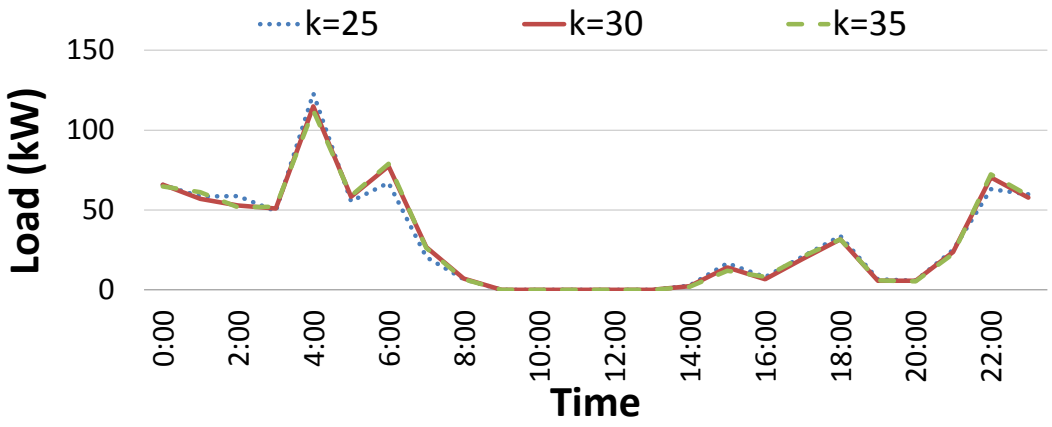

Figure 3.14: Bootstrap estimates of the mean PEV load at bus 41 phase b in the real distribution feeder for different sample sizes.

independent [74].

Table 3.2: Bootstrap estimates of mean daily feeder peak demand for the real distribution feeder for various penetration levels.

Statistic [kW]	**PEV penetration level**			
	30%	**40%**	**50%**	**60%**
Sample mean	13,190.02	13,258.73	13,368.27	13,477.59
Bootstrap mean	13,190.02	13,258.73	13,368.60	13,477.44
Bootstrap σ	11.02	11.24	17.49	16.44
95% CI	[13,167.98, 13,211.92]	[13,236.78, 13,280.71]	[13,335.23, 13,403.01]	[13,445.6, 13,510.45]

For various PEV penetration levels, using a sample size of k=25, the mean of the Bootstrap distribution is very close to the sample mean, as seen in Table 3.2, which also shows that the standard deviation and confidence intervals for the Bootstrap distribution are

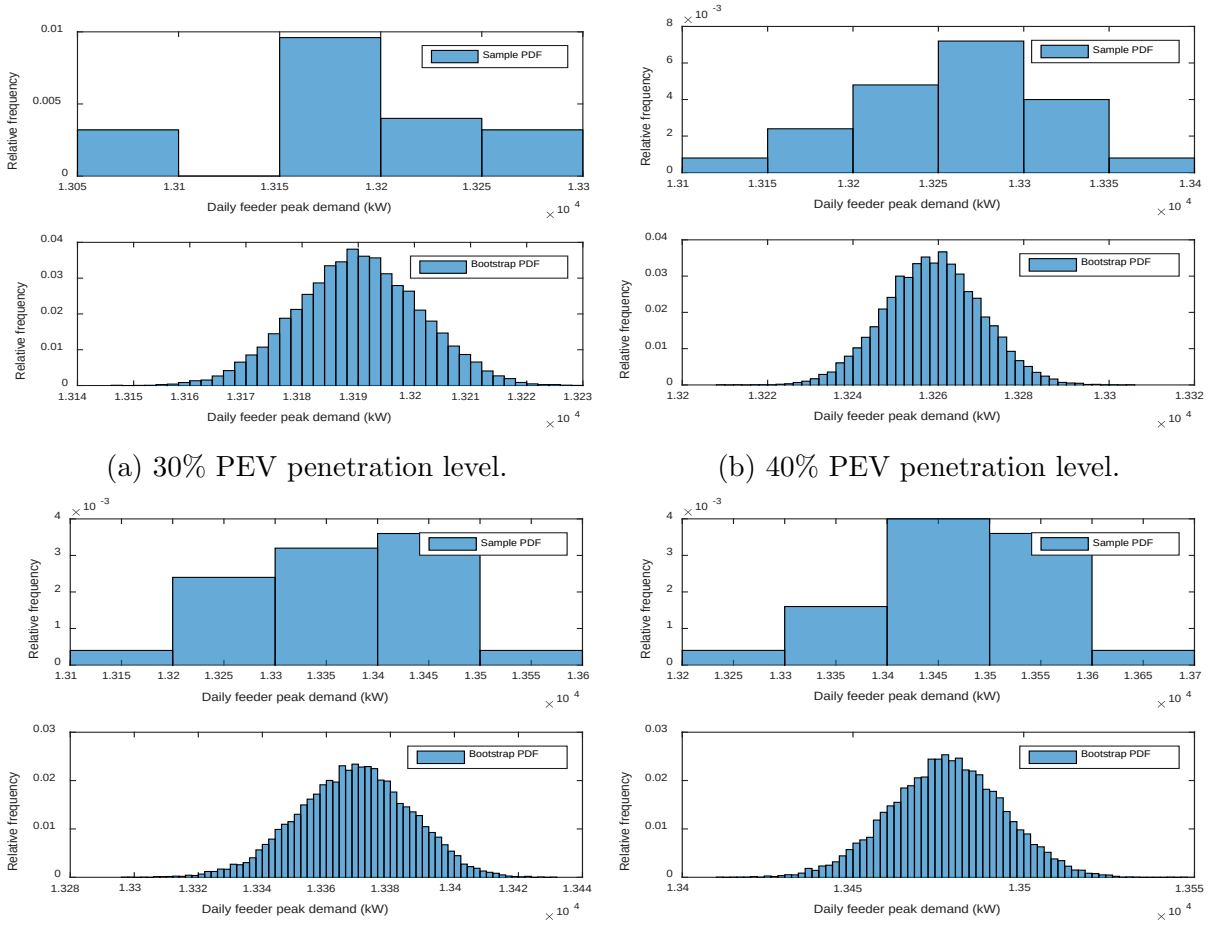

(a) 30% PEV penetration level.

(b) 40% PEV penetration level.

(c) 50% PEV penetration level.

(d) 60% PEV penetration level.

Figure 3.15: Estimation of mean daily system peak demand for the real distribution feeder for various PEV penetration levels.

relatively small. This close proximity of the Bootstrap mean to the sample mean means that the estimated mean of the original sample has almost no bias. Since the distribution of the Bootstrap replicate means is centered at the population mean, this implies that the Bootstrap estimate of the mean is an unbiased estimator of the population mean. In addition, the resulting Bootstrap distribution is approximately symmetrical and continuous; hence, the percentile method is used to compute the Bootstrap CI, while the variance and

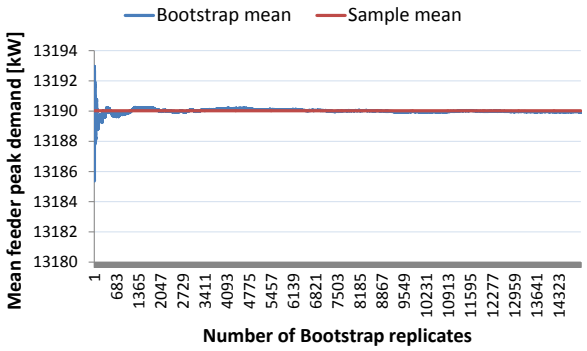

(a) 30% PEV penetration level.

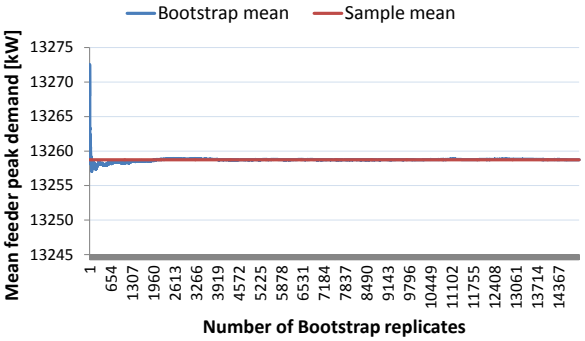

(b) 40% PEV penetration level.

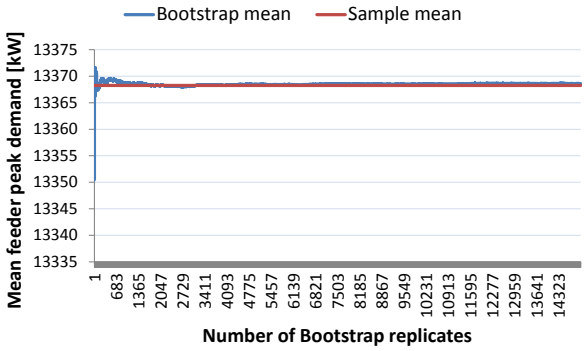

(c) 50% PEV penetration level.

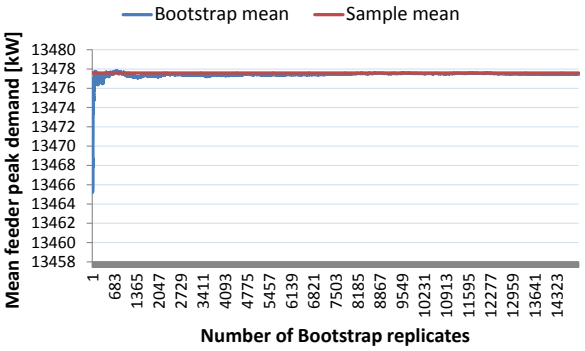

(d) 60% PEV penetration level.

Figure 3.16: Convergence of Bootstrap estimate of the mean daily feeder peak demand with respect to the number of Bootstrap replicates for the real distribution feeder, for various PEV penetration levels.

standard deviation of the mean is the variance and standard deviation of the distribution of the mean. Furthermore, Figure 3.16 shows that, for various PEV penetration levels, the Bootstrap mean converges to the original sample mean as the number of Bootstrap replicates increases. This indicates that the number of Bootstrap replicates taken is large enough to get a good estimate of the statistic.

The Bootstrap estimates of the hourly tap settings are found to be very close to the original sample mean. In addition, simulation results show that the maximum hourly tap

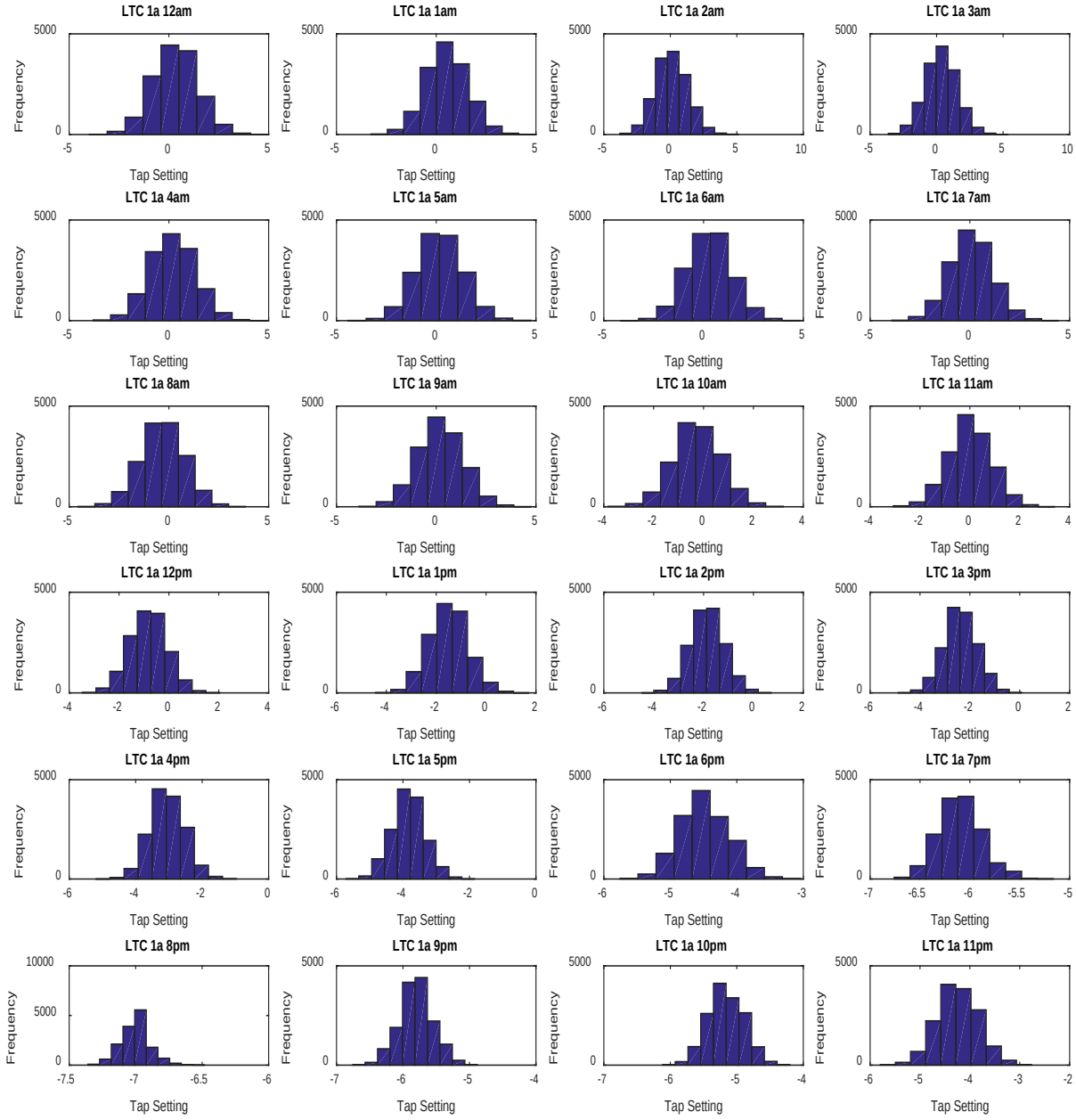

Figure 3.17: Histograms for the tap setting of LTC transformer $T1$ phase a in the real distribution feeder during each time interval.

operations is preserved in the Bootstrap estimate. For a PEV penetration level of 30%, Figure 3.17 presents the histograms for the tap settings of LTC transformer T1 phase a during each time interval, which also approximate to normal p.d.f.s. The histograms of all the other LTC taps are presented in Appendix A. Furthermore, each PEV charging schedule from the original sample is found to be feasible for the Bootstrap feeder control schedule; i.e., no feeder operating limits are violated.

3.5.4 Results For IEEE 13-Bus Test Feeder

Estimation of Mean Daily Feeder Peak Demand and Feeder Control Schedules

A sample size of k=25 is used to compute the mean daily feeder peak demand and the feeder control schedules using the Bootstrap technique for the IEEE 13-bus test feeder, for a PEV penetration level of 60%. As in the case of the real distribution feeder, Figure 3.18 shows that the Bootstrap distribution for the mean daily feeder peak demand approximates to a normal distribution. Figure 3.19 shows the convergence of the Bootstrap mean to the sample mean, as the number of Bootstrap replicates (samples) increases. Table 3.3 shows that the Bootstrap mean is centered around the sample mean, and hence has almost no bias. Furthermore, this table also shows that the standard deviation and confidence intervals for the Bootstrap distribution are small.

The Bootstrap estimates of the hourly tap and capacitor settings are found to be very close to the original sample mean, and their Bootstrap distributions also approximate to normal distributions, as seen in Figures 3.20 and 3.21.

3.5.5 Computational Performance

The proposed approach is implemented using MATLAB [64] and OpenDSS [42], where the former is used to code the optimization and heuristic models, and the latter is used

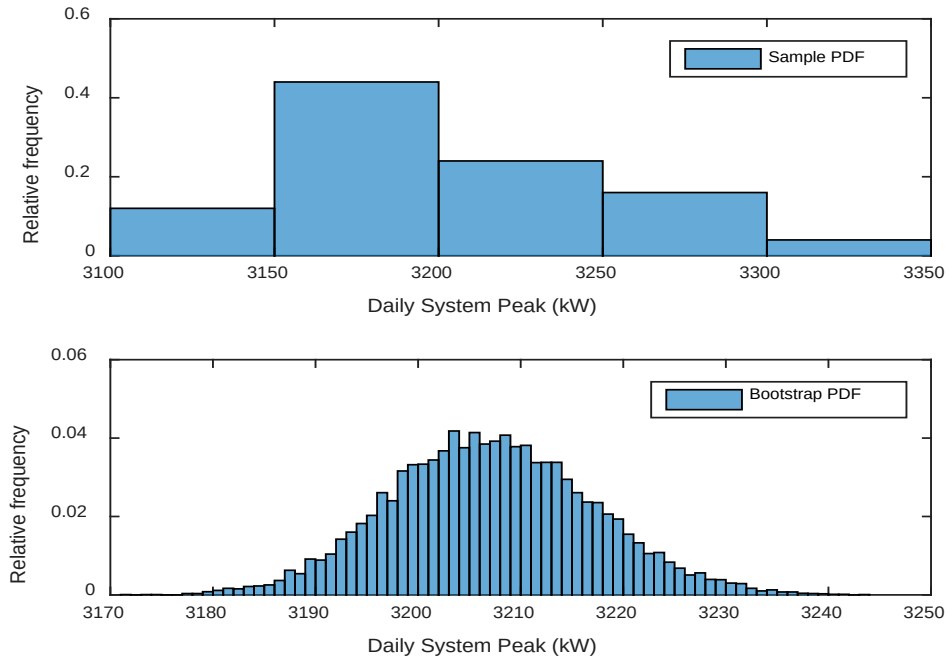

Figure 3.18: Estimation of mean daily system peak demand for the IEEE 13-bus test feeder for 60% PEV penetration level.

Table 3.3: Bootstrap estimates of mean daily feeder peak demand for the IEEE 13-bus test feeder for PEV penetration level = 60%.

Statistic [kW]	**pr=60%, k=25**
Sample mean	3,207.17
Bootstrap mean	3,207.12
Bootstrap σ	9.82
95% CI	[3,187.24, 3,225.94]

for feeder modeling and power flow computations. The execution is carried out on a workstation with Intel Core i7-2600 CPU running at 3.40 GHz and 8 GB RAM.

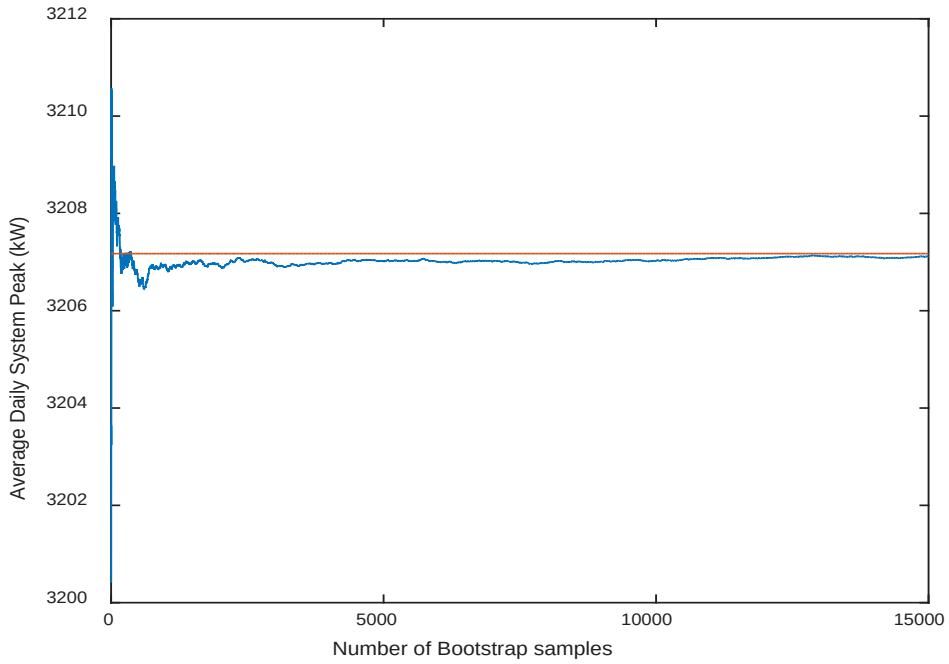

Figure 3.19: Convergence of Bootstrap estimate of the mean daily feeder peak demand with respect to the number of Bootstrap replicates for the IEEE 13-bus test feeder, for 60% PEV penetration level.

- *Real Distribution Feeder*: As every GA solution takes T = 2.5-3.0 h for the real distribution feeder, the MCS approach with a GA-based optimization model would be infeasible to implement in practice, thereby requiring 37,500-45,000 h of computation time for 15,000 samples. However, using the Bootstrap technique reduced the computation times significantly to (kT/NC) h, where NC is the number of computers. Thus, for NC=1, it took 63-75 h for k=25 to run the full 24 h simulation; to obtain a solution in a reasonable 3 h, it would require NC=k=25 desktops, or a multiprocessor server.

- *IEEE 13-Bus Test Feeder*: Similarly, for the IEEE 13-bus test feeder, every GA solution takes T = 1.0-1.5 h, hence 15,000-22,500 h of computation time would be required for 15,000 samples. Using the Bootstrap technique, this time was reduced

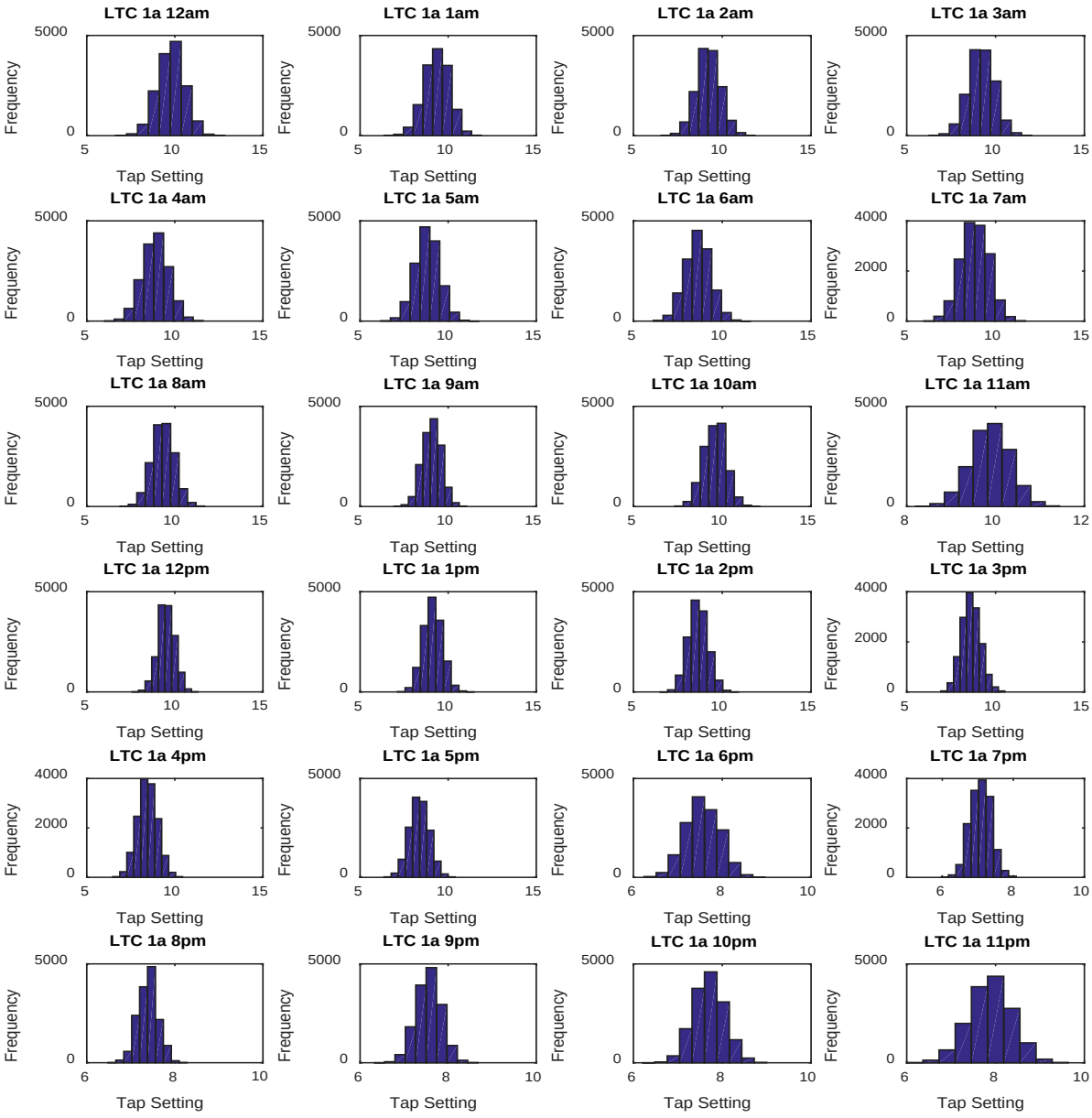

Figure 3.20: Histograms for the tap setting of LTC transformer $T1$ phase a in the IEEE 13-bus test feeder during each time interval.

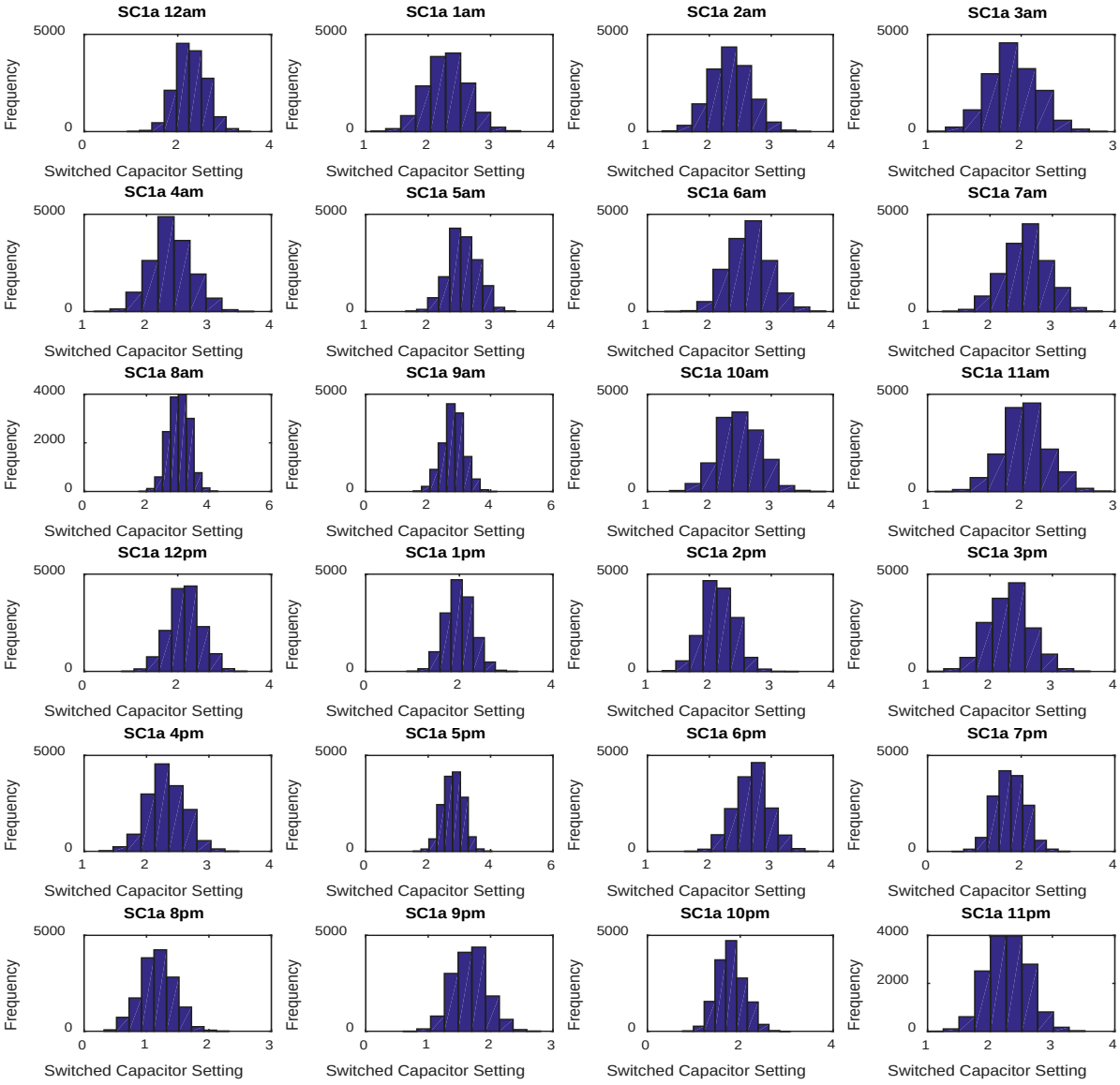

Figure 3.21: Histograms for the tap setting of switched capacitor $C1$ phase a in the IEEE 13-bus test feeder during each time interval.

to 25-38 h (NC=1).

3.6 Summary

This chapter presented the problem formulation for the proposed two-step approach, including the first step, i.e., the day-ahead dispatch of distribution feeders to compute the hourly feeder control schedule, as well as the daily feeder peak demand, with the objective of minimizing the daily peak demand, while considering PEV uncertainties based on a Bootstrap approach. A detailed description of the methods used in this step, i.e., the GA-based optimization model, and the Bootstrap estimation, was presented. The results for the day-ahead dispatch of distribution feeders were also discussed and analyzed for a real test feeder and the IEEE 13-bus test feeder, which were described in detail, together with the assumptions made. The discussions on the impact of sample size on Bootstrap estimates, and the estimation of mean daily feeder peak demand and feeder control schedule show that the resulting sampling distributions of the feeder daily peak demand, charging PEV loads and LTC taps approximately resulted in normal distributions, and that the sample size used was sufficiently large. In addition, the Bootstrap method using the GA model was shown to be able to significantly reduce the computational burden, hence demonstrating the feasibility of the proposed approach. The fair charging of PEVs, which is the second step of the proposed approach, is presented in the next chapter.

Chapter 4

Fair Charging of PEVs Considering PEV Uncertainties

Nomenclature

Indices

N	Total number of nodes in the system
LN	Number of load nodes in the system
B	Number of feeders in the system
n	Node index
b	Feeder index
t	Time interval index
i	LTC tap index
j	Switched capacitor index
k	Number of elements in the sample
l	Vehicle index

Parameters

τ_1,τ_2	Time steps
$\overline{\|I\|}_b$	Current carrying capacity of feeder [A]
$\underline{V}_n$	Minimum voltage limit [p.u.]
$\overline{V}_n$	Maximum voltage limit [p.u.]
nev_n	Number of PEVs
Mcp_l	Maximum limit of single charging point [kW]
Mop	Maximum control operations per hour for taps (Mop_{tap}) and capacitors (Mop_{cap})
$\overline{Pcp}_n$	Charging point limit of aggregate PEV load [kW]
$\|V^{bc}\|_n$	Base case voltage magnitude [p.u.]

Variables

δ_n	Voltage angle [rad]
P_n^{bl}	Base load active power demand [kW]
P_n^{pev}	PEV load active power demand [kW]
$\|I\|_b$	Magnitude of feeder current [A]
$\|V\|_n$	Magnitude of node voltage [p.u.]
J	Jacobian matrix
Q_n	Reactive power demand [kVAr]
P_n	Real power demand [kW]
$\Delta\|V\|_n$	Available voltage margin [p.u.]
ΔP_n^{pev}	Change in PEV load [kW]
$\Delta\delta_n$	Change in node voltage angle [rad]
ΔQ_n	Change in reactive power demand [kVar]
$E[P^{max}]$	Bootstrap estimate of daily feeder minimum peak demand [kW]
$E[Con]$	Bootstrap estimate of hourly feeder control schedule
P^{total}	Total feeder active power demand [kW]

4.1 Introduction

The hourly feeder controls $E[Con]$ computed in the first step of the day-ahead dispatch, discussed in the previous chapter, are assumed fixed in the second step, presented in this chapter. This step concentrates on the aggregated PEV charging control performed periodically every τ_2 interval (every few minutes) at each node, and is implemented using a GA-based optimization approach. The power allocated to aggregate PEV loads is computed every few minutes (e.g., 5 minutes), to be applied for the next time interval, and hence, this computation has to be fast.

The current industry practice in Ontario is to charge PEVs without the use of any coordinated charging strategy, i.e., maximum possible power is allocated to the PEVs, and LTC taps and capacitors are adjusted automatically to maintain node voltages within operating limits. In addition, a popular sensitivity-based heuristic approach is also discussed here. Hence, the performance of the proposed technique is compared with the current industry practice and the heuristic approach, to highlight its feasibility and advantages.

The remainder of this chapter is organized as follows: A fair PEV charging technique is proposed in Section 4.2, which is fast, fair to all aggregated PEV loads, and does not impact the feeder operation and control. Next, Sections 4.3 and 4.4 discuss the current industry practice in Ontario and a popular heuristic approach, respectively, and the performance of the proposed technique is compared with them. Finally, the results for the fair charging of PEVs, which is the second step of the proposed approach, as well as its computational performance, are discussed and analyzed for the test feeders used in this thesis.

4.2 Optimization Approach

Considering the perspective of PEV customers, the utility faces the challenge of allocating limited amount of power or resources among all the PEV customers without exceeding the daily feeder peak demand, and with the feeder controls remaining fixed for the day.

Aggregate PEV loads at some nodes of a radial primary distribution feeder may be at a disadvantage compared to others in the same feeder due to their location which affects node voltages across the feeder; thus, an increase in power to some PEV loads would come at the expense of reducing power delivered to other loads. Hence, this work focuses on a well-accepted notion of fairness in the area of telecommunications and networks, known as proportional fairness scheduling [84]. Proportional fairness scheduling provides a balance between two competing interests, i.e., maximizing the total power delivered to the aggregate PEV loads, as well as providing a minimum level of power to all PEV loads connected for charging.

Based on the previous discussion, the objective is to maximize the charging of connected PEV loads in a fair manner using the proportional fairness scheme, for each time interval τ_2, as follows:

$$\max \left\{ \prod_{n=1}^{N} \left\{ \frac{P_n^{pev}}{\overline{Pcp}_n} \right\} \right\} \quad \forall\, nev_n \neq 0 \tag{4.1}$$

The ratio of P_n^{pev} to $\overline{Pcp}_n$ achieves its maximum value of 1, if $P_n^{pev} = \overline{Pcp}_n$. Hence, by maximizing the product of these ratios, the objective function maximizes the power delivered to the charging PEVs at each node, and provides a minimum level of service to all nodes where there are PEVs to charge.

The constraints of the proposed optimization model are as follows:

- *System limits*: The physical and operational limits of the system, i.e., power delivered to the PEV at the charging point, as well as the node voltage and feeder current limits, are considered, as follows:

$$0 \leq P_n^{pev} \leq \overline{Pcp}_n \quad \forall\, n = 1, ..., LN \tag{4.2}$$

$$\underline{V}_n \leq |V|_n \leq \overline{V}_n \quad \forall\, n = 1, .., LN \tag{4.3}$$

$$0 \leq |I|_b \leq \overline{|I|}_b \quad \forall\, b = 1, .., B \tag{4.4}$$

where

$$\overline{Pcp}_n = \sum_{l=1}^{nev_n} Mcp_l \quad \forall\ n = 1, .., LN \tag{4.5}$$

- *Power flows*: The power flows are determined using OpenDSS [42].
- *Peak demand constraint*: This constraint ensures that the total feeder load does not exceed the peak demand setpoint $E[P^{max}]$ computed in the first step, as follows:

$$\sum_{n=1}^{N} \left(P_n^{bl} + P_n^{pev}\right) \leq E[P^{max}] \tag{4.6}$$

Note that the feeder controls are fixed at the values $E[Con]$ determined in the first step. This optimization problem is also solved using GA, so that power flows can be readily computed using an external solver; in this work, the external power flow solver used is OpenDSS.

4.3 Current Industry Practice

In North America, the current industry practice is to provide whatever power is required by the charging PEVs, while trying to maintain node voltages within operating limits through automatic regulation of LTC taps and capacitors [85]. The real distribution feeder used in this thesis has no switched capacitors, and hence, in this case, only LTC taps are considered for feeder voltage regulation. However, the IEEE 13-bus test feeder has both LTC taps and switched capacitors. In this case, feeder voltage regulation is done by increasing or decreasing the reactive power injected by switched capacitors, and the LTC taps are used only if the switched capacitors have reached their upper or lower physical limits and the feeder is still operating outside its limits.

Typically, the up or down voltage regulation using LTC taps is performed based on the node voltages at the midpoint of the feeder, i.e., if the voltage at this node is higher or lower than the maximum or minimum voltage threshold, the taps are adjusted until

this node voltage is within the operating limits; however, for the test feeders used in this work, this approach results in voltage violations in the most remote nodes. Hence, these farthest nodes are used here as the voltage regulated nodes, while still maintaining all nodes downstream from the voltage regulator within operating limits. This may result in frequent tap changing operations, which can decrease the lifetime of LTC taps in the real distribution feeder. Furthermore, the maximum power given to the PEVs at a node is limited by the charging point threshold.

4.4 Heuristic Approach

The sensitivity-based heuristic approach (e.g. [29, 53]) computes the charging rates of PEVs at each node using the Jacobian matrix J and the available voltage margin. This Jacobian matrix J is computed from the base case (without PEV loads) Y-bus matrix (extracted from OpenDSS [42]), obtained by linearizing the power flow equations. Thus, every τ_2 min, the Jacobian matrix can be calculated as follows:

$$J = \begin{bmatrix} \frac{\partial P}{\partial \delta} & \frac{\partial P}{\partial |V|} \\ \frac{\partial Q}{\partial \delta} & \frac{\partial Q}{\partial |V|} \end{bmatrix} = \begin{bmatrix} J_1 & J_2 \\ J_3 & J_4 \end{bmatrix} \tag{4.7}$$

The base-case Jacobian matrix corresponds to the operating point associated with base loads in the feeder, with PEV load being zero. Changes in active power P_n correspond to changes in PEV load ΔP_n^{pev} at each node, which can be computed as follows:

$$\begin{bmatrix} \Delta P_n^{pev} \\ \Delta Q_n \end{bmatrix} = J \begin{bmatrix} \Delta \delta_n \\ \Delta |V|_n \end{bmatrix} \quad \forall\ n = 1, .., N \tag{4.8}$$

The base-case node voltages $|V^{bc}|_n$ are computed for the known base load at each node, which is then used to calculate the available voltage margin to the lower operating threshold as follows:

$$\Delta |V|_n = \underline{|V|}_n - |V^{bc}|_n \quad \forall\ n = 1, .., N \tag{4.9}$$

In this work, since PEVs are assumed to be purely active power loads, and the node voltage limits only depend on $|V|_n$, then $\Delta Q_n = 0$, and $\Delta\delta_n = 0$. Consequently:

$$\Delta P_n^{pev} = J_2 \ \Delta|V|_n \ \ \forall \ n = 1, .., N \tag{4.10}$$

From (4.10), there may be load nodes where the resulting ΔP_n^{pev} is a negative value or exceeds the charging point limit for the node; these are corrected to $\Delta P_n^{pev} = 0$, since the initial operating point has zero PEV load, and to $\Delta P_n^{pev} = \overline{Pcp}_n$, respectively. In addition, for the nodes, $\Delta P_n^{pev} = 0$ with no PEV loads. The corrected ΔP_n^{pev} is, then, sent to OpenDSS, which computes the actual charging rate allocated to the PEV loads at each node n every τ_2 min.

4.5 Results

4.5.1 Results For Real Distribution Feeder

Optimization vs Heuristic

The performances of the sensitivity-based heuristic and the optimization approaches in allocating maximum possible power to the charging PEVs at a 30% PEV penetration level, while considering the operational and physical limits of the feeder, are compared in Figure 4.1. It is clear that the optimization approach performs better than the heuristic approach in satisfying the feeder and peak demand constraints, especially during the peak hours. Observe that the load profile obtained using the heuristic approach violates the peak demand value $E[P^{max}]$; however, the latter does not violate the node voltage limits at the farthest node in the feeder, which is heavily loaded, i.e., bus 41 phase c, as seen in Figure 4.2.

In addition to the $E[P^{max}]$ violation, the heuristic approach also violates the voltage operational limits of the feeder during the peak hours, i.e., from 7 pm to 9 pm, as seen in

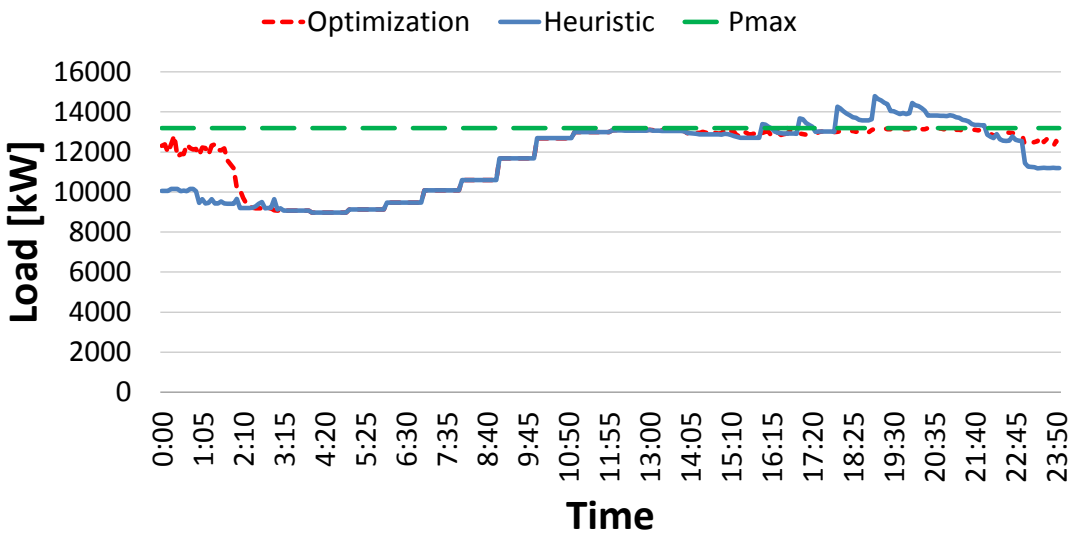

Figure 4.1: System load profile comparison between the optimization and sensitivity-based heuristic approaches for the real distribution feeder.

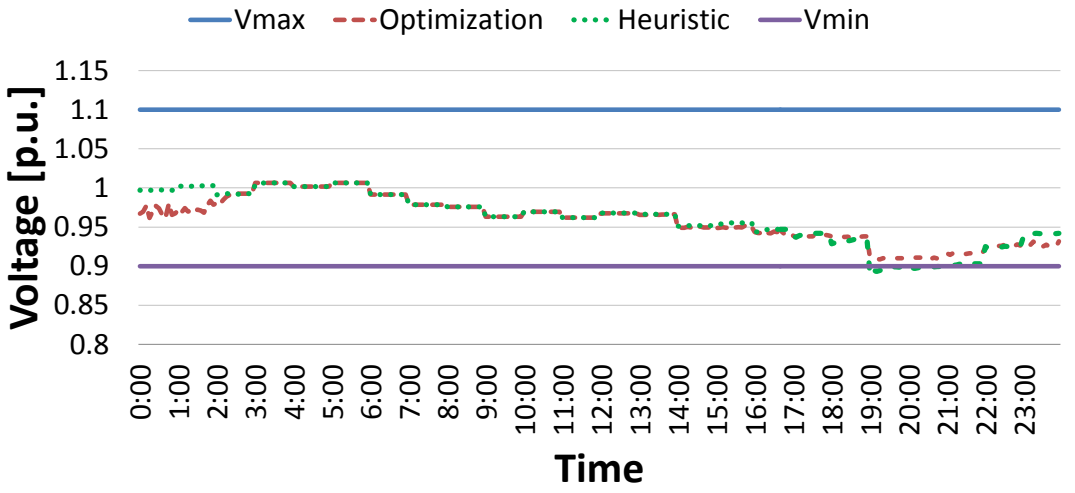

Figure 4.2: Voltage profile comparison between the GA-based optimization and sensitivity-based heuristic approach for the farthest node in the real distribution feeder, i.e., bus 41 phase *c*.

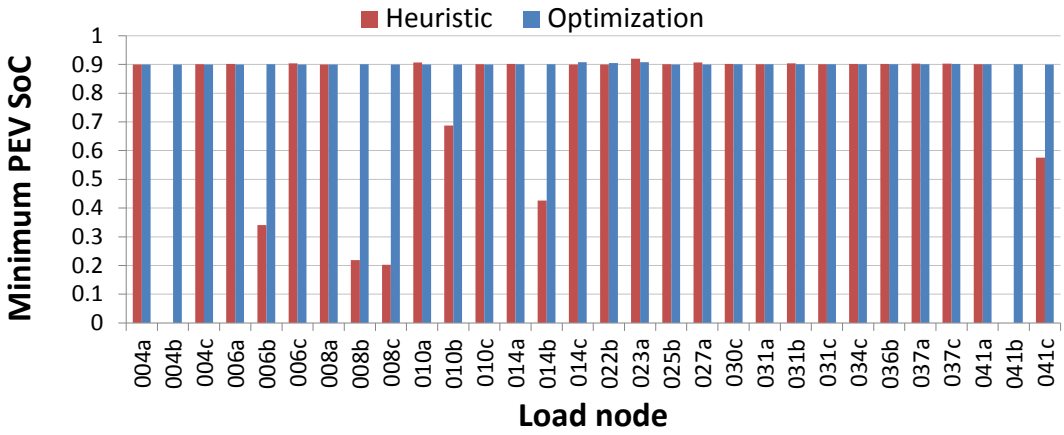

Figure 4.3: Minimim PEVs' SoC at load nodes at the end of the charging period using the optimization and heuristic approaches for the real distribution feeder.

Figure 4.2. This is because the heuristic approach is based on a linearization of the power flow equations around operating points, and thus it only works for a small range of voltages around the base case. Furthermore, Figure 4.3 shows that the optimization approach is able to charge all the PEVs to the desired battery SoC level at the end of the charging period, while the heuristic approach fails to do the same.

Optimization vs Base Schedule and Current Practices

Other methods for operating feeder controls to maintain node voltages within the feeder operating limits are compared to the proposed technique in this section, in particular, with respect to the current industry practice of automatic voltage regulation, and a feeder control strategy obtained from a base schedule with no PEVs. The base schedule has the advantage to be a best case scenario in terms of risks, since there is no possibility of under or overvoltages, but it potentially may not be able to charge all the PEVs to the desired battery SoC level, as the penetration level increases. Indeed, a consequence of choosing the Bootstrap feeder control schedule is that there is a possibility that the actual aggregated

PEV load may be higher or lower than the expected value, and hence there is a risk of under or overvoltage, respectively.

- *Impact on PEV Charging Time, Feeder Peak Demand, and Final Battery SoC*: The base schedule, Bootstrap schedule, and automatic regulation are applied to 20 randomly generated realizations of initial battery SoC, and arrival and departure times of individual PEVs at each node, for PEV penetration levels of 30%, 40%, 50%, and 60%. Figure 4.4 shows that as the PEV penetration level increases, it takes more time to charge all the PEVs using the base schedule compared to the Bootstrap schedule. Furthermore, Figure 4.5 shows that as the PEV penetration increases, the charging time difference increases until it reaches saturation; this is because the base schedule is not able to deliver the expected energy to all PEVs within the charging period, as the PEV penetration level increases. For a PEV penetration level of 30%, the difference in charging time is not significant, which means that the base schedule may be sufficient for the day-ahead dispatch of feeders with low-to-medium PEV penetration levels. However, for high PEV penetration levels, it may be more advantageous to use the Bootstrap schedule (feeder control schedule computed using the Bootstrap technique, as previously described in Chapter 3).

  In the case of automatic regulation, for all the PEV penetration levels, the PEVs finish charging in a short period of time, compared to the base and Bootstrap schedules; however, this is at the cost of significant increase in the daily feeder peak demand, as can be seen in Figure 4.6. In addition to higher feeder peak demands, voltage limit violations are also seen at load nodes, particularly at higher PEV penetration levels, which are discussed later.

  In terms of the final battery SoC of PEVs, for low PEV penetration levels, all the vehicles are able to achieve the desired final battery SoC at the end of the charging period using any of the feeder control methods. However, at medium-to-high PEV penetration levels, there are instances when the base schedule is unable to charge all the PEVs to the desired SoC level, as shown in Figure 4.7. This is because, as the PEV

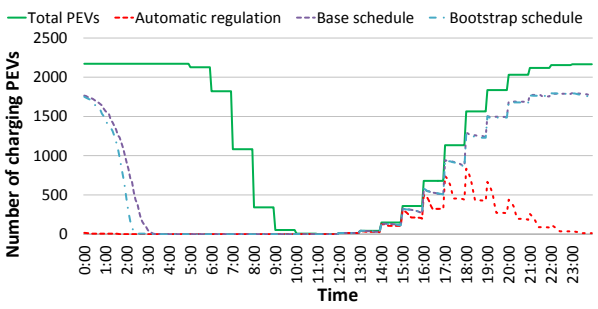

(a) 30% PEV penetration level.

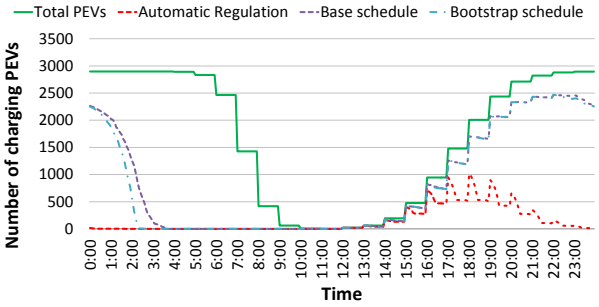

(b) 40% PEV penetration level.

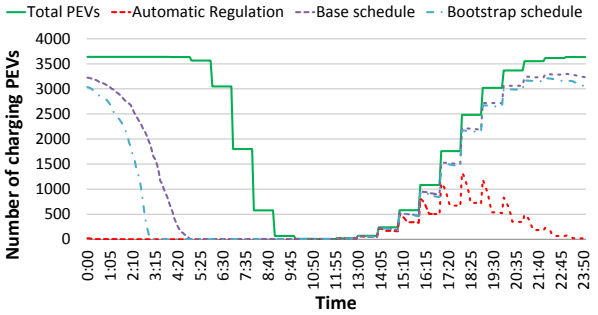

(c) 50% PEV penetration level.

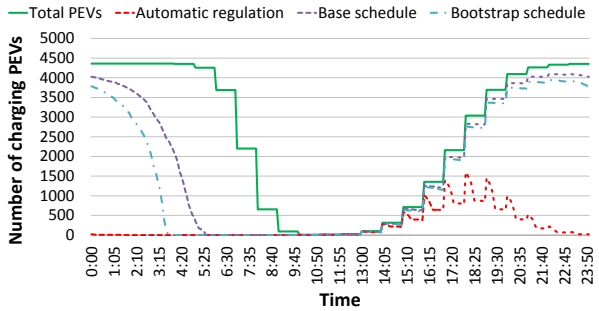

(d) 60% PEV penetration level.

Figure 4.4: Comparison of the number of charging PEVs in each interval for the real distribution feeder for various PEV penetration levels.

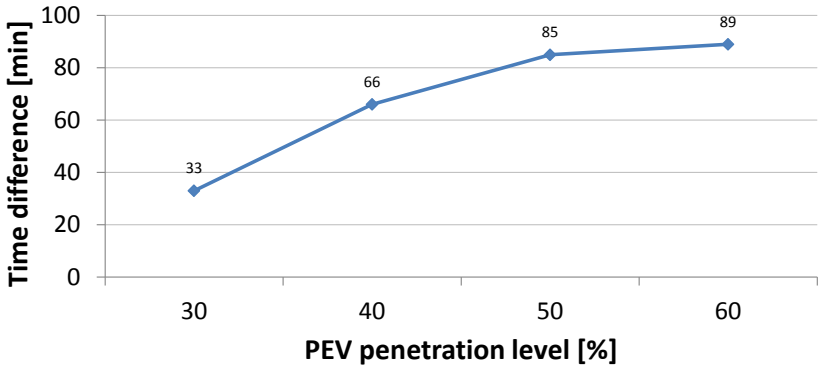

Figure 4.5: Difference in time taken by the base and Bootstrap schedules to charge all the PEVs for the real distribution feeder.

penetration level increases, it takes longer to charge the PEVs using the base schedule, resulting in some instances of PEVs departing before being fully charged. Hence, based on the above discussion, charging the PEVs using the Bootstrap schedule outperforms both the base schedule and automatic regulation, in terms of charging time, achieving final battery SoC, and maintaining the feeder operating limits.

- *Impact of Estimated Aggregated PEV Load and Feeder Control Method on Node Voltages*: The impact of the estimated aggregated PEV load can be analyzed in two ways. If the aggregated PEV load is higher than the expected value, the power given to the aggregated PEVs at each node will be lower than it could be, and hence, this would impact the total energy delivered to the PEVs. On the other hand, if the aggregated PEV load is less than the expected value, then there is a risk of overvoltage, which is undesirable from the utility perspective, and hence the optimization will not be feasible, since the voltages would not meet the node voltage limit constraints. The risk of overvoltage can be alleviated at the cost of reducing the total energy delivered to the PEVs, by using the base feeder control schedule (without PEVs).

  For PEV penetration levels of 30%, 40%, 50%, and 60%, the base schedule, Bootstrap schedule, as well as the current industry practice in Ontario, i.e., automatic voltage

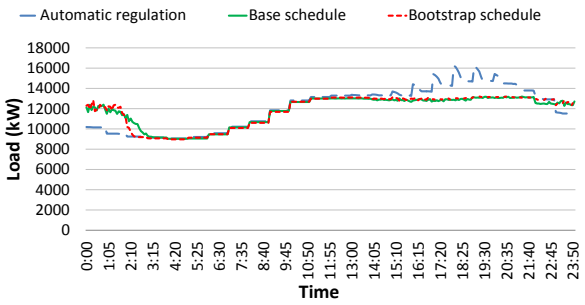

(a) 30% PEV penetration level.

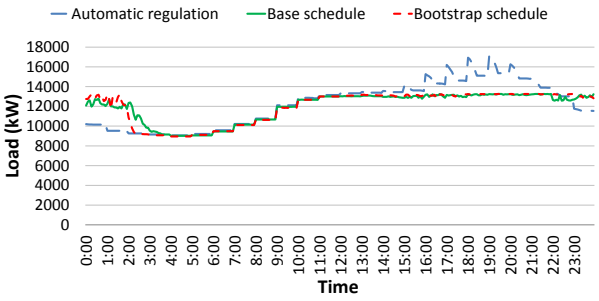

(b) 40% PEV penetration level.

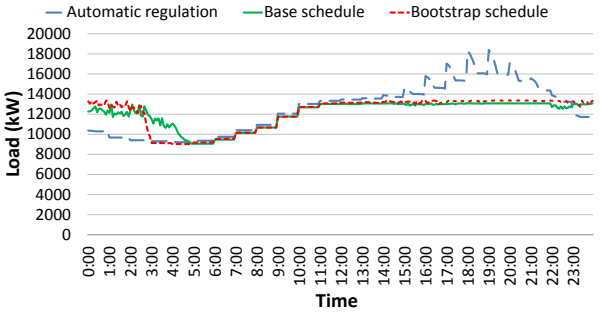

(c) 50% PEV penetration level.

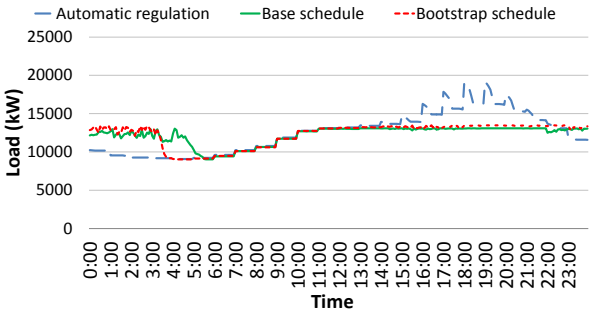

(d) 60% PEV penetration level.

Figure 4.6: Comparison of feeder load profiles for the real distribution feeder for various PEV penetration levels.

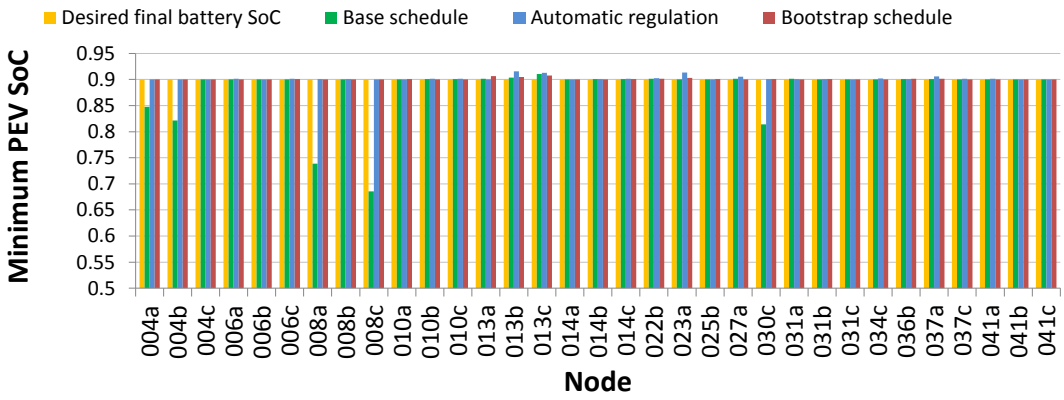

Figure 4.7: Minimim final battery SoC per load node at the end of the charging period for the real distribution feeder for a PEV penetration level of 60%.

regulation with no PEV charging control, are used to charge the PEVs in a fair manner, for the 20 randomly generated realizations of initial battery SoC, and arrival and departure times of PEVs. The results here show that for the test feeder, even in the extreme case of no charging PEVs, while using the Bootstrap and base feeder control schedules, no instances of overvoltage occurred at any of the load nodes over the 24 h period for any of the generated realizations. However, the results for the current industry practice show that voltage violations occur at buses located before transformer $T2$, mostly in phases a and c. This is because of the absence of any voltage control mechanisms in that section of the feeder, and the nodes selected for voltage control in the feeder, which in this case are the farthest nodes, per-phase, as previously discussed. Nevertheless, there may be a loading condition for this test feeder in which overvoltage may occur, as there are no voltage control mechanisms considered in the second step. Furthermore, it is seen that as the PEV penetration level increases, more nodes violate the minimum voltage limit for automatic regulation. Thus, for a PEV penetration level of 30%, violations occured only for bus 14 phase a for the automatic regulation case for all the generated realizations, as observed in Figure 4.8, whereas Figure 4.9 shows more buses violating the voltage

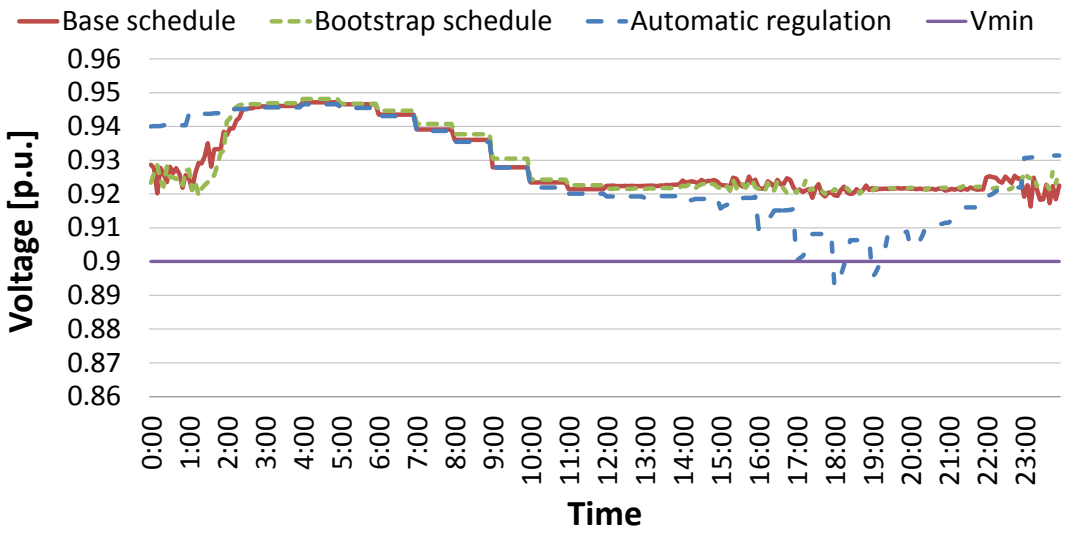

Figure 4.8: Voltage profile comparison of bus 14 phase a in the real distribution feeder for a PEV penetration level of 30%.

limits for a 60% PEV penetration level.

- *Impact on Number of Control Operations*: The choice of feeder control schedules to charge PEVs has an impact on the number of control operations. The test feeder used in this thesis does not have any capacitors, and hence, the discussion is limited to tap operations; however, this discussion can be extended to capacitors in a similar manner. Thus, Figure 4.10 presents the 24 h tap schedule using automatic regulation, base schedule, and the Bootstrap schedule, for various PEV penetration levels, showing that the base schedule has the highest number of tap changes at all PEV penetration levels, while the number of tap changes using automatic regulation are the lowest, with the exception of 60% penetration level. However, the number of tap operations for the Bootstrap schedule are in between the two extremes, except for 60% penetration level, in which case it is the lowest. This is because the base and Bootstrap schedules are optimized, as previously discussed, for minimum feeder peak demand, without voltage violations at any load node; on the other hand, automatic

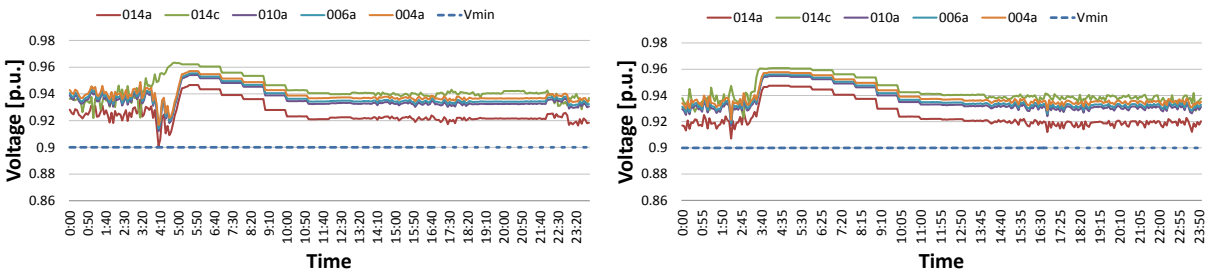

(a) Base schedule.

(b) Bootstrap schedule.

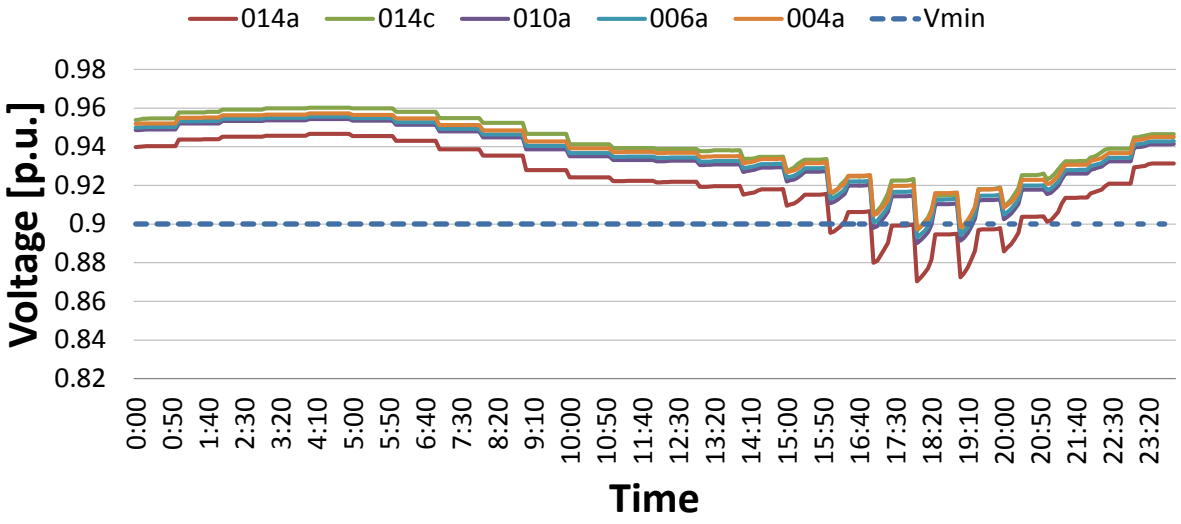

(c) Automatic regulation.

Figure 4.9: Voltage profile comparisons for the real distribution feeder for a PEV penetration level of 60%.

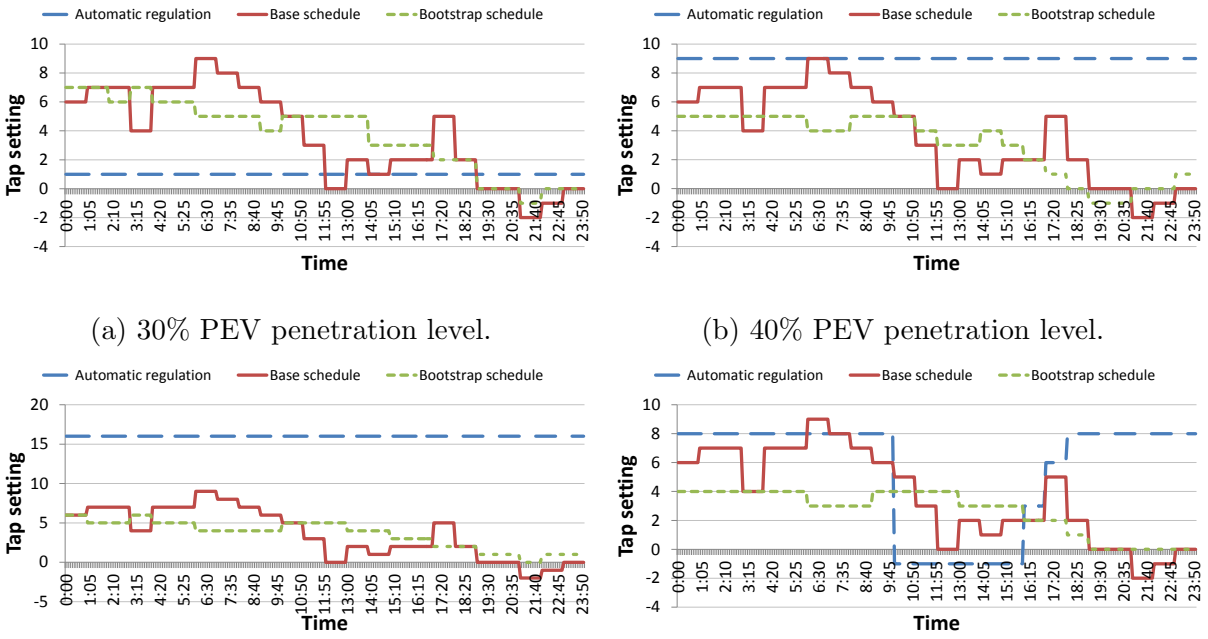

(a) 30% PEV penetration level.

(b) 40% PEV penetration level.

(c) 50% PEV penetration level.

(d) 60% PEV penetration level.

Figure 4.10: Comparison of tap operations at transformer $T4$ phase c in the real distribution feeder for various PEV penetration levels.

regulation results in voltage violations at some nodes, and hence does not operate the feeder in an optimal manner.

Bootstrap Schedule vs Optimal Schedule

The peak demand value and feeder control schedule obtained using the Bootstrap technique may be the best choice for all possible realizations; however, these values may not be the optimal solution for a given realization. Hence, for this realization at 30% and 60% PEV penetration levels, the Bootstrap and optimal feeder control schedules are used to compute the peak demand values, PEV charging profiles, and voltage profiles, to evaluate the deviation of the Bootstrap results from the optimal solution. Thus, Figure 4.11 shows

that the PEV charging profiles for the Bootstrap and optimal feeder control schedules are approximately the same for 30% and 60% PEV penetration levels. Observe that, at 30% PEV penetration level, the feeder peak demands for both schedules are approximately the same (0.37% difference), while at the 60% PEV penetration level, there is a small difference of 1.9% between the two peak demands. Furthermore, Figure 4.12 shows that for both schedules, all the PEVs finish charging at approximately the same time for both PEV penetration levels. Hence, the deviation of the Bootstrap solution from the optimal is small, with respect to the PEV charging profiles, peak demands, and charging times.

It is important to highlight that the optimal feeder control schedules are quite different from the Bootstrap schedule for the chosen PEV penetration levels, as shown in Figure 4.13. As a result, the voltage profiles at the heavily loaded and remote bus 41 phase c also differ a bit, though not significantly, for these two feeder control schedules, as seen in Figure 4.14. Hence, the Bootstrap schedule, though different from the optimal schedule for a particular realization, is an acceptable choice, since it's performance is comparable to the optimal schedule in terms of PEV charging.

4.5.2 Results For IEEE 13-Bus Test Feeder

Optimization vs Base Schedule and Current Practices

As in the case of the real distribution feeder, the proposed technique is compared to other feeder control methods, i.e., the base schedule and the current industry practice of automatic voltage regulation, to validate the performance of the presented approach.

- *Impact on PEV Charging Time, Feeder Peak Demand, and Final Battery SoC*: The base schedule, Bootstrap schedule, automatic regulation are applied to randomly generated realizations of initial battery SoC, and arrival and departure times of individual PEVs at each node, for a high PEV penetration level of 60%. Figure 4.15 shows that for a high PEV penetration level, the base schedule takes a significantly

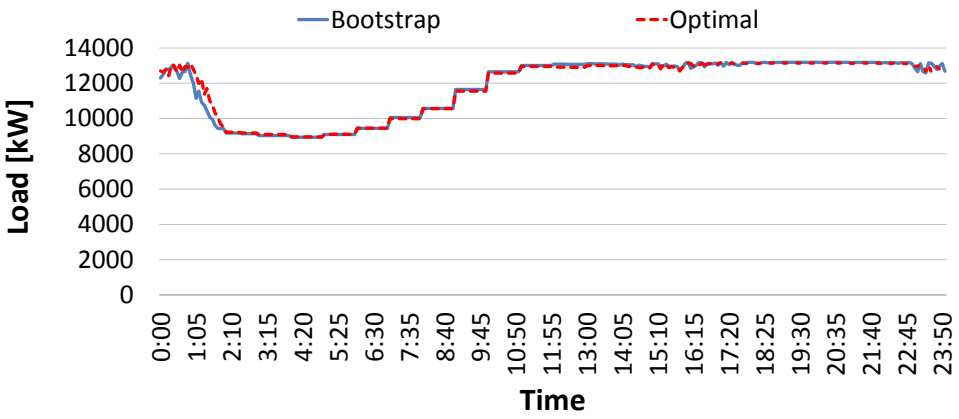

(a) 30% PEV penetration level.

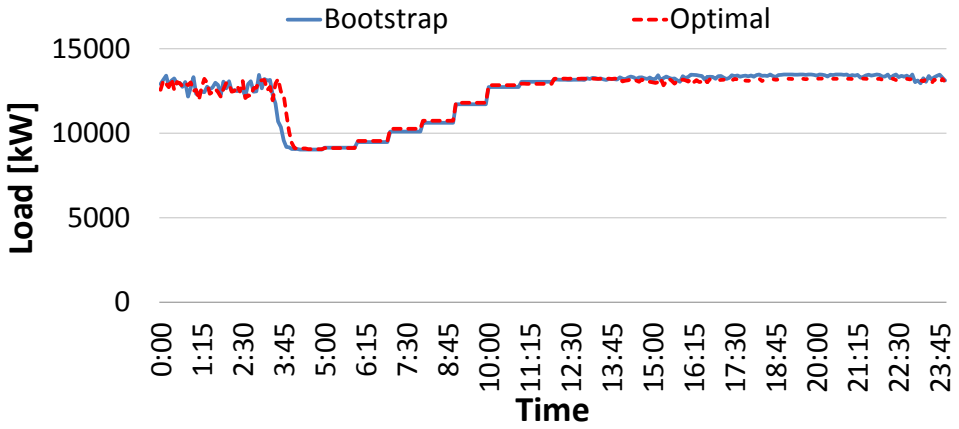

(b) 60% PEV penetration level.

Figure 4.11: System load profile comparison between the optimal and Bootstrap feeder control schedules for the real distribution feeder, for 30% and 60% PEV penetration levels.

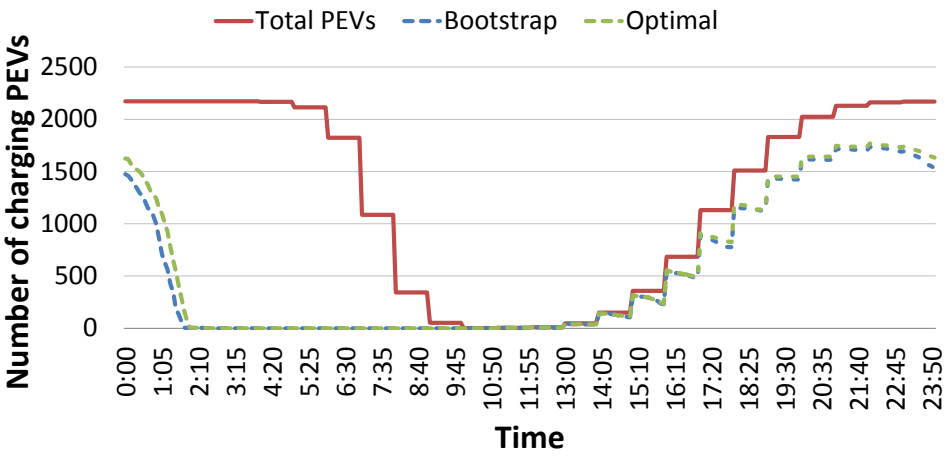

(a) 30% PEV penetration level.

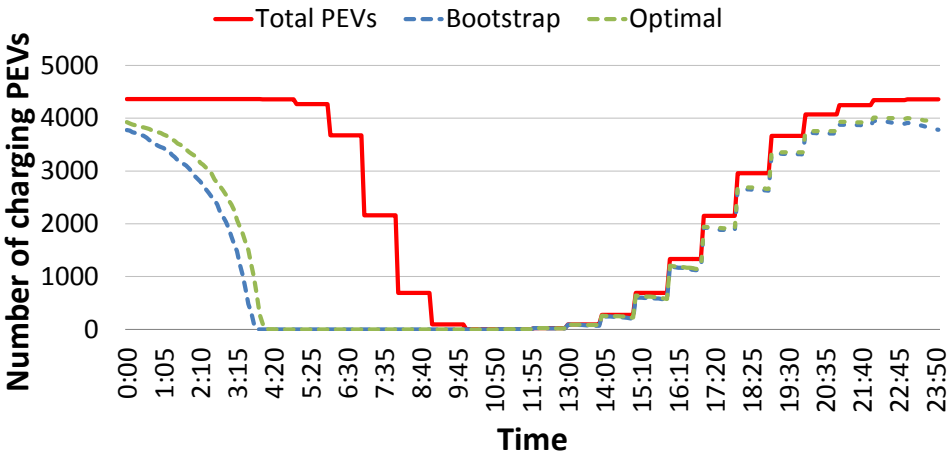

(b) 60% PEV penetration level.

Figure 4.12: Comparison of number of charging PEVs between the optimal and Bootstrap feeder control schedules for the real distribution feeder, for 30% and 60% PEV penetration levels.

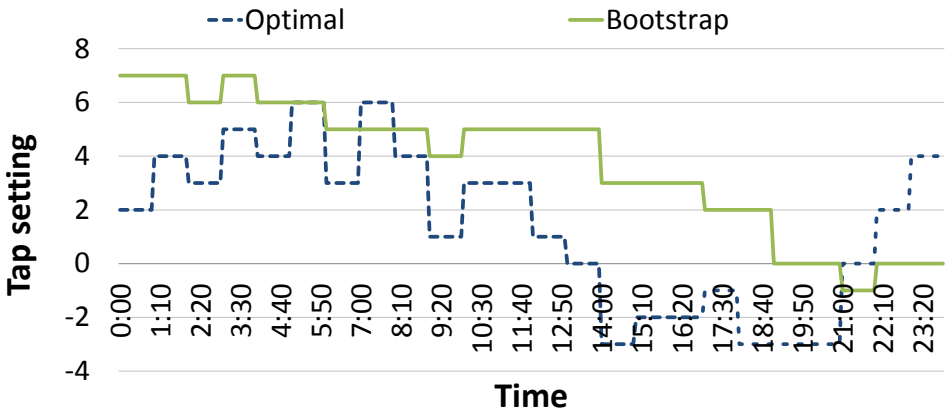

(a) 30% PEV penetration level.

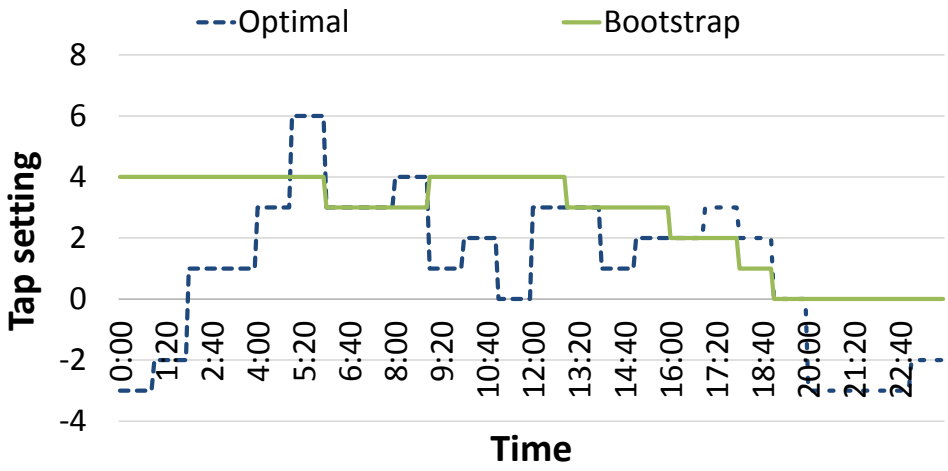

(b) 60% PEV penetration level.

Figure 4.13: Comparison between the optimal and Bootstrap feeder control schedules for transformer $T4$ phase c in the real distribution feeder, for 30% and 60% PEV penetration levels.

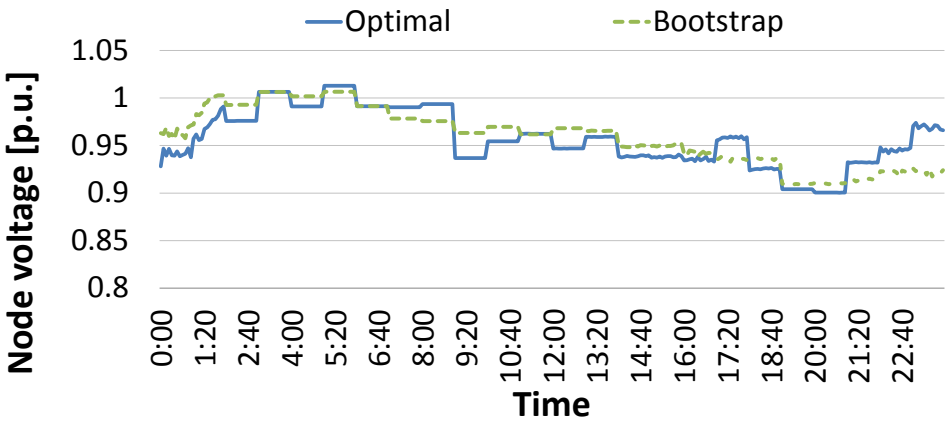

(a) 30% PEV penetration level.

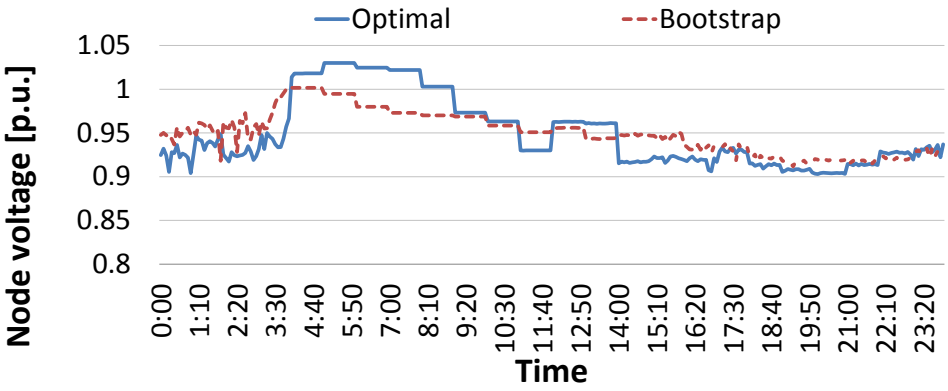

(b) 60% PEV penetration level.

Figure 4.14: Voltage profile comparison between the optimal and Bootstrap feeder control schedules for bus 41 phase c in the real distribution feeder, for 30% and 60% PEV penetration levels.

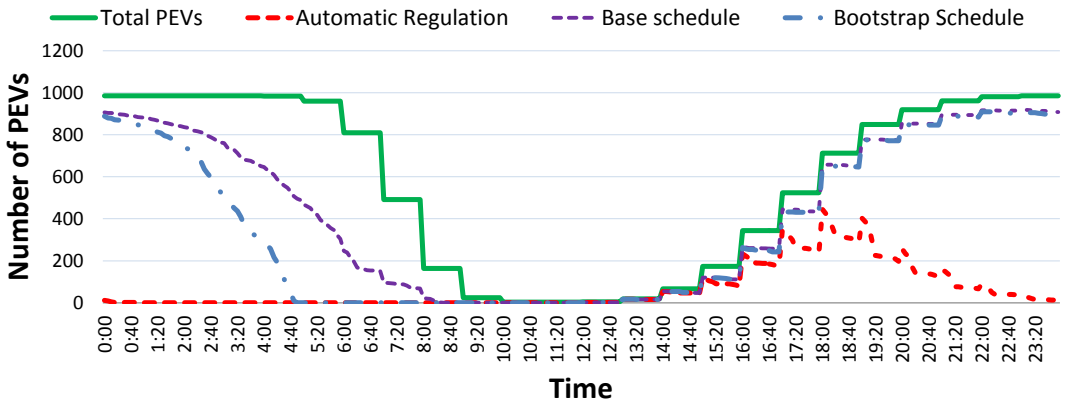

Figure 4.15: Comparison of the number of charging PEVs for the IEEE 13-bus test feeder in each time interval.

longer time to charge the vehicles, compared to the Bootstrap schedule, similar to Figure 4.4. Furthermore, the Bootstrap schedule is able to charge the majority or all of the PEVs to the desired final battery SoC, while the base schedule is unable to do the same (Figure 4.16) resulting in many PEVs departing without being fully charged.

In the case of automatic regulation, it is able to charge all the PEVs to the desired final battery SoC in the shortest time; however, as in the case of the real distribution feeder, this is at the cost of significant peak demand violation, as seen in Figure 4.17.

- *Impact of Estimated Aggregated PEV Load and Feeder Control Method on Node Voltages*: Similar to the case of the real distribution feeder, the results show that even in the case of the IEEE 13-bus test feeder, no instances of overvoltages occurred at any of the load nodes over the 24 h period, while using the base and Bootstrap schedules, even in the extreme case of no PEVs.

  As in the case of the real distribution feeder, there are voltage limit violations at some nodes using automatic regulation, is shown in Figure 4.18. This is because the IEEE 13-bus test feeder has switched capacitors at the remote nodes in addition to

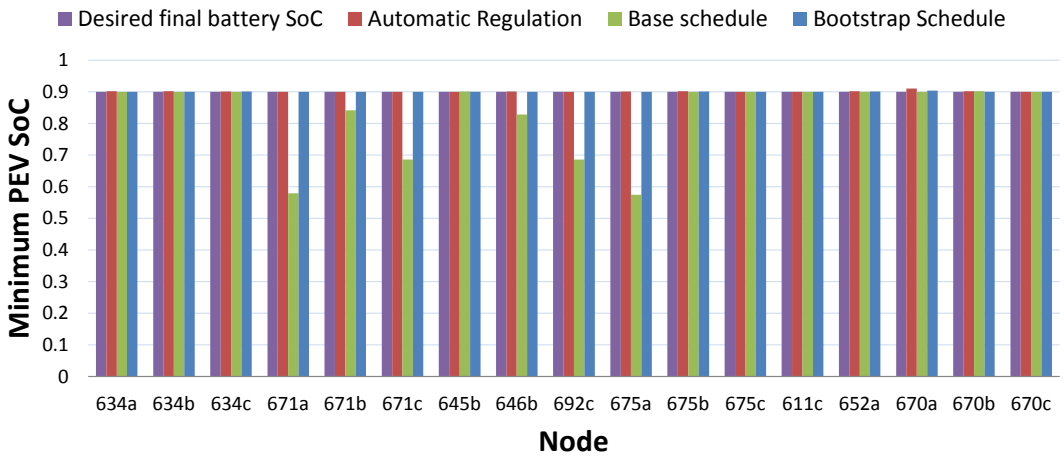

Figure 4.16: Minimim final battery SoC per load node at the end of the charging period for the IEEE 13-bus test feeder for a PEV penetration level of 60%.

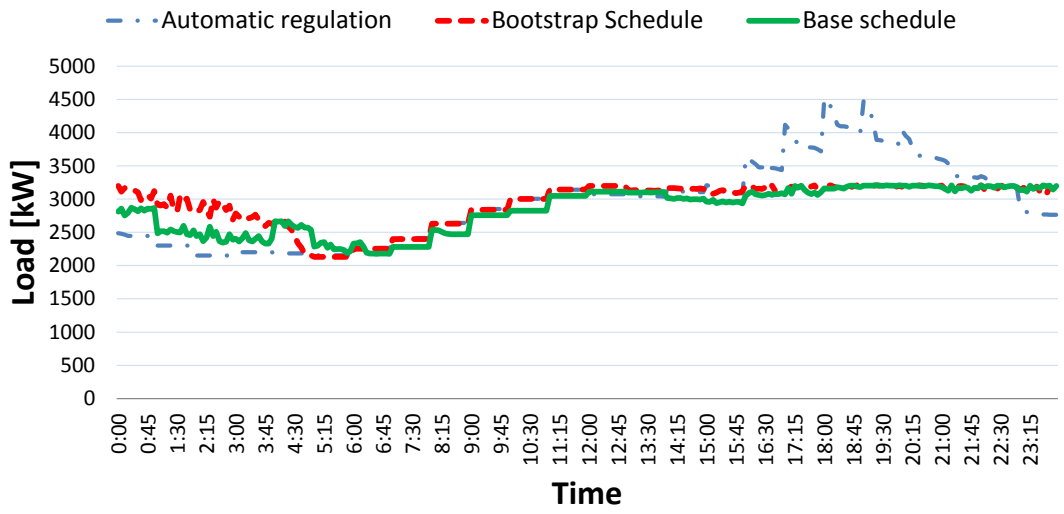

Figure 4.17: Comparison of feeder load profiles for the IEEE 13-bus test feeder at 60% PEV penetration level.

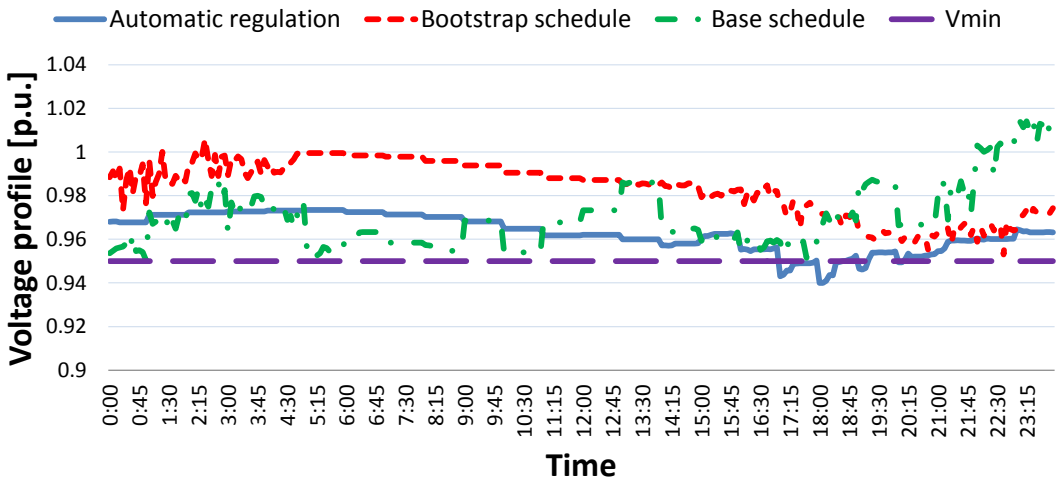

Figure 4.18: Comparison of voltage profiles at bus 634 phase b in the IEEE 13-bus test feeder at 60% PEV penetration level.

LTC taps, which results in better voltage regulation, and the length of this feeder is much smaller compared to the real distribution feeder, which results in a smaller voltage drop at the end of the feeder.

- *Impact on Number of Control Operations*: The choice of feeder control schedules to charge PEVs has an impact on the number of tap and capacitor operations in the IEEE 13-bus test feeder, similar to the real distribution feeder. Figures 4.19 and 4.20 present the 24 h tap and capacitor schedules, using automatic regulation, base schedule, and the Bootstrap schedule, which show that the Bootstrap schedule has the least number of tap and capacitor operations, compared to the other two methods.

4.5.3 Computational Performance

The computation of the day-ahead feeder control schedules faciliates the time-decoupling of the periodic scheduling problem, thereby enabling fast computations. Hence, in the

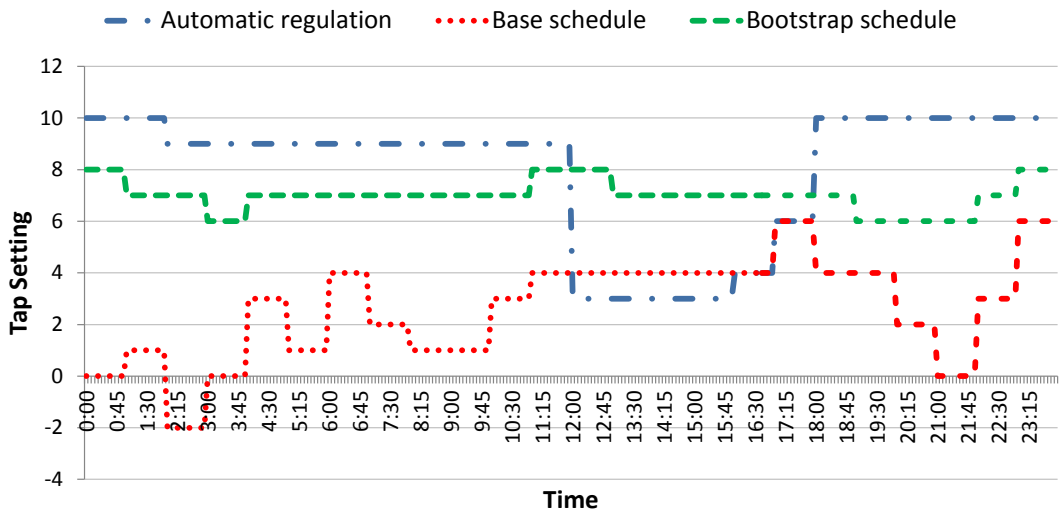

Figure 4.19: Comparison of tap operations for LTC transformer $T1$ phase c in the IEEE 13-bus test feeder at 60% PEV penetration level.

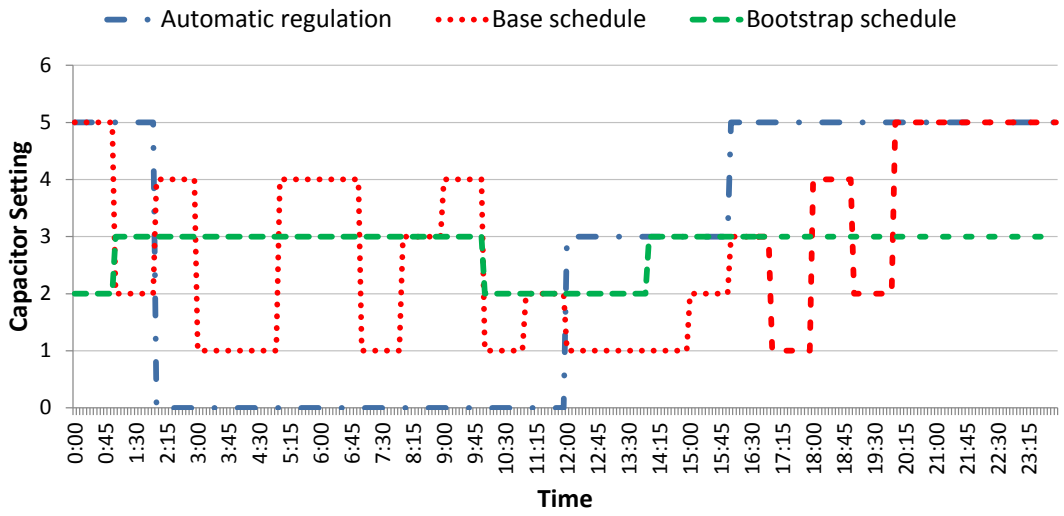

Figure 4.20: Comparison of capacitor operations for Capacitor $C2$ phase c in the IEEE 13-bus test feeder at 60% PEV penetration level.

second step of the proposed technique, the optimization approach on average takes approximately 20-30 s every τ_2, which would clearly be sufficiently fast for computing fair charging schedules of PEVs for the assumed τ_2= 5 min.

4.6 Summary

This chapter presented the second step of the proposed technique, i.e., the fair charging of PEVs. First, a detailed description was provided of the optimization model, which performs the fair charging of PEVs, while considering the distribution feeder operating constraints. A brief overview of the current industry practice in Ontario was then discussed, followed by a popular sensitivity-based heuristic approach for PEV charging and feeder voltage regulation; these other approaches were used to evaluate the performance of the proposed optimization approach. Finally, the results for the fair charging of PEVs for both feeders, as well as its computational performance for various PEV penetration levels, were discussed and analyzed, showing that the optimization technique outperformed the heuristic method in terms of maintaining feeder operating limits and the peak demand constraint. Comparison of the load profiles, voltage profiles, and the feeder control schedules between the Bootstrap estimate and the optimal solution for a particular PEV charging scenario show that the deviation from the optimal is small.

Chapter 5

Conclusions

5.1 Summary

This thesis presented a two-step approach for the fair charging of PEVs, considering the primary distribution feeder characteristics and limitations, and the uncertainties associated with these loads. The motivation for this research was presented in Chapter 1, and the main research objectives and contributions were outlined based on a critical review of the existing literature.

In Chapter 2, a background review of the main concepts and tools relevant to this research on fair charging of PEVs, while considering their uncertainties, is first presented. The DOPF model, including objective functions and constraints, were then discussed, followed by some basic concepts related to PEVs, such as their types, charging levels, charging schemes, their basic design concepts, battery charging principles, and optimal dispatch techniques. An overview of mathematical programming and modeling tools used was also provided, and the main concepts of GA were discussed. Finally, a brief summary of the non-parametric Bootstrap technique, and computation of confidence intervals, variance, and standard deviation, was presented.

Chapter 3 presented the problem formulation for the proposed two-step approach, including the first step, i.e., the day-ahead dispatch of distribution feeders to compute the hourly feeder control schedule, as well as the daily feeder peak demand, with the objective of minimizing the daily peak demand, while considering PEV uncertainties based on a Bootstrap approach. A detailed description of the methods used in this step, i.e., the GA-based optimization model, and the Bootstrap estimation, was presented. The results for the day-ahead dispatch of distribution feeders were also discussed and analyzed for a real test feeder and the IEEE 13-bus test feeder, which were described in detail, together with the assumptions made. The discussions on the impact of sample size on Bootstrap estimates, and the estimation of mean daily feeder peak demand and feeder control schedule show that the resulting sampling distributions of the feeder daily peak demand, charging PEV loads and LTC taps approximately resulted in normal distributions, and that the sample size used was sufficiently large. In addition, the Bootstrap method using the GA model was shown to be able to significantly reduce the computational burden, hence demonstrating the feasibility of the proposed approach. The fair charging of PEVs, which is the second step of the proposed approach, is presented in the next chapter.

Chapter 4 presented the second step of the proposed technique, i.e., the fair charging of PEVs. First, a detailed description was provided of the optimization model, which performs the fair charging of PEVs, while considering the distribution feeder operating constraints. A brief overview of the current industry practice in Ontario was then discussed, followed by a popular sensitivity-based heuristic approach for PEV charging and feeder voltage regulation; these other approaches were used to evaluate the performance of the proposed optimization approach. Finally, the results for the fair charging of PEVs for both feeders, as well as its computational performance for various PEV penetration levels, were discussed and analyzed, showing that the optimization technique outperformed the heuristic method in terms of maintaining feeder operating limits and the peak demand constraint. Comparison of the load profiles, voltage profiles, and the feeder control schedules between the Bootstrap estimate and the optimal solution for a particular PEV charging scenario show that the deviation from the optimal is small.

5.2 Contributions

The main contributions of the research presented in this thesis are as follows:

- Proposed a new method to obtain day-ahead hourly feeder control schedules using an accurate and realistic model of a 3-phase unbalanced feeder, considering PEV uncertainty. Realistic discrete variables were used to represent feeder voltage controls.
- For the first time, a non-parametric Bootstrap technique was applied in the context of PEV integration and feeder dispatch, to estimate feeder control schedules and daily peak demand, accounting for PEV uncertainties.
- For the first time, a method is proposed for maximum possible power allocation to charge PEV loads using the proportional fairness approach, without exceeding a peak demand setpoint or the feeder operational limits.
- The benefits and feasibility of the proposed two-step approach were demonstrated in terms of computational effort and practical application using an actual primary distribution feeder, and realistic assumptions regarding PEV charging uncertainties. These results were also validated using the IEEE 13-bus test feeder.

The main contents and contributions of Chapter 3 have been published in IEEE PES General Meeting Proceedings [86] and IEEE PowerTech Conference Proceedings [76]. The main contents of Chapter 4 will be submitted to the IEEE Transactions on Smart Grids shortly.

5.3 Limitations

The limitations of this research are as follows:

- This work does not investigate the impact of communication lag in relaying real-time information to the optimization model, and how the model would perform the optimization with missing information.
- The first step of the proposed optimization approach relies on driver behaviour and travel patterns to generate uncertainty p.d.f.s to model the arrival and departure times, and initial battery size of PEVs, which may not be readily available.
- The first step of the presented approach also needs information related to PEV battery sizes and their location in the feeder, which may be not easily available.

5.4 Future Work

Based on the research presented in this thesis, the following are some possible directions for further research:

- The issue of how to properly allocate the PEV power determined by the proposed technique to the actual PEVs at each node is currently being investigated considering the secondary low-voltage distribution network.
- The impact of deviation from base load forecasts on feeder control and PEV charging needs further investigation.
- Cost-based analysis to evaluate benefit to both utilities and PEV customers needs further investigation.
- Modifications to the proposed approach to consider V2G and voltage control by PEV chargers should be investigated.
- The impact of distributed generation sources on the control and operation of distribution feeders needs further investigation.

APPENDICES

Appendix A

Additional Bootstrap Results

Additional Bootstrap distributions of LTC transformer tap settings for transformers $T1$ phases b and c, $T2$ phases a, b, and c, and $T4$ phases a, b, and c during each time interval, are presented in Figures A.1, A.2, A.3, A.4, A.5, A.6, A.7, and A.8, respectively, for a PEV penetration level of 30% (Real distribution feeder).

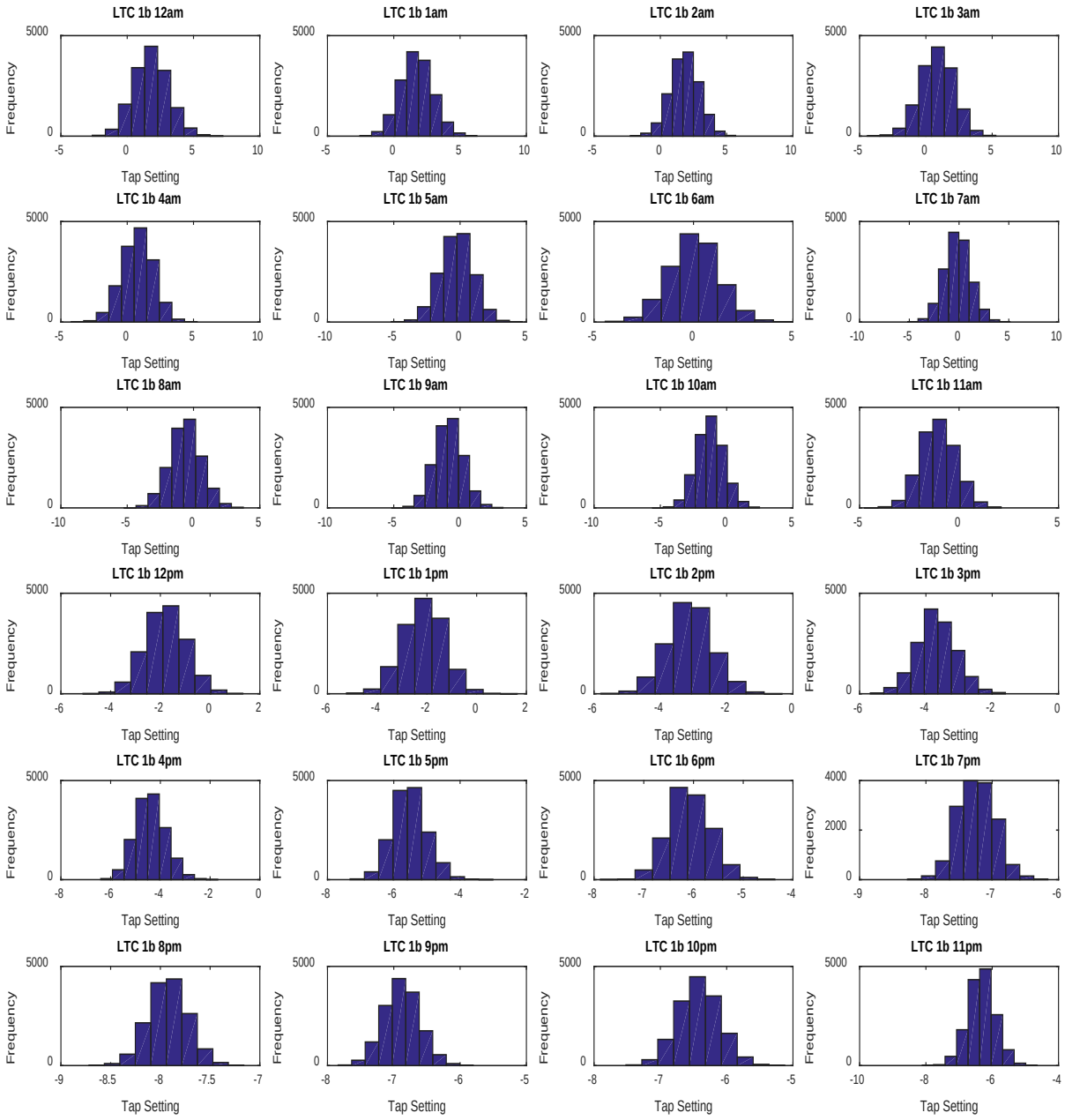

Figure A.1: Histograms for the tap setting of LTC transformer $T1$ phase b in the real distribution feeder during each time interval.

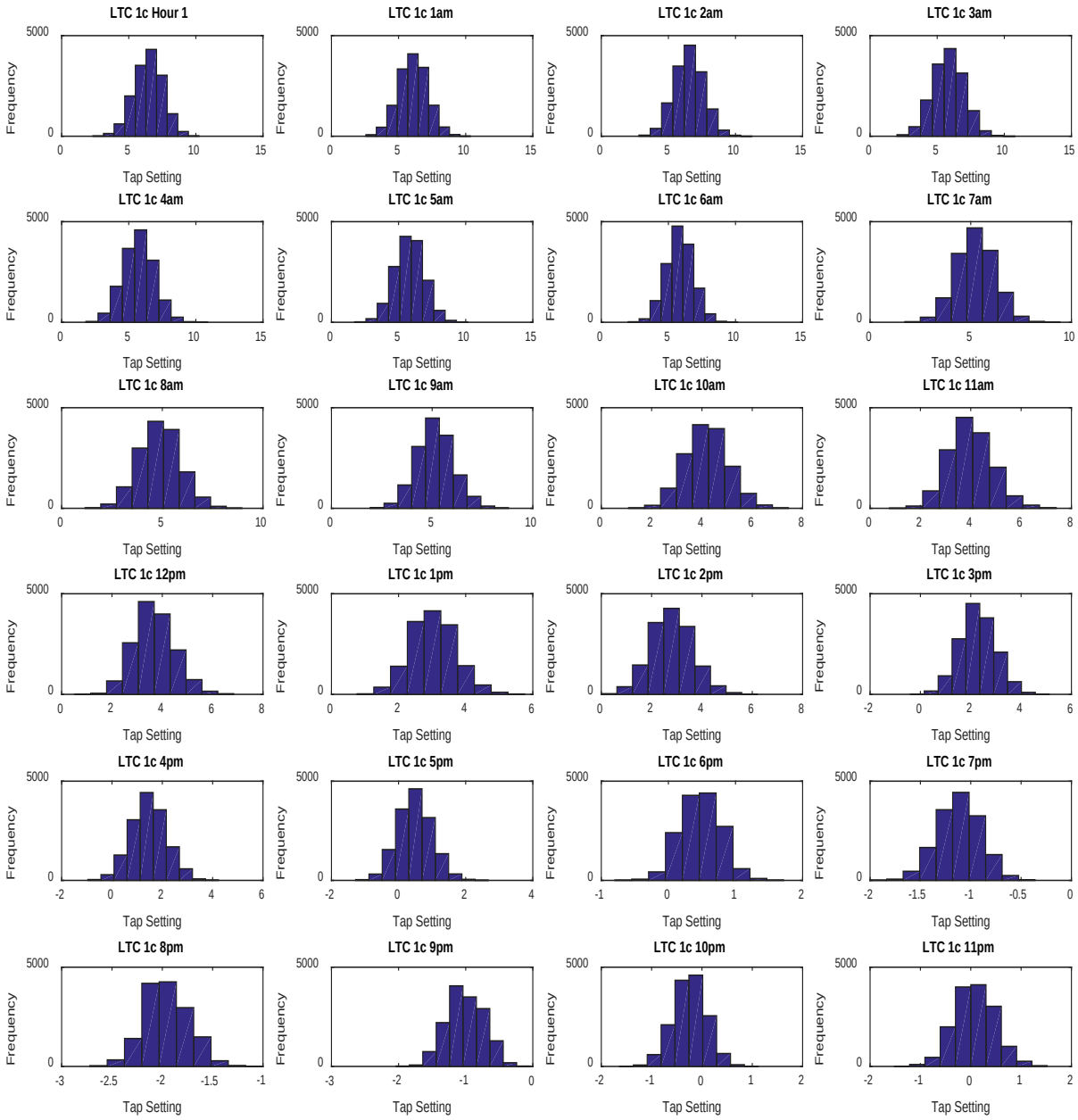

Figure A.2: Histograms for the tap setting of LTC transformer $T1$ phase c in the real distribution feeder during each time interval.

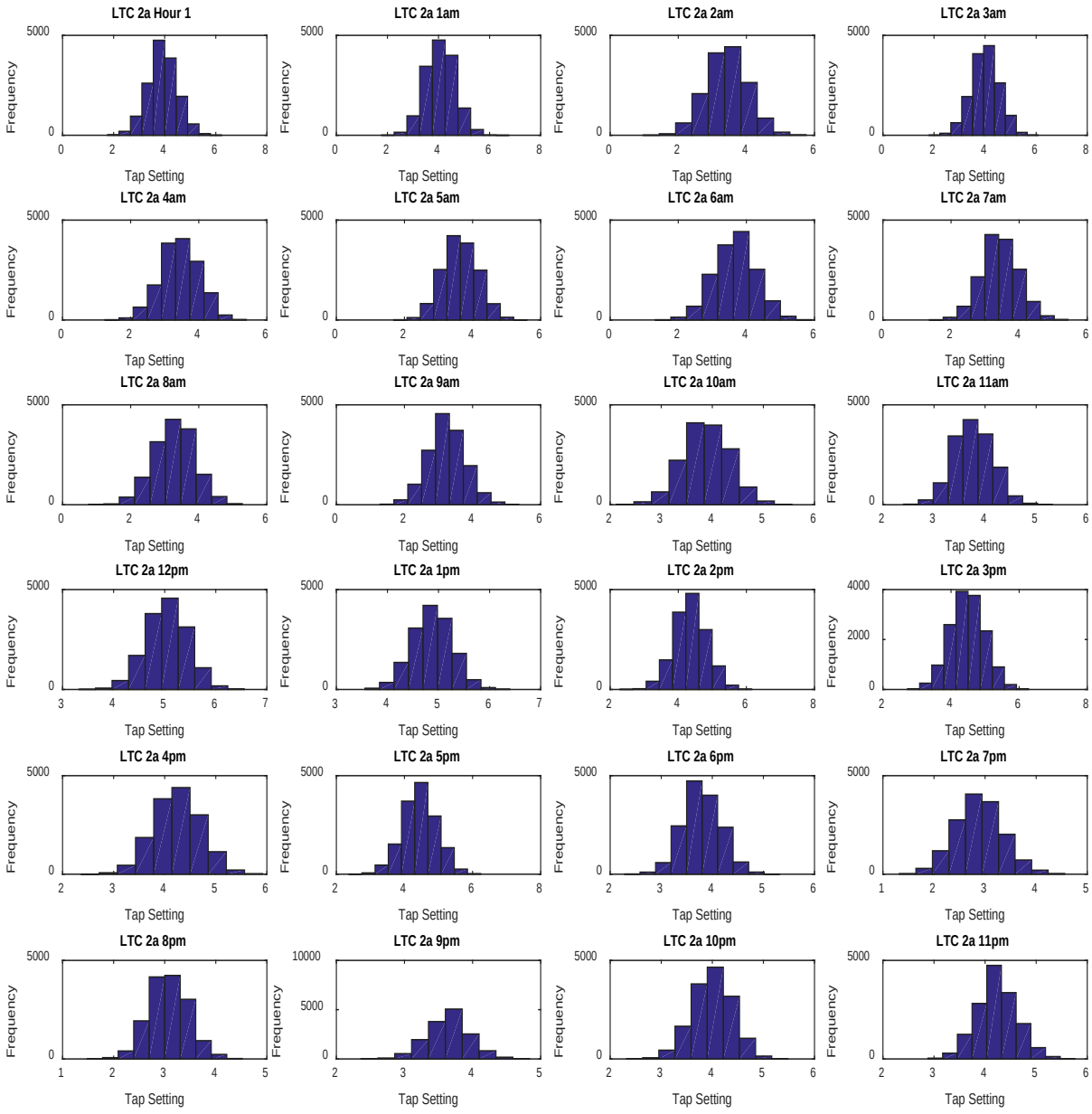

Figure A.3: Histograms for the tap setting of LTC transformer $T2$ phase a in the real distribution feeder during each time interval.

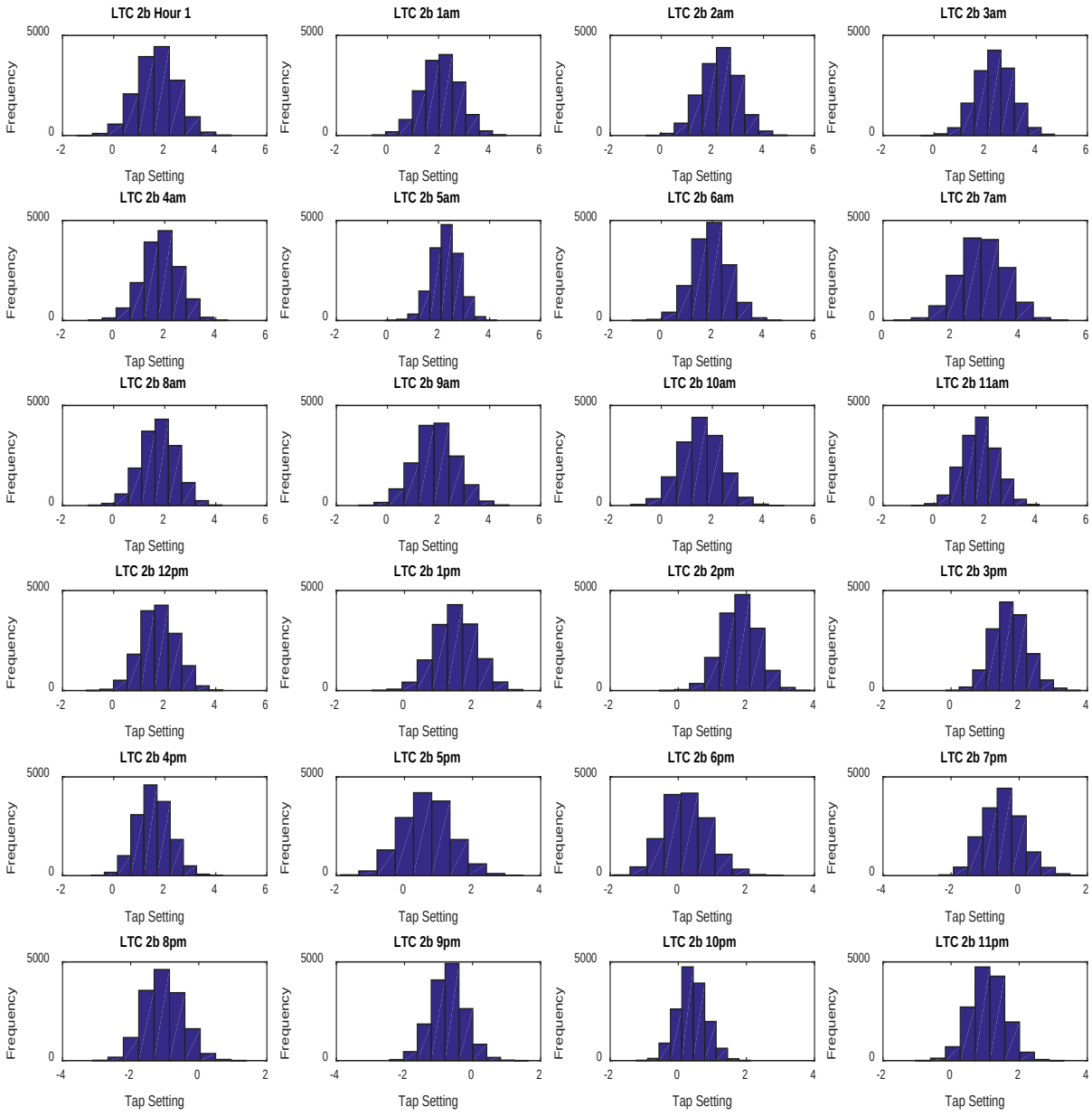

Figure A.4: Histograms for the tap setting of LTC transformer $T2$ phase b in the real distribution feeder during each time interval.

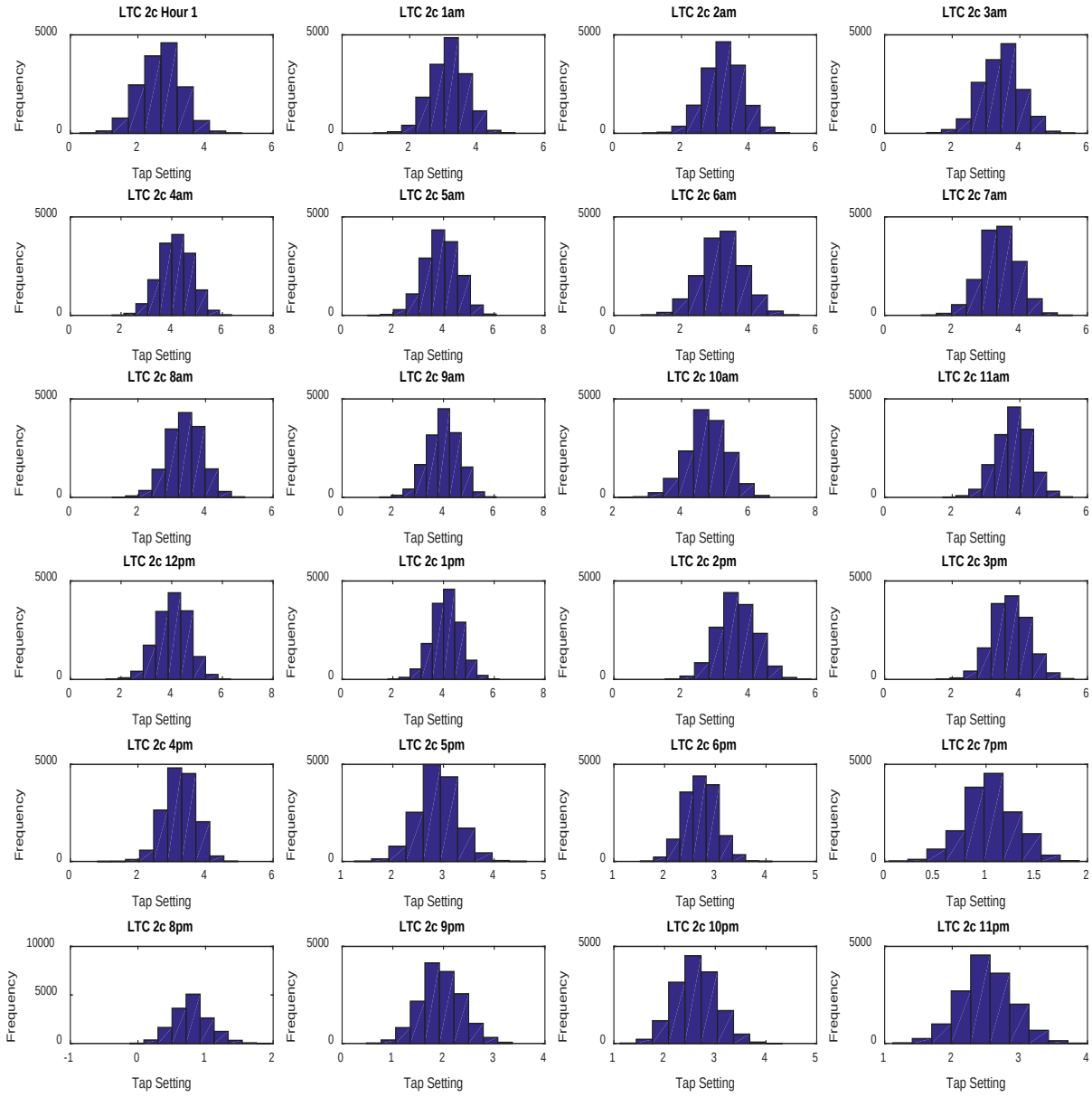

Figure A.5: Histograms for the tap setting of LTC transformer $T2$ phase c in the real distribution feeder during each time interval.

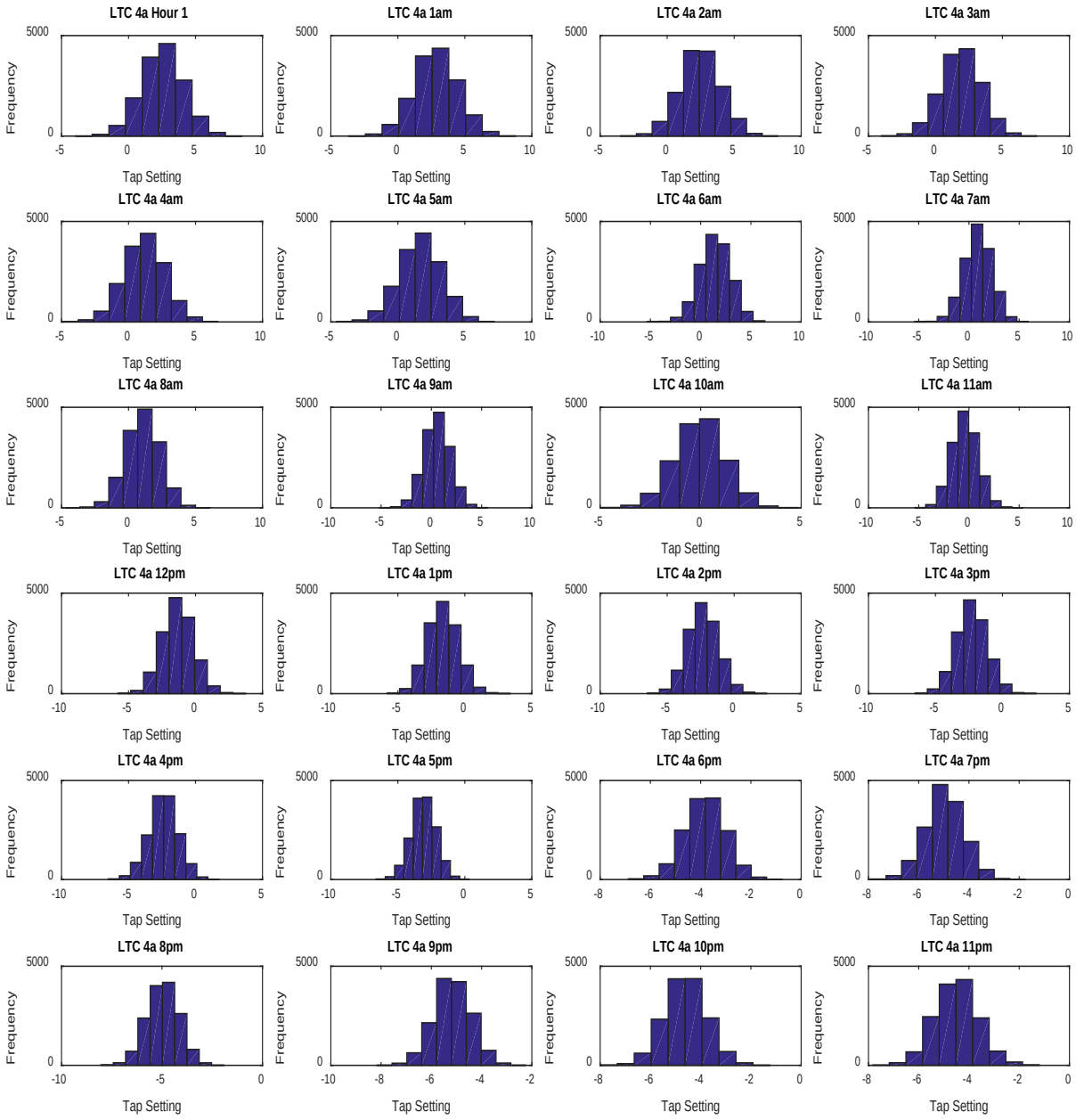

Figure A.6: Histograms for the tap setting of LTC transformer $T4$ phase a in the real distribution feeder during each time interval.

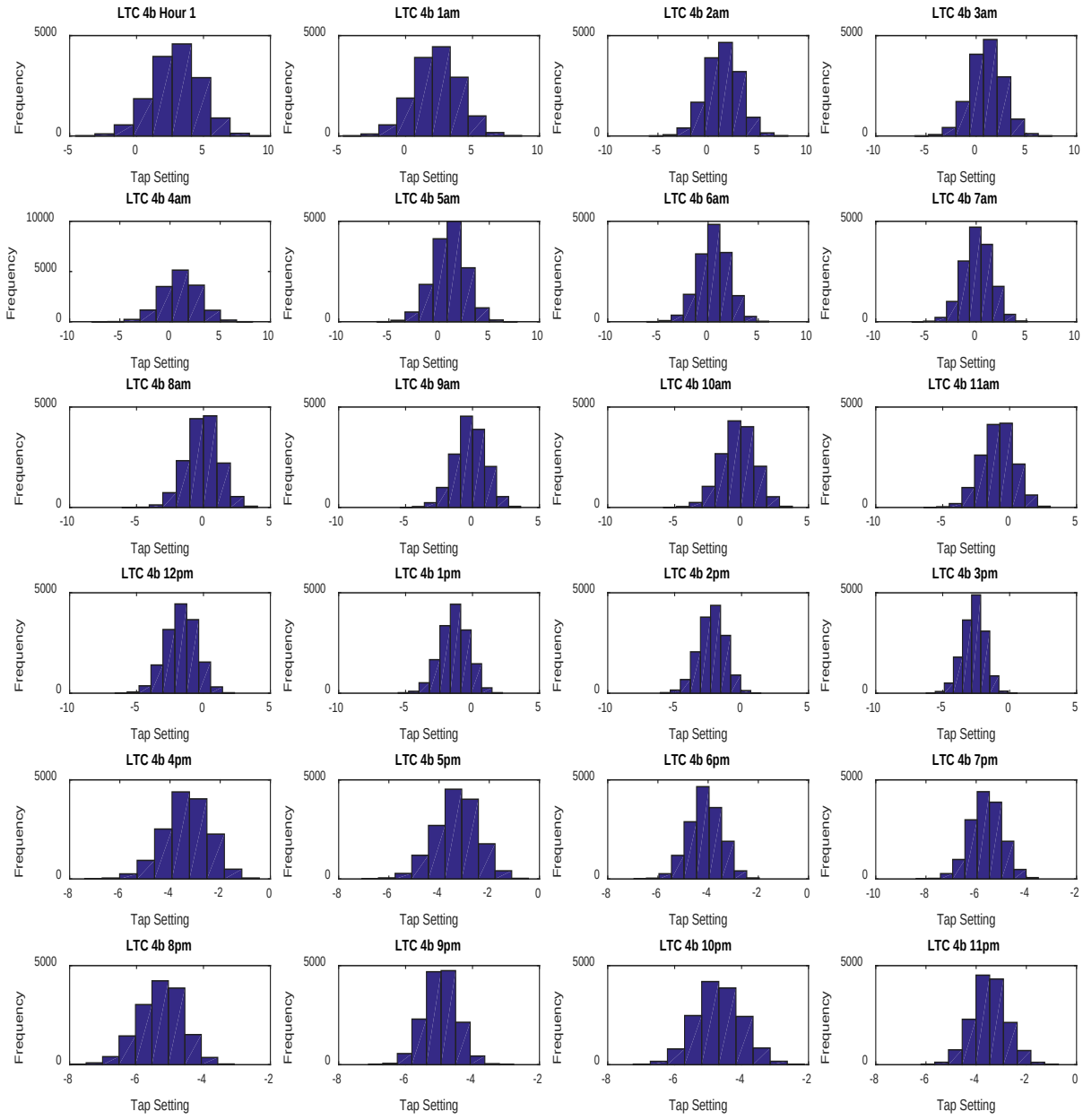

Figure A.7: Histograms for the tap setting of LTC transformer $T4$ phase b in the real distribution feeder during each time interval.

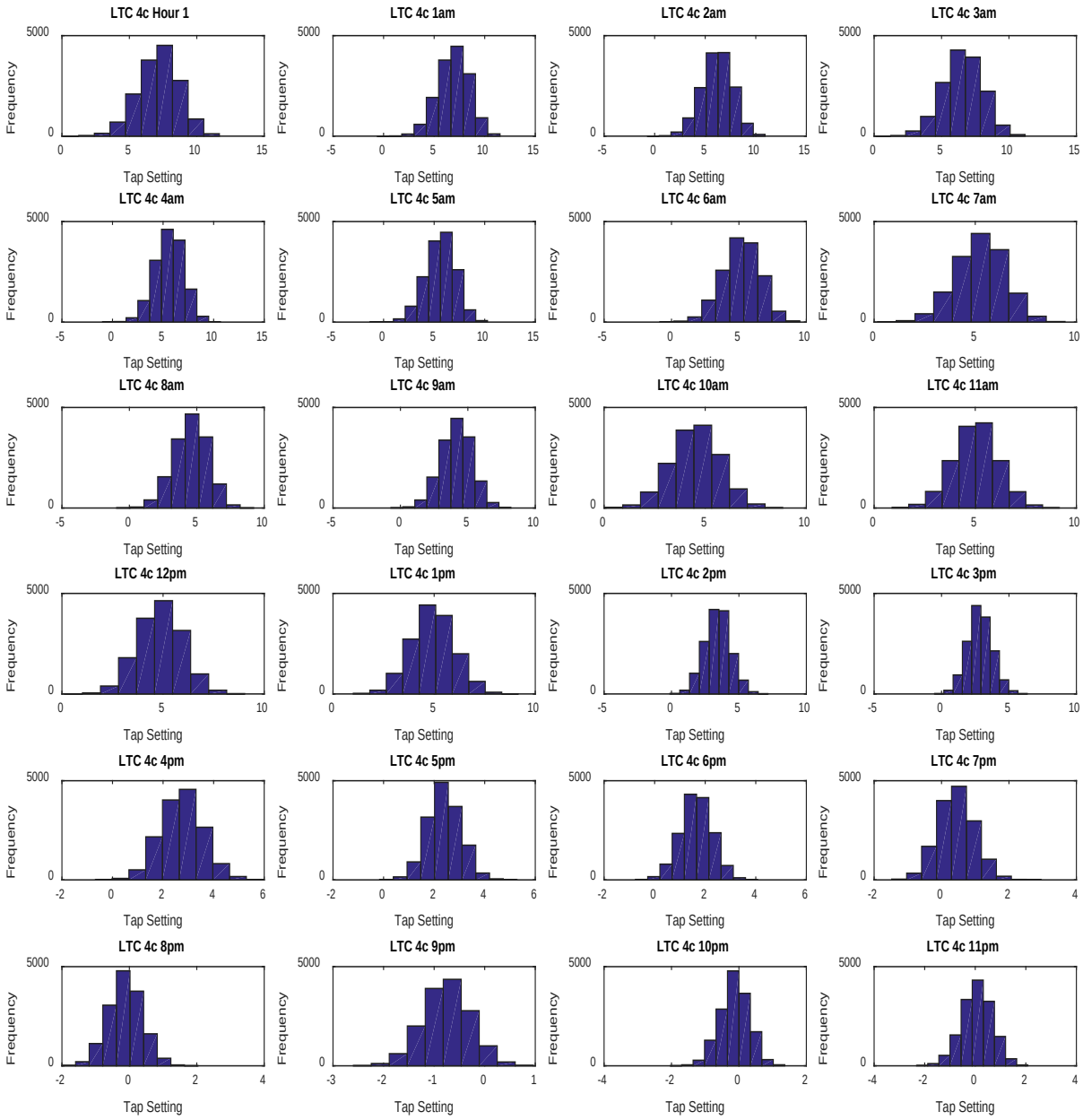

Figure A.8: Histograms for the tap setting of LTC transformer $T4$ phase c in the real distribution feeder during each time interval.

References

[1] "Canada's Action on Climate Change," 2015. [Online]. Available: http://www.climatechange.gc.ca/default.asp?lang=En&n=72F16A84-1

[2] "Greenhouse Gas Emissions by Economic Sector," 2013. [Online]. Available: https://www.ec.gc.ca/indicateurs-indicators/default.asp?lang=en&n=F60DB708-1

[3] WISE, "Towards an Ontario Action Plan for Plug-in Electric Vehicles," University of Waterloo, 2010. [Online]. Available: http://www.ieso.ca/imoweb/pubs/smart_grid/materials/20100907/\WATERLOO%20PHEV_Report%20Final%20May_17.pdf

[4] I. Sharma, C. Canizares, and K. Bhattacharya, "Smart charging of PEVs penetrating into residential distribution systems," *IEEE Transactions on Smart Grid*, vol. 5, no. 3, pp. 1196–1209, May 2014.

[5] "Peaksaver PLUS helps Ontarios electricity system get smarter," 2015. [Online]. Available: http://www.powerauthority.on.ca/conservation/peaksaver-plus-helps-ontarios-electricity-system-get-smarter

[6] Kankar Bhattacharya, "Power System Operation Notes (ECE 666)," 2012.

[7] S. Paudyal, C. Canizares, and K. Bhattacharya, "Optimal operation of distribution feeders in smart grids," *IEEE Transactions on Industrial Electronics*, vol. 58, no. 10, pp. 4495–4503, 2011.

[8] P. Richardson, D. Flynn, and A. Keane, "Local versus centralized charging strategies for electric vehicles in low voltage distribution systems," in *IEEE Power and Energy Society General Meeting (PES)*, July 2013, pp. 1–1.

[9] A. Vargas and M. Samper, "Real-time monitoring and economic dispatch of smart distribution grids: High performance algorithms for dms applications," *IEEE Transactions on Smart Grid*, vol. 3, no. 2, pp. 866–877, June 2012.

[10] B. Zhang, A. Lam, A. Dominguez-Garcia, and D. Tse, "An optimal and distributed method for voltage regulation in power distribution systems," *IEEE Transactions on Power Systems*, vol. 30, no. 4, pp. 1714–1726, July 2015.

[11] S. Shao, M. Pipattanasomporn, and S. Rahman, "Grid integration of electric vehicles and demand response with customer choice," *IEEE Transactions on Smart Grid*, vol. 3, no. 1, pp. 543–550, March 2012.

[12] M. Azzouz, M. Shaaban, and E. El-Saadany, "Real-time optimal voltage regulation for distribution networks incorporating high penetration of pevs," *IEEE Transactions on Power Systems*, vol. 30, no. 6, pp. 3234–3245, Nov 2015.

[13] Z. Fan, "A distributed demand response algorithm and its application to PHEV charging in smart grids," *IEEE Transactions on Smart Grid*, vol. 3, no. 3, pp. 1280–1290, Sept 2012.

[14] Y. He, B. Venkatesh, and L. Guan, "Optimal scheduling for charging and discharging of electric vehicles," *IEEE Transactions on Smart Grid*, vol. 3, no. 3, pp. 1095–1105, Sept 2012.

[15] C. Jin, J. Tang, and P. Ghosh, "Optimizing electric vehicle charging: A customer's perspective," *IEEE Transactions on Vehicular Technology*, vol. 62, no. 7, pp. 2919–2927, Sept 2013.

[16] S. Bahrami and M. Parniani, "Game theoretic based charging strategy for plug-in hybrid electric vehicles," *IEEE Transactions on Smart Grid*, vol. 5, no. 5, pp. 2368–2375, Sept 2014.

[17] Y. Mou, H. Xing, Z. Lin, and M. Fu, "Decentralized optimal demand-side management for PHEV charging in a smart grid," *IEEE Transactions on Smart Grid*, vol. 6, no. 2, pp. 726–736, March 2015.

[18] R. Abousleiman and R. Scholer, "Smart charging: System design and implementation for interaction between plug-in electric vehicles and the power grid," *IEEE Transactions on Transportation Electrification*, vol. PP, no. 99, pp. 1–1, 2015.

[19] L. Gan, U. Topcu, and S. Low, "Stochastic distributed protocol for electric vehicle charging with discrete charging rate," in *IEEE Power and Energy Society General Meeting*, July 2012, pp. 1–8.

[20] N. Rotering and M. Ilic, "Optimal charge control of plug-in hybrid electric vehicles in deregulated electricity markets," *IEEE Transactions on Power Systems*, vol. 26, no. 3, pp. 1021–1029, Aug 2011.

[21] P. Zhang, K. Qian, C. Zhou, B. Stewart, and D. Hepburn, "A methodology for optimization of power systems demand due to electric vehicle charging load," *IEEE Transactions on Power Systems*, vol. 27, no. 3, pp. 1628–1636, Aug 2012.

[22] N. O'Connell, Q. Wu, J. Ostergaard, A. Nielsen, S. T. Cha, and Y. Ding, "Electric vehicle (EV) charging management with dynamic distribution system tariff," in *IEEE PES International Conference and Exhibition on Innovative Smart Grid Technologies (ISGT Europe)*, Dec 2011, pp. 1–7.

[23] N. Blaauwbroek, D. Issicaba, and J. Pecas Lopes, "Multi-agent scheme to handle flexible loads on low voltage distribution grids," in *Power Systems Computation Conference (PSCC)*, Aug 2014, pp. 1–7.

[24] O. Ardakanian, S. Keshav, and C. Rosenberg, "Real-time distributed control for smart electric vehicle chargers: From a static to a dynamic study," *IEEE Transactions on Smart Grid*, vol. 5, no. 5, pp. 2295–2305, Sept 2014.

[25] M. Esmaili and M. Rajabi, "Optimal charging of plug-in electric vehicles observing power grid constraints," *IET Generation, Transmission Distribution*, vol. 8, no. 4, pp. 583–590, April 2014.

[26] A. Masoum, S. Deilami, A. Abu-Siada, and M. Masoum, "Fuzzy approach for online coordination of plug-in electric vehicle charging in smart grid," *IEEE Transactions on Sustainable Energy*, vol. PP, no. 99, pp. 1–10, 2015.

[27] F. Baccino, S. Grillo, S. Massucco, and F. Silvestro, "A two-stage margin-based algorithm for optimal plug-in electric vehicles scheduling," *IEEE Transactions on Smart Grid*, vol. 6, no. 2, pp. 759–766, March 2015.

[28] N. Chen, C. W. Tan, and T. Quek, "Electric vehicle charging in smart grid: Optimality and valley-filling algorithms," *IEEE Journal on Selected Topics in Signal Processing*, vol. 8, no. 6, pp. 1073–1083, Dec 2014.

[29] S. Deilami, A. Masoum, P. Moses, and M. Masoum, "Real-time coordination of plug-in electric vehicle charging in smart grids to minimize power losses and improve voltage profile," *IEEE Transactions on Smart Grid*, vol. 2, no. 3, pp. 456–467, Sept 2011.

[30] K. Clement-Nyns, E. Haesen, and J. Driesen, "The impact of charging plug-in hybrid electric vehicles on a residential distribution grid," *IEEE Transactions on Power Systems*, vol. 25, no. 1, pp. 371–380, Feb 2010.

[31] J. de Hoog, T. Alpcan, M. Brazil, D. Thomas, and I. Mareels, "Optimal charging of electric vehicles taking distribution network constraints into account," *IEEE Transactions on Power Systems*, vol. 30, no. 1, pp. 365–375, Jan 2015.

[32] F. Baccino, S. Grillo, S. Massucco, and F. Silvestro, "A two-stage margin-based algorithm for optimal plug-in electric vehicles scheduling," *IEEE Transactions on Smart Grid*, vol. 6, no. 2, pp. 759–766, March 2015.

[33] S. Sojoudi and S. Low, "Optimal charging of plug-in hybrid electric vehicles in smart grids," in *IEEE Power and Energy Society General Meeting*, July 2011, pp. 1–6.

[34] Z. Darabi and M. Ferdowsi, "Aggregated impact of plug-in hybrid electric vehicles on electricity demand profile," *IEEE Transactions on Sustainable Energy*, vol. 2, no. 4, pp. 501–508, Oct 2011.

[35] M. Shaaban, Y. Atwa, and E. El-Saadany, "PEVs modeling and impacts mitigation in distribution networks," *IEEE Transactions on Power Systems*, vol. 28, no. 2, pp. 1122–1131, May 2013.

[36] L. Pieltain-Fernandez, T. Roman, R. Cossent, C. Domingo, and P. Frias, "Assessment of the impact of plug-in electric vehicles on distribution networks," *IEEE Transactions on Power Systems*, vol. 26, no. 1, pp. 206–213, Feb 2011.

[37] K. Qian, C. Zhou, M. Allan, and Y. Yuan, "Modeling of load demand due to EV battery charging in distribution systems," *IEEE Transactions on Power Systems*, vol. 26, no. 2, pp. 802–810, May 2011.

[38] G. Li and X.-P. Zhang, "Modeling of plug-in hybrid electric vehicle charging demand in probabilistic power flow calculations," *IEEE Transactions on Smart Grid*, vol. 3, no. 1, pp. 492–499, March 2012.

[39] R. Verzijlbergh, M. Grond, Z. Lukszo, J. Slootweg, and M. Ilic, "Network impacts and cost savings of controlled EV charging," *IEEE Transactions on Smart Grid*, vol. 3, no. 3, pp. 1203–1212, Sept 2012.

[40] W. H. Kersting, *Distribution System Modeling and Analysis*. CRC Press, 2006.

[41] "Nebraska Power Association," 2013. [Online]. Available: http://www.nepower.org/npa-on-energy-issues/transmission/

[42] R. Dugan, "OpenDSS," 2010. [Online]. Available: http://electricdss.svn.sourceforge.net/viewvc/electricdss/Doc/OpenDSSManual.doc?view=log

[43] "OpenDSS Training Workshop," 2014. [Online]. Available: http://sourceforge.net/p/electricdss/code/HEAD/tree/trunk/Training/SRP-ASU2014/

[44] Canadian Standards Association, *Electrical Engineering Standards: CAN3-C235-83 (R2010) - Preferred Voltage Levels for AC Systems, 0 to 50 000 V*, 2010.

[45] M. Yilmaz and P. Krein, "Review of battery charger topologies, charging power levels, and infrastructure for plug-in electric and hybrid vehicles," *IEEE Transactions on Power Electronics*, vol. 28, no. 5, pp. 2151–2169, May 2013.

[46] J. Axsen, A. Burke, and K. Kurani, "Batteries for plug-in hybrid electric vehicles (PHEVs): Goals and the state of technology," 2008.

[47] A. Hajimiragha, C. Canizares, M. Fowler, and A. Elkamel, "Optimal transition to plug-in hybrid electric vehicles in ontario, canada, considering the electricity-grid limitations," *IEEE Transactions on Industrial Electronics*, vol. 57, no. 2, pp. 690–701, Feb 2010.

[48] M. Duval, "Advanced batteries for electric-drive vehicles: A technology and cost-effectiveness assessment for battery electric vehicles, power assist hybrid electric vehicles, and plug-in hybrid electric vehicles."

[49] Z. Darabi and M. Ferdowsi, "Aggregated impact of plug-in hybrid electric vehicles on electricity demand profile," *IEEE Transactions on Sustainable Energy*, vol. 2, no. 4, pp. 501–508, Oct 2011.

[50] E. Rigas, S. Ramchurn, and N. Bassiliades, "Managing electric vehicles in the smart grid using artificial intelligence: A survey," *IEEE Transactions on Intelligent Transportation Systems*, vol. PP, no. 99, pp. 1–17, 2015.

[51] M. Vaya and G. Andersson, "Centralized and decentralized approaches to smart charging of plug-in vehicles," in *IEEE Power and Energy Society General Meeting*, July 2012, pp. 1–8.

[52] Z. Ma, D. Callaway, and I. Hiskens, "Decentralized charging control of large populations of plug-in electric vehicles," *IEEE Transactions on Control Systems Technology*, vol. 21, no. 1, pp. 67–78, Jan 2013.

[53] P. Richardson, D. Flynn, and A. Keane, "Local versus centralized charging strategies for electric vehicles in low voltage distribution systems," *IEEE Transactions on Smart Grid*, vol. 3, no. 2, pp. 1020–1028, June 2012.

[54] O. Ardakanian, C. Rosenberg, and S. Keshav, "Distributed control of electric vehicle charging," in *Proceedings of the Fourth International Conference on Future Energy Systems*, ser. e-Energy '13. New York, NY, USA: ACM, 2013, pp. 101–112. [Online]. Available: http://doi.acm.org/10.1145/2487166.2487178

[55] L. Yang, J. Zhang, and H. Poor, "Risk-aware day-ahead scheduling and real-time dispatch for electric vehicle charging," *IEEE Transactions on Smart Grid*, vol. 5, no. 2, pp. 693–702, March 2014.

[56] S. G. Nash and A. Sofer, *Linear and Non-Linear Programming*. The McGraw-Hill Companies, Inc., 1996.

[57] W. Winston and M. Venkataramanan, *Introduction to Mathematical Programming: Applications and Algorithms*. Cengage Learning, 2002. [Online]. Available: https://books.google.ca/books?id=pr9EnwEACAAJ

[58] J. Zhu, *Optimization of Power System Operation*. John Wiley & Sons, Inc., 2009.

[59] "Mixed-Integer Nonlinear Programming," 2003. [Online]. Available: http://www.math.tu-bs.de/~bussieck/siagopt.pdf

[60] A. Kunjur and S. Krishnamurty, "Genetic Algorithms in Mechanism Synthesis." [Online]. Available: http://www.ecs.umass.edu/mie/labs/mda/mechanism/papers/genetic.html

[61] M. Dorigo and T. Stützle, "Ant colony optimization: overview and recent advances," *Techreport, IRIDIA, Universite Libre de Bruxelles*, 2009.

[62] "A comparison of Particle Swarm Optimization and the Genetic Algorithm," 2004. [Online]. Available: http://web.mit.edu/deweck/www/PDF_archive/3%20Refereed%20Conference/3_50_AIAA-2005-1897.pdf

[63] C. A. C. Coello, G. B. Lamont, and D. A. V. Veldhuizen, *Evolutionary Algorithms for Solving Multi-Objective Problems (Genetic and Evolutionary Computation)*. Secaucus, NJ, USA: Springer-Verlag New York, Inc., 2006.

[64] The Mathworks, Inc., "MATLAB," 1994-2015. [Online]. Available: http://www.mathworks.com/products/matlab/

[65] J. Miller, W. Potter, R. Gandham, and C. Lapena, "An evaluation of local improvement operators for genetic algorithms," *IEEE Transactions on Systems, Man and Cybernetics*, vol. 23, no. 5, pp. 1340–1351, Sep 1993.

[66] D. E. Goldberg, *Genetic Algorithms in Search, Optimization, and Machine Learning*. Addison-Wesley Publishing Company, Inc., 1953.

[67] D. A. Coley, *An Introduction to Genetic Algorithms for Scientists and Engineers*. World Scientific Publishing Co. Pte. Ltd., 2010.

[68] D. Greenhalgh and S. Marshall, "Convergence criteria for genetic algorithms," *SIAM Journal on Computing*, vol. 30, no. 1, pp. 269–282, 2000. [Online]. Available: http://dx.doi.org/10.1137/S009753979732565X

[69] B. Efron, "Bootstrap methods: Another look at the jackknife," *The Annals of Statistics*, vol. 7, no. 1, pp. 1–26, 01 1979. [Online]. Available: http://dx.doi.org/10.1214/aos/1176344552

[70] B. Efron and R. Tibshirani, *An Introduction to the Bootstrap*. Chapman and Hall/CRC, 1994.

[71] Z. R. Yang, M. Zwolinski, and C. Chalk, "Bootstrap, an alternative to monte carlo simulation," *Electronics Letters*, vol. 34, no. 12, pp. 1174–1175, Jun 1998.

[72] Wendy Post, "Bootstrapping: A Non-parametric Approach to Statistical Inference," 2012. [Online]. Available: http://www.gmw.rug.nl/~huisman/sgs/2012_10_25_Bootstrap.pdf

[73] L. Kogan, "Small-Sample Inference and Bootstrap," 2010. [Online]. Available: http://ocw.mit.edu/courses/sloan-school-of-management/15-450-analytics-of-finance-fall-2010/lecture-notes/MIT15_450F10_lec09.pdf

[74] T. Hesterberg, S. Monaghan, D. Moore, A. Clipson, and R. Epstein, "Bootstrap methods and permutation tests," 2003. [Online]. Available: http://hsta559s12.pbworks.com/w/file/fetch/50747070/Hesterberg.Bootstrappng.chpt18.pdf

[75] F. Scholz, "The bootstrap small sample properties," 2007. [Online]. Available: http://www.stat.washington.edu/fritz/Reports/bootstrap-report.pdf

[76] N. Mehboob, C. Canizares, and C. Rosenberg, "Day-ahead dispatch of distribution feeders considering temporal uncertainties of pevs," in *IEEE Eindhoven PowerTech*, June 2015, pp. 1–6.

[77] S. Villalba and C. Bel, "Hybrid demand model for and short term load forecasting in distribution electric systems," *IEEE Transactions on Power Delivery*, vol. 15, no. 2, pp. 764–769, Apr 2000.

[78] N. Ding, C. Benoit, G. Foggia, Y. Besanger, and F. Wurtz, "Neural network-based model design for short-term load forecast in distribution systems," *IEEE Transactions on Power Systems*, vol. PP, no. 99, pp. 1–10, 2015.

[79] B. K. Sovacool and R. F. Hirsh, "Beyond batteries: An examination of the benefits and barriers to plug-in hybrid electric vehicles (PHEVs) and a vehicle-to-grid (V2G) transition," *Energy Policy*, vol. 37, no. 3, pp. 1095 – 1103, 2009. [Online]. Available: http://www.sciencedirect.com/science/article/pii/S0301421508005934

[80] J. D. Bishop, C. J. Axon, D. Bonilla, M. Tran, D. Banister, and M. D. McCulloch, "Evaluating the impact of V2G services on the degradation of batteries in PHEV and EV," *Applied Energy*, vol. 111, pp. 206 – 218, 2013. [Online]. Available: http://www.sciencedirect.com/science/article/pii/S0306261913004121

[81] I. Sharma, C. Canizares, and K. Bhattacharya, "Modeling and impacts of smart charging PEVs in residential distribution systems," in *IEEE Power and Energy Society General Meeting*, 2012, pp. 1–8.

[82] T.-K. Lee, Z. Bareket, T. Gordon, and Z. Filipi, "Stochastic modeling for studies of real-world PHEV usage: Driving schedule and daily temporal distributions," *IEEE Transactions on Vehicular Technology*, vol. 61, no. 4, pp. 1493–1502, May 2012.

[83] Hydro One Networks Inc., "Distribution Customers Conditions of Service," 2013. [Online]. Available: http://www.hydroone.com/MyHome/MyAccount/ConditionsofService/Documents/Hydro_One_Conditions_of_Service_2013_ENGLISH.pdf

[84] E. Liu and K. Leung, "Proportional fair scheduling: Analytical insight under rayleigh fading environment," in *IEEE Wireless Communications and Networking Conference*, March 2008, pp. 1883–1888.

[85] Noel, Kanishk, private communication.

[86] N. Mehboob, C. Canizares, and C. Rosenberg, "Day-ahead dispatch of PEV loads in a residential distribution system," in *IEEE Power and Energy Society General Meeting*, July 2014, pp. 1–5.